UCLouvain
Institute for Information
and Communication Technologies,
Electronics and Applied Mathematics

A model- and experiment-based study of gait variability in health and Parkinson's disease

Clémence Vandamme

Thesis submitted in partial fulfillment
of the requirements for the degree of
Doctor in Applied Sciences

Dissertation committee:

Prof. Frédéric Crevecoeur (Advisor), UCLouvain, Belgium
Prof. Renaud Ronsse (Advisor), UCLouvain, Belgium
Prof. Philippe Lefèvre (Secretary), UCLouvain, Belgium
Prof. Pierre-Antoine Absil (Chair), UCLouvain, Belgium
Prof. Leslie Decker, Université Caen-Normandie, France
Dr. Thibault Warlop, Centre Hospitalier Wallonie Picarde, Belgium
Prof. Vivian Weerdesteyn, Radboud University Medical Center, The Netherlands

Version of September 2026.

Remerciements

TOUT au long de ces cinq années qui ont abouti à la rédaction de cette thèse, j'ai pu compter sur l'aide et le soutien de nombreuses personnes. Je tiens ici à toutes et tous les remercier comme il se doit.

Merci tout d'abord à Fred et Renaud pour m'avoir aidée et guidée tout au long de cette aventure. Votre expertise, vos encouragements et vos conseils toujours très pertinents m'ont permis de m'épanouir et de progresser au fil des années. Merci Fred pour ta disponibilité et pour ton optimisme à toute épreuve, qui m'a toujours aidée à voir le positif dans mes résultats. Merci Renaud pour ton enthousiasme lors de nos réunions régulières et pour tes relectures attentives, toujours accompagnées d'un commentaire positif ou d'un mot encourageant. Je tiens également à remercier Thibault Warlop pour son aide autour des expériences avec les patients et pour son enthousiasme pour ce projet. Merci également aux Prof. Philippe Lefèvre, Leslie Decker, Vivian Weerdesteyn et Pierre-Antoine Absil d'avoir accepté de faire partie de ce jury, pour le temps investi dans la lecture de mon manuscrit et pour les discussions très instructives que nous avons eues lors de la défense privée.

Au cours de toutes ces années, j'ai eu la chance de collaborer avec des collègues (et amis !) exceptionnels. Merci Virginie de m'avoir aidée à faire mes premiers pas avec beaucoup de bienveillance, et merci François pour ta motivation et ton investissement dans un mémoire qui me tenait à coeur. Un merci tout particulier à Astrid, avec qui je n'ai pas seulement partagé une collaboration, mais également un bureau, des voyages, des rires et les difficultés de la fin de thèse. Merci pour ton écoute, ta flexibilité et ta bonne humeur. Je voudrais évidemment remercier les membres du SenseMotion Lab pour les discussions scientifiques et les bons moments passés en conférence et en retraite, et plus largement tous les habitants de l'Euler, anciens et actuels. Vous avez embelli mon quotidien avec une bonne dose d'humour, de café, de papotes, d'afterworks, de spikeball, de courses piou-piou et de paninis parmigiana. Merci également à Marie-Christine, Dora, Pascale, Astrid, François, John et Etienne, qui rendent la vie à l'Euler toujours plus facile.

Je tiens également à remercier mes amis, notamment Lucas, Jeanne, Alice, Pauline, Seb, Anne, *les colocs de Kraainem* - Constance, Perrine et Florine -, et *les 6 ways to Sunday* - Juliette, Lisa, Alix et Martin. Votre amitié m'est très précieuse. Merci à mes parents, mon frère et mes sœurs pour vos nombreux encouragements. Et surtout, merci Augu de m'avoir soutenue, rassurée et donné le sourire au quotidien.

Contents

Contents iii

List of acronyms vii

1 General introduction 1
1.1 Parkinson's disease 2
1.1.1 Pathophysiology 2
1.1.2 Symptoms 5
1.1.3 Current therapeutic approaches 6
1.2 Long-range autocorrelations in gait variability 7
1.2.1 Impact of aging and disease 8
1.2.2 Impact of contextual constraints 10
1.2.3 Synchronization with rhythmic cues 12
1.2.4 Modeling approach 14
1.3 Aim of this work 16
1.4 Publications and communications 17

2 Long-Range Autocorrelations: Mathematical foundations 19
2.1 Definition 19
2.2 Self-similarity and fractal structure 20
2.3 Spectral representation 21
2.4 Methods to assess LRA in a time series 21
2.4.1 Frequency domain method 22
2.4.2 Time domain methods 22
2.4.3 Evenly-spacing 24
2.4.4 Integrated methods 24
2.5 Discussion 25

3 Model of gait control in Parkinson's disease and prediction of robotic assistance 29
3.1 Introduction 30
3.2 Materials and Methods 31
3.2.1 Data 31
3.2.2 Assessment of the Long-range autocorrelation 32
3.2.3 Gait model for young and healthy population 32

3.2.4 Model adaptations to Parkinson's disease and robotic assistance . . . 35
3.3 Results . . . 37
3.3.1 Healthy gait . . . 37
3.3.2 Gait in Parkinson's Disease . . . 38
3.3.3 Simulation of robotic assistance . . . 40
3.4 Discussion . . . 41
3.5 Complementary discussion . . . 45
3.5.1 From computational predictions to experimental intervention . . . 45
3.5.2 Impact of methodological heterogeneity between datasets . . . 46

4 Measured and modeled transitions between self-paced walking and synchronization with rhythmic auditory cues . . . 47
4.1 Introduction . . . 48
4.2 Material and Methods . . . 49
4.2.1 Experimental procedure . . . 49
4.2.2 Data acquisition and processing . . . 51
4.2.3 Data analysis . . . 52
4.2.4 Model . . . 53
4.2.5 Statistical analyses . . . 56
4.3 Results . . . 57
4.3.1 Behavioural experiments . . . 57
4.3.2 Model . . . 61
4.4 Discussion . . . 65

5 Assessing gait control from short time series using a geometric characterization of stride-by-stride corrections . . . 69
5.1 Introduction . . . 70
5.2 Material & Methods . . . 71
5.2.1 Experimental data . . . 71
5.2.2 Model . . . 73
5.2.3 Data analysis . . . 74
5.2.4 Statistics . . . 76
5.3 Results . . . 77
5.3.1 Model description . . . 77
5.3.2 Comparison with experimental data . . . 79
5.3.3 Impact of initial asynchrony in cued condition . . . 81
5.3.4 Results summary . . . 84
5.4 Discussion . . . 84

6 Preserved behavioral flexibility during locomotion and reaching in Parkinson's disease 89
6.1 Introduction . . . 90
6.2 Materials & Methods . . . 92
6.2.1 Recruitment and Assessment . . . 92
6.2.2 Experimental procedure . . . 92

6.2.3 Data acquisition and processing . . . 93
6.2.4 Data analysis . . . 93
6.2.5 Statistical analyses . . . 96
6.2.6 Reaching experiment . . . 96
6.2.7 Evaluation of redundancy across tasks . . . 98
6.3 Results . . . 98
6.3.1 Flexible modulation of gait control . . . 98
6.3.2 Flexible modulation of reaching control . . . 101
6.3.3 Evaluation of redundancy across tasks . . . 103
6.3.4 Results summary . . . 105
6.4 Discussion . . . 106
6.5 Supplementary material . . . 109

7 Conclusion and perspectives . . . **113**
7.1 Main contributions . . . 113
7.2 Future work . . . 115
7.2.1 LRA and gait adaptability . . . 115
7.2.2 Foot placement . . . 115
7.2.3 Fractal cueing . . . 116
7.2.4 State estimation . . . 117
7.2.5 Selection of preferred gait parameters . . . 117
7.3 Concluding words . . . 118

Bibliography . . . **119**

List of acronyms

AFA	Adaptive Fractal Analysis
AUC	Area Under Curve
CPG	Central Pattern Generator
DFA	Detrended Fluctuation Analysis
fBm	fractional Brownian motion
fGn	fractional Gaussian noise
GEM	Goal-Equivalent Manifold
H&Y	Hoehn & Yahr
HC	Healthy Control
IMU	Inertial Measurement Unit
LRA	Long-Range Autocorrelation
PD	Parkinson's disease
POP	Preferred Operating Point
PSD	Power Spectral Density
RMSE	Root Mean Square Error
ROC	Receiver Operating Characteristics
RRA	Rescaled Range Analysis
SCPG	Super Central Pattern Generator

1

General introduction

THE emergence of bipedal locomotion marked a defining chapter in the evolutionary journey of hominids (Harcourt-Smith and Aiello, 2004), just as the first independent steps of a child symbolize a pivotal moment in early motor development (Iverson, 2010). Beneath an apparent simplicity, walking depends on the precise coordination of numerous neural structures, including cortical areas, basal ganglia, brainstem structures, spinal circuits, and peripheral sensory systems (Takakusaki, 2017). A key challenge faced by the locomotor system is to simultaneously ensure stability and adaptability: successful locomotion requires maintaining balance while remaining flexible enough to respond to changing environmental conditions.

With advancing age and in neurological disorders, such as Parkinson's disease, this finely tuned locomotor machinery becomes increasingly vulnerable. Impairments in the neural circuits underlying gait and balance can lead to reduced mobility, increased risk of falls, and a progressive loss of independence, all of which substantially affecting quality of life. Understanding the neural mechanisms that govern stable and adaptable locomotion is therefore essential for developing effective interventions to preserve mobility and independence in individuals with Parkinson's disease.

Because locomotor deficits often emerge before severe disability becomes apparent, sensitive markers of gait control are needed to characterize these impairments and monitor their progression. In this context, gait variability has emerged as a valuable tool for investigating locomotor control. Rather than being perfectly repetitive, healthy walking exhibits a certain degree of stride-to-stride fluctuation that reflects the continuous adaptation of the locomotor system to internal and external perturbations. While some variability is a natural feature of flexible and adaptive movement, excessive or altered variability may indicate impairments in the mechanisms responsible for regulating locomotion. In Parkinson's disease, alterations in gait variability, both in magnitude and temporal structure, have been linked to disease severity, fall risk, and deficits in motor automaticity, highlighting its potential as a relevant biomarker of locomotor impairment. Consequently, the quantification of gait variability has gained con-

siderable interest as a means of probing the integrity of the neural processes governing gait control. Beyond the amount of variability, increasing attention has been devoted to its temporal organization,commonly quantified through the presence of long-range autocorrelations, reflecting statistical dependencies between stride intervals separated by multiple steps.

The present thesis builds upon decades of research dedicated to understanding the mechanisms underlying gait variability, in health and in Parkinson's disease. More specifically, this work investigates how gait regulation shapes the temporal structure of stride-to-stride fluctuations by combining experimental observations with theoretical models. Before addressing these questions, it is essential to establish the clinical and theoretical foundations of this work. The first section introduces Parkinson's disease, describing its pathophysiology, clinical manifestations, and current therapeutic approaches. The second section reviews the existing literature on gait variability, with a particular focus on its temporal structure, its alterations in pathological and experimentally constrained conditions, and the theoretical frameworks that have been proposed to explain its emergence. Together, these elements provide the conceptual background for the research questions and hypotheses developed throughout this thesis.

1.1 Parkinson's disease

Parkinson's disease (PD) is a progressive neurodegenerative disorder and the second most common neurodegenerative disease after Alzheimer's disease. In 2019, an estimated 8.5 million people worldwide were living with PD, with prevalence increasing markedly across older age groups (Ou et al. 2021). The clinical manifestations of PD encompass both motor and non-motor symptoms. The cardinal motor features include bradykinesia, resting tremor, and rigidity, often accompanied by gait and balance impairments (Kalia and Lang, 2015). Non-motor manifestations include sleep disturbances, anxiety and depression, cognitive decline, and dysfunction of the autonomic nervous system (Faivre et al. 2019; Schapira et al. 2017; Williams-Gray et al. 2007).

1.1.1 Pathophysiology

The pathophysiology of PD is characterized by the progressive degeneration of dopaminergic neurons within the substantia nigra pars compacta (SNpc). This neurodegeneration has been associated with the formation of Lewy bodies, which consist largely of misfolded α-synuclein (Surmeier, 2018). While the loss of dopamine neurons are believed to produce the core motor symptoms of PD, Lewy body depositions are also found in different brain regions. Neurodegeneration can therefore affect brainstem nuclei, including autonomic areas like the dorsal motor nucleus of the vagus, motor nuclei such as the pedunculopontine nucleus, and neuromodulatory nuclei like the locus coeruleus and raphe (Seidel et al. 2015).

The loss of dopaminergic neurons in SNpc affects the proper functioning of the basal ganglia system, a group of interconnected subcortical nuclei. The basal ganglia are composed of

five principal structures: the caudate nucleus, putamen, globus pallidus (divided into the internal and external segments, GPi and GPe), substantia nigra (pars compacta and pars reticulata, SNpc and SNpr), and subthalamic nucleus (STN). The caudate nucleus and putamen together constitute the striatum, which serves as the primary input structure of the basal ganglia. The major connections within the basal ganglia network are illustrated in Figure 1.1A.

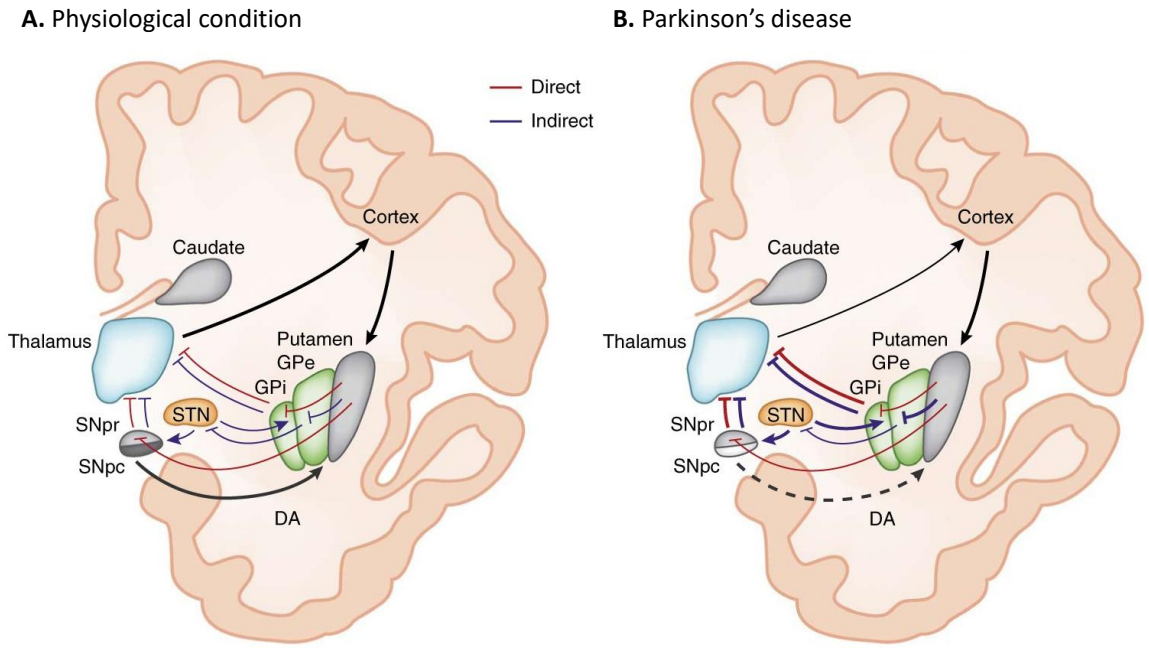


Figure 1.1 Schematic representation of basal ganglia circuitry in healthy conditions (A) and Parkinson's disease (B), adapted from Calabresi et al. (2014). Red pathways denote the direct pathway and blue pathways denote the indirect pathway. Arrowheads indicate excitatory projections, whereas T-heads indicate inhibitory projections. Line thickness qualitatively represents changes in pathway activity associated with dopamine depletion.

The corticostriatal pathway constitutes the main input pathway of the basal ganglia. Cortical activation excites striatal neurons, which subsequently modulate the activity of downstream nuclei through inhibitory GABAergic projections. Under normal physiological conditions, neurons of the GPi exert a tonic inhibitory influence on the thalamus. Since the thalamus projects excitatory signals to cortical motor areas, modulation of pallidal output directly influences motor cortical activity. Two major functional pathways can be distinguished within the basal ganglia circuitry:

- **Direct pathway**. Striatal neurons project directly to the GPi. Activation of this pathway inhibits GPi activity, thereby reducing its inhibitory influence on the thalamus. The resulting thalamic disinhibition increases excitatory feedback to the motor cortex and facilitates movement initiation and execution.
- **Indirect pathway**. Striatal neurons project to the GPe, which in turn modulates activity in the STN. The STN excites the GPi, increasing thalamic inhibition and consequently reducing cortical excitation. This pathway therefore suppresses competing or unwanted motor programs.

The coordinated regulation of movement depends on a finely balanced interaction between these two pathways. Within the striatum, medium spiny neurons expressing D1 dopamine receptors give rise primarily to the direct pathway, whereas neurons expressing D2 receptors contribute predominantly to the indirect pathway. Dopamine exerts opposing effects on these neuronal populations: it enhances activity in D1-expressing neurons while suppressing activity in D2-expressing neurons. Dopaminergic projections from the SNpc simultaneously facilitate the direct pathway and inhibit the indirect pathway, producing a net increase in thalamocortical excitation and promoting voluntary movement.

In PD, progressive degeneration of dopaminergic neurons within the SNpc disrupts this regulatory mechanism. The resulting dopamine depletion reduces activation of the direct pathway while simultaneously enhancing the influence of the indirect pathway. Consequently, inhibitory output from the GPi to the thalamus increases, reducing thalamocortical excitation and impairing the initiation and execution of voluntary movements (Figure 1.1B).

In addition to the GPi, the SNpr constitutes a major output nucleus of the basal ganglia. Similar to the GPi, the activity of the SNpr is regulated by the direct and indirect pathways of the basal ganglia, such that dopamine depletion in PD affects the output of both nuclei in a comparable manner. Like the GPi, the SNpr is composed predominantly of GABAergic neurons that exert tonic inhibitory control over several motor-related structures. Its projections target not only thalamic nuclei but also brainstem regions involved in motor control, particularly the superior colliculus and the pedunculopontine nucleus. Through these connections, the SNpr contributes to the regulation of eye movements, postural control, gait initiation, and orienting behaviors. In PD, increased activity of the SNpr resulting from dopamine depletion enhances inhibitory output toward these downstream targets. This excessive inhibition has been proposed to contribute to impaired movement initiation, oculomotor abnormalities, and gait disturbances, including freezing of gait (Calabresi et al. 2014).

One important extension of the classical model is the incorporation of the hyperdirect pathway, a monosynaptic projection from the cortex to the STN (Nambu et al. 2002). Through this pathway, cortical activity can rapidly influence basal ganglia output without first passing through the striatum. Activation of the hyperdirect pathway excites the STN, which in turn increases the inhibitory output of the GPi toward the thalamus. This mechanism is believed to provide a rapid and global suppression of competing motor programs, contributing to action selection and behavioral inhibition. STN excitation is also shaped by release of GPe-mediated inhibition. While direct and indirect pathways are often viewed as opposed responses to dopamine, the hyperdirect pathway highlights the complementary function of these two pathways in movement initiation and action selection.

While many symptoms arise directly from neuronal loss and dopamine depletion, increasing evidence suggests that motor dysfunction also reflects abnormal activity patterns and pathological synchronization within surviving neural networks (McGregor and Nelson, 2019). Dopamine depletion modifies the balance of activity within basal ganglia circuits, which in turn promotes the emergence of pathological oscillations and synchronized firing across the

network. Electrophysiological recordings in patients and animal models have discovered abnormally synchronized oscillatory activity at multiple levels of the basal ganglia–cortical loop (Hammond et al. 2007). In particular, PD is associated with excessive oscillatory activity in the beta frequency band ($13 - 30$ Hz) throughout the cortico-basal ganglia network. Elevated beta-band synchronization has been linked to impaired movement initiation, reduced movement vigor, and motor rigidity (Jenkinson and Brown, 2011).

1.1.2 Symptoms

The alterations in basal ganglia activity described above manifest clinically as a progressive spectrum of motor impairments. Bradykinesia, defined as a reduction in movement speed and amplitude, is considered the cardinal motor feature of Parkinson's disease. In severe cases, movement initiation may become extremely difficult, leading to episodes of akinesia (Fasano et al. 2022). These impairments are generally attributed to reduced facilitation of cortical motor areas resulting from dopamine depletion within basal ganglia circuits. Beyond movement execution, PD also affects motor preparation and automaticity (Redgrave et al. 2010). Patients typically exhibit prolonged reaction times and increased difficulty performing complex or sequential motor tasks. Activities that are largely automatic in healthy individuals often require conscious attention in PD, contributing to impaired dual-task performance and increased cognitive load during movement (Yogev et al. 2005). Interestingly, several studies have shown that externally triggered or visually guided movements may be relatively preserved compared with internally generated movements, suggesting that motor deficits arise not from a general inability to move but from impaired initiation and automatic control of movement (Redgrave et al. 2010).

Additional motor manifestations include resting tremor, muscular rigidity, and postural instability (defined as an inability to keep the body's center of mass controlled relative to the base of support) (Jankovic, 2008). Resting tremor typically occurs when the affected limb is relaxed and often decreases during voluntary movement. Rigidity reflects an abnormal increase in muscle tone and contributes to movement stiffness and discomfort. Postural instability emerges later in the disease course and is associated with impaired balance control and an increased risk of falls (Bloem et al. 2001). Gait dysfunction is among the most disabling manifestations of PD. Typical gait alterations include reduced walking speed, shorter stride length, increased gait variability, impaired interlimb coordination, and diminished movement automaticity (Mirelman et al. 2019). In advanced stages of the disease, some patients experience freezing of gait, a transient inability to initiate or continue walking despite the intention to move. Freezing of gait typically occurs during gait initiation, turning, or when navigating narrow spaces, and is a major contributor to falls and loss of independence (Nutt et al. 2011).

The progressive loss of neurons leads to a gradual worsening of symptoms over the course of the disease. Disease severity is commonly evaluated using the Hoehn & Yahr (H&Y) scale, which is based on motor dysfunction (Hoehn and Yahr, 1967). The scale ranges from stage 1, where symptoms are limited to one side of the body, to stage 5, where patients are confined to a wheelchair or bed. Intermediate stages reflect increasing bilateral involvement, the develop-

ment of postural instability, and the loss of functional independence. The revised version of the H&Y scale includes stages 1.5 and 2.5 to provide a more refined assessment of patients whose condition falls between the original categories (Goetz et al. 2004).

1.1.3 Current therapeutic approaches

Current interventions aim primarily to alleviate symptoms, improve functional mobility, and maintain quality of life, as no therapy has yet been shown to stop or reverse the degenerative process. Because clinical presentation and disease progression vary substantially across patients, treatment strategies must be individualized and are often adjusted throughout the course of the disease.

Pharmacological therapy remains the cornerstone of Parkinson's disease management. Most available medications seek to compensate for dopamine depletion within the basal ganglia or to enhance dopaminergic neurotransmission. One common treatment is levodopa (L-DOPA), a metabolic precursor of dopamine capable of crossing the blood-brain barrier. Once converted into dopamine within the central nervous system, levodopa partially restores dopaminergic signaling and improves many of the cardinal motor symptoms of PD, including bradykinesia, rigidity, and, to a lesser extent, tremor. Levodopa is typically administered in combination with a decarboxylase inhibitor to prevent it from being converted into dopamine before crossing the blood-brain barrier.

Additional pharmacological options include dopamine agonists, which directly stimulate dopamine receptors; monoamine oxidase B inhibitors, which reduce dopamine degradation; and catechol-*O*-methyltransferase inhibitors, which prolong the action of levodopa. These medications may be used alone during the early stages of the disease or in combination with levodopa as symptoms progress.

Although dopaminergic therapies often provide substantial symptomatic relief, their effectiveness tends to fluctuate over time. Long-term treatment is frequently associated with motor complications such as wearing-off phenomena and levodopa-induced dyskinesias (Salat and Tolosa, 2013). Furthermore, several symptoms, particularly postural instability, gait impairments, and freezing of gait, often become progressively less responsive to dopaminergic medication as the disease advances (Nutt et al. 2011).

For patients whose symptoms cannot be adequately controlled by medication alone, advanced therapeutic options may be considered. Deep Brain Stimulation (DBS) is currently the most widely used surgical treatment for Parkinson's disease. In this procedure, electrodes are implanted within deep brain structures, most commonly the STN or the GPi, and connected to a pulse generator implanted subcutaneously in the chest. DBS can substantially reduce motor symptoms and medication requirements in appropriately selected patients. Although the precise mechanisms remain incompletely understood, DBS is increasingly understood not simply as a modulation of firing rates but as an intervention capable of disrupting pathological

synchronization and restoring more physiological patterns of network activity (McGregor and Nelson, 2019).

Finally, pharmacological and surgical treatments are frequently complemented by rehabilitation programs aimed at preserving mobility, balance, and functional independence. In gait, numerous interventions have been proposed, including external cueing, aerobic exercises, resistance training, treadmill-based training and balance training (Osborne et al. 2022). Dance-based interventions combine several of these components, including cueing, aerobic and balance training, and have shown beneficial effects in people with Parkinson's disease (Earhart, 2009). More recently, robotic devices and technology-assisted rehabilitation approaches have been developed to provide intensive, repeatable, and task-specific training (Marchal-Crespo and Riener, 2018).

The persistence of gait impairments despite effective treatment of other motor symptoms highlights the complexity of locomotor control in Parkinson's disease and motivates continued research into the neural mechanisms underlying gait dysfunction and its rehabilitation.

1.2 Long-range autocorrelations in gait variability

The study of biological variability has progressively moved from focusing solely on the amount of variability to addressing both its magnitude and its temporal organization. Indeed, two signals can exhibit identical variability magnitudes while differing substantially in the way fluctuations are organized across time. In gait, Hausdorff, Peng, et al. (1995) first demonstrated that consecutive stride durations exhibit Long-Range Autocorrelation (LRA), also referred to as statistical persistence or fractal dynamics, during unconstrained walking. This means that each stride statistically depends on previous gait cycle, with this dependency extending over hundreds of strides. Such patterns have also been reported in heartbeat dynamics (Peng, Havlin, et al. 1995), respiration (Fadel et al. 2004), neural activity (Bédard et al. 2006) and finger tapping (Gilden et al. 1995), making this feature a recurring observation across numerous physiological and behavioral processes.

The interpretation of these fractal fluctuations remains an active area of research. According to complexity-based approaches, LRA may naturally emerge from interactions among the many components of the locomotor system operating across multiple temporal scales (Wagenmakers et al. 2004). Within this framework, fractal dynamics are often considered signatures of adaptability and healthy system organization. Consistent with this interpretation, alterations of LRA have been reported in several pathological conditions and have often been associated with reduced adaptability and increased fall risk (Hausdorff, 2007). In addition, this metric is also highly sensitive to context, as evidenced by its alteration in various conditions. However, the relationship between LRA and locomotor control remains incompletely understood. The following sections review the various interpretations proposed in the literature, drawing on studies of LRA in aging and pathology, experimentally constrained walking, and modeling approaches.

1.2.1 Impact of aging and disease

A substantial body of literature has shown that aging and neurological disorders altered both the magnitude and temporal organization of gait variability. Beyond simple increases in stride-to-stride variability, these populations often exhibit modifications in the structure of fluctuations. Those findings have contributed to the growing interest in nonlinear analyses of gait variability as potential markers of mobility decline, fall risk, and disease progression.

First, aging is generally associated with increased gait variability, which has been often interpreted as a loss of automaticity, reduced balance performance and increased fall risk (Beauchet et al. 2017; Herssens et al. 2018; Hollman, McDade, and Petersen, 2011; Malatesta et al. 2003). As older adults commonly adopt slower walking patterns and because walking at slower speeds increases gait variability in young adults, it was initially hypothesized that the greater variability observed in elderly individuals might simply result from reduced walking velocity. However, Kang and Dingwell (2008) showed that increased variability in aging was more strongly related to declines in muscle strength, flexibility, and sensorimotor function than to slower speed itself. In addition, increased variability in older adults does not necessarily imply an alteration of control strategies (Dingwell, Salinas, and Cusumano, 2017).

Conversely, the effect of aging on the fractal dynamics of stride variability is not entirely consistent across studies. Several authors observed reduced stride correlations in elderly individuals compared with healthy young adults (Hausdorff, Mitchell, et al. 1997; Kobsar et al. 2014), interpreting this alteration as evidence of impaired gait regulation. Subsequent studies confirmed that persistence tended to decrease with age, reporting significant alterations of LRA already observable in a group of adults between 40 and 60 years old (Chien et al. 2015). In contrast, other studies reported no significant differences in the temporal structure of variability between young adults and elderly (Dingwell, Salinas, and Cusumano, 2017; Kosse et al. 2016; Malatesta et al. 2003; Marmelat, Reynolds, and Hellman, 2018; Stout et al. 2016). In a systematic review, an overall decrease was reported, but with a modest effect size (Ravi et al. 2020).

To explain this discrepancy, some authors suggested that the alteration of fractal gait dynamics may depend on the functional status or physical activity of older individuals (Ducharme, Kent, and Van Emmerik, 2019; Stout et al. 2016). For example, highly active older adults exhibited more complex locomotor patterns than less active older adults, even in the absence of differences in the magnitude of variability (Cavanaugh et al. 2010; Hausdorff, Nelson, et al. 2001). It has also been shown that measures of LRA had promising ability to distinguish older fallers from non-fallers (Gonabadi et al. 2021; Hausdorff, 2007). Older adults who experienced past falls could use compensatory strategies aimed at enhancing safety and reducing the risk of falling, strategies which may influence the temporal organization of strides. In that sense, Herman et al. (2005) hypothesized that the scaling exponent may reflect the degree of voluntary gait control and cautiousness adopted during locomotion. Finally, changes in gait dynamics could also be an early sign for underlying pathology.

Indeed, gait variability alterations are generally more pronounced in several pathologies,

such as Parkinson's disease (PD). Compared with healthy controls, individuals with PD exhibit increased stride-to-stride variability together with weaker correlations in gait parameters (Frenkel-Toledo et al. 2005; Hausdorff, Ashkenazy, et al. 2001; Hausdorff, Cudkowicz, et al. 1998; Marmelat, Reynolds, and Hellman, 2018). Still, some studies reported no difference compared to age-matched subjects (Dotov, Bayard, et al. 2017; Ota et al. 2014), and a review published in 2020 indicated a moderate effect size and substantial heterogeneity (Ravi et al. 2020). Two main factors may account for these inconsistencies. First, heterogeneity within the PD population itself may play a role, as individuals in the early stages of the disease are often less affected. In this regard, reduced persistence has been associated with greater disease severity (Bartsch et al. 2007; Warlop, Detrembleur, Bollens, et al. 2016) and an increased risk of falling (Hausdorff, 2009), suggesting that fractal gait dynamics may capture clinically relevant aspects of locomotor dysfunction in PD. Second, methodological heterogeneity across studies, including differences in experimental paradigms and approaches used to quantify LRA, may also contribute to the variability in findings.

Similar alteration of LRA have been reported in Huntington's disease, which also involves basal ganglia dysfunction, although trough distinct pathological mechanisms (Hausdorff, Mitchell, et al. 1997). Therefore, the loss of LRA in PD has often been interpreted as reflecting impaired gait automaticity resulting from basal ganglia degeneration. Given the central role of the basal ganglia in the coordination and timing of sequential motor activity, their dysfunction may disrupt the temporal organization of locomotion. However, patients with advanced amyotrophic lateral sclerosis also exhibit diminished LRA despite relatively preserved basal ganglia function (Hausdorff, Lertratanakul, et al. 2000). In addition, temporal correlations of stride intervals appear largely preserved in individuals with peripheral neuropathy or multiple sclerosis, despite slower walking speeds and increased gait variability (Gates and Dingwell, 2007; Kaipust, Huisinga, et al. 2012; Lizrova Preiningerova et al. 2015). Together, this suggest that alterations in LRA cannot be explained solely by reduced gait speed, increased variability, or even basal ganglia dysfunction. Rather, they may reflect a more general deterioration of central neural mechanisms responsible for the temporal regulation and coordination of locomotion.

Overall, studies conducted in aging and pathological populations have substantially contributed to the interpretation of LRA in gait variability. Although the physiological mechanisms responsible for the emergence of LRA during healthy locomotion remain incompletely understood, converging evidence suggested that they reflected the integrity of neural processes involved in the regulation of gait. Altered LRA have been reported in several neurological disorders and were often associated with impaired automaticity, reduced adaptability, and increased fall risk. Importantly, changes in the magnitude of gait variability and changes in its temporal organization do not systematically occur together. Increased variability may be observed in the absence of altered LRA, whereas diminished LRA can emerge without an simultaneous increase in magnitude. This dissociation indicates that conventional variability measures and LRA capture different dimensions of gait control. In this context, the temporal organization of gait variability has been proposed as a distinctive marker of locomotor impairment across neurological disorders (Moon et al. 2016). Consistent with this view, Dierick et al. (2021) ar-

gued that nonlinear indices such as the fractal exponent provide information that complements traditional measures of variability and may improve the characterization of gait dysfunction in neurodegenerative diseases. Together, these findings highlight the potential of LRA analyses both as a tool for investigating gait regulation and as a clinically relevant marker of locomotor health.

1.2.2 Impact of contextual constraints

In addition to the impact of specific pathologies, several experimental studies have investigated how different walking contexts modulated the fractal structure of stride fluctuations. These analyses are particularly informative because they help clarify both the physiological meaning of LRA and the methodological factors that may influence their estimation in clinical settings. Importantly, the effects of these contextual constraints may differ between healthy adults and individuals with gait impairments, and some paradigms may (partially) restore a fractal pattern similar to that of healthy controls. Broadly, many findings suggested that gait dynamics vary according to the level of constraint imposed on locomotion, although the direction of these changes may depend on the specific nature of the constraint.

Walking speed constitutes one important factor of gait dynamics. In healthy young adults, walking at speeds different from preferred walking speed (PWS) has been associated with higher fractal exponents, following a U-shaped relationship with a minimum near PWS (Jordan et al. 2007). This observation is consistent with the idea that PWS corresponds to an energetically optimal and mechanically efficient locomotor state (Brisswalter and Mottet, 1996; Holt et al. 1991). Humans naturally select walking speeds that minimize metabolic cost and exploit the passive dynamics of the musculoskeletal system. Deviating from this optimal velocity may increase the demands imposed on locomotor regulation and thereby alter the temporal organization of gait variability. Similar quadratic relationships between speed and gait persistence have also been observed in older adults and this relationship appeared steeper than in young adults, suggesting a greater sensitivity to deviations from preferred speed (Chien et al. 2015).

Because treadmill walking is frequently used in experimental and clinical settings for practical reasons, its effects on gait dynamics should be also carefully considered. By imposing a constant external speed, the range of available motor solutions becomes more constrained on a treadmill, which potentially impacts gait regulation. In healthy young adults, average stride length, duration and velocity on treadmill are similar to those observed in overground walking, but the variability of these parameters is significantly reduced on the treadmill (Hollman, Watkins, et al. 2016). In contrast, the level of LRA in series of stride duration is not affected by the treadmill in this population (Bollens, Crevecoeur, Nguyen, et al. 2010), provided that the walker do not rely on the handrails (Chang et al. 2009). Indeed, using handrails has been associated with increased persistence compared with unsupported treadmill or overground walking. Mechanical stabilization through upper-limb support may reduce postural demands and permit looser control of stepping dynamics, thereby increasing temporal correlations between strides. However, this interpretation contrasts with findings showing increased persistence

under destabilizing conditions such as non-preferred walking speeds. In addition, treadmill walking has been associated with anti-persistence in stride-to-stride fluctuations of stride velocity (Dingwell, John, and Cusumano, 2010; Terrier and Dériaz, 2012), whereas overground walking tends to preserve persistent dynamics in these same time series (Terrier, Turner, and Schutz, 2005). Moreover, a clear association between the degree of attentional focus on gait and the anti-persistence observed in stride velocity has been evidence by Decker et al. (2013).

The effects of treadmill walking on gait variability differ in patients with Parkinson's disease compared to healthy young adults. In patients, treadmill walking has been shown to increase gait variability, further exacerbating the increased variability associated with the disease, but also increase gait complexity, partially restoring patterns similar to that of healthy young adults (Hollman, Von Arb, et al. 2020; Warlop, Detrembleur, Stoquart, et al. 2018). Several hypotheses were raised to explain this effect. Patients could take advantage of the hip extension, the constant gait speed or the absence of visual flow on the treadmill (Bello and Fernandez-Del-Olmo, 2012). Sensory inputs from the treadmill could also provide the necessary trigger to maintain some gait rhythmicity and overcome the defective internal rhythm of the basal ganglia disorders (Van Wegen et al. 2006). In this way, the fixed timing of leg movements could reduce the regulatory load on defective areas, allowing relative adaptations of gait parameters (Frenkel-Toledo et al. 2005; Nanhoe-Mahabier et al. 2011).

Additional experimental manipulations reinforced the idea that increasing task constraints modifies gait complexity. Forced marching and load carriage, for example, reduce gait variability and alter LRA, leading to more tightly regulated stepping patterns (Krajewski et al. 2020). Under increased mechanical constraints, a more restricted workspace of gait parameters is available to achieve successful locomotion and strides therefore become more tightly controlled and less adaptable. Similarly, turning tasks has been shown to affect gait correlation structures, likely because they require additional anticipatory and postural adjustments (Dotov, Bardy, and Dalla Bella, 2016). Finally, attentional and cognitive demands may also influence gait dynamics. Nevertheless, the extent and nature of this influence remain unclear, as studies on dual tasking have produced heterogeneous and sometimes contradictory results (Bollens, Crevecoeur, Detrembleur, et al. 2014; Lamoth et al. 2011; Sejdić, Findlay, et al. 2013; Yano et al. 2024). This heterogeneity may partly arise from differences in experimental paradigms, including the nature of the secondary task (cognitive versus motor), walking conditions (overground versus treadmill walking, with or without visual flow), and task difficulty.

Taken together, these findings suggest that long-range autocorrelations are not fixed properties of locomotion but emerge from the interaction between the individual and the constraints imposed by the task and environment. Changes in walking speed, mechanical support, treadmill walking, load carriage, turning, or cognitive demands all modify the temporal organization of stride fluctuations, indicating that LRA are sensitive to the strategies used to regulate gait. Importantly, these manipulations do not affect gait dynamics in a uniform manner: some constraints appear to increase persistence whereas others reduce it, and the effects may differ between healthy individuals and clinical populations. This interpretation is consistent with the theoretical framework proposed by Stergiou, Harbourne, and Cavanaugh (2006), who argued

that healthy biological systems operate in an intermediate state between excessive order and excessive randomness. Within this perspective, movement variability exhibits a complex structure that reflects the system's ability to adapt to changing internal and external constraints. Building on this concept, Stergiou and Decker (2011) proposed the Optimal Movement Variability framework, according to which both overly regular and overly random movement patterns may indicate reduced adaptability.

1.2.3 Synchronization with rhythmic cues

Among the various contextual constraints that influence gait variability, rhythmic cueing represents one of the most impactful manipulations of gait dynamics. Numerous studies have demonstrated beneficial effects of rhythmic cueing on gait performance in Parkinson's disease. Auditory cueing has been shown to improve gait speed, stride length and cadence, while reducing stride-to-stride variability (Lim et al. 2005; Spaulding et al. 2013). Similar benefits have also been reported in other populations presenting gait impairments, including stroke, multiple sclerosis, and orthopedic patients (Ghai and Ghai, 2018; Ghai and Ghai, 2019; Thaut, McIntosh, and Rice, 1997).

Despite these beneficial effects, rhythmic cueing substantially alters the temporal organization of gait variability. Several studies have shown that synchronizing gait to an isochronous metronome converted persistent stride duration fluctuations into anti-persistent dynamics across all populations (Delignières and Torre, 2009; Jordão et al. 2022; Kaipust, McGrath, et al. 2013; Marmelat, Torre, et al. 2014; Sejdić, Fu, et al. 2012; Terrier and Dériaz, 2012; Vaz, Groff, et al. 2019), a phenomenon also reminiscent of the effects observed on stride velocity under treadmill walking. When treadmill walking and rhythmic cueing are combined, stride length time series also exhibit anti-persistent dynamics (Terrier and Dériaz, 2012). In contrast to statistical persistence, which indicates that deviations from the mean are statistically more likely to be followed by deviations in the same direction, anti-persistence means that deviations in one direction are statistically more likely to be followed by deviations in the opposite direction. Thus, the changes induced by rhythmic cues are though to represent a fundamental reorganization of locomotor control rather than a simple alteration of gait variability.

Assuming that this change in variability structure would be an unwanted side effect, several authors have proposed to introduce variability, whether random or with a fractal structure, into the external rhythm to mimic the variability observed in healthy locomotion (Hunt et al. 2014; Lheureux et al. 2020). Several studies indicated that those type of cues can maintain the beneficial effects of synchronization while restoring, at least partially, statistical persistence in gait fluctuations in healthy older adults and in individuals with Parkinson's disease (Hove et al. 2012; Rhea et al. 2014; Vaz, Knarr, and Stergiou, 2020).

Adaptive cueing systems have also recently emerged. These systems continuously adjust cue characteristics in real time according to ongoing gait performance, thereby accommodating natural fluctuations in motor capacity and potentially reducing habituation and dependency

to the stimulus (Ginis et al. 2018; Mancini et al. 2018). Music-based cueing constitutes another alternative to simple metronomic stimulation. In addition to providing rhythmic information, music may increase motivation, enjoyment, and adherence to training programs while eliciting gait improvements comparable to those observed with metronome cueing (Braun Janzen et al. 2022). In addition, music naturally have a more complex structure than isochronous cues, and have therefore less impact on LRA (Moumdjian, Maes, et al. 2020; Sowalsky et al. 2026).

Cueing interventions can also differ according to the gait parameter being targeted. Whereas auditory metronomes primarily act on cadence, visual stepping targets such as floor markers mainly encourage modulation of stride length (Azulay et al. 2006; Spaulding et al. 2013; Terrier, 2016). Whether based on cadence or stride length, in addition to restoring rhythm, cues can encourage a faster pace and longer strides by setting targets that are more challenging than natural gait parameters. Moreover, significantly higher LRA have been observed when walking at higher tempi (Moumdjian, Maes, et al. 2020).

Another important dimension concerns cueing modality as auditory, visual, and tactile cues have all been employed successfully, either alone or in combination. Auditory cues are typically delivered through rhythmic stimuli such as a metronome, visual cueing through external visual targets (Spaulding et al. 2013), and tactile cueing through rhythmic vibrotactile stimulation, including wrist vibration (Van Wegen et al. 2006). Auditory cueing remains the most extensively studied approach, but multimodal cueing may enhance effectiveness by engaging complementary sensory pathways (Ginis et al. 2018). A distinction can also be made between external and internal cueing strategies. Internal cueing strategies, counting silently, has also been shown to improve some gait parameters such as stride time varaibility, stride length and gait speed (Tosserams, Keijsers, et al. 2022). Although external cues generally produce larger immediate effects in Parkinson's disease, internal cueing approaches may promote greater autonomy and transfer to everyday locomotion (Haussler et al. 2026; Rochester et al. 2011).

Finally, interpersonal synchronization has recently emerged as an alternative form of cueing. Rather than synchronizing with an artificial external signal, individuals coordinate their movements with those of another person. This approach has been shown to restore LRA in gait fluctuations in healthy older adults and may provide a more ecologically valid means of promoting adaptive locomotor control (Almurad, Roume, Blain, and Delignières, 2018; Almurad, Roume, and Delignières, 2017; Ezzina et al. 2025).

In summary, rhythmic cueing encompasses a wide range of intervention designs, each of them offering specific advantages and limitations with respect to gait performance and user engagement. Beyond their clinical applications, these cueing paradigms have provided important insights into the interpretation of LRA in gait variability. The observation that more rigid and predictable cueing structures tend to induce anti-persistent dynamics, particularly in the gait variable directly constrained by the cue, supports the view that LRA reflect underlying control processes. Cueing is generally thought to shift locomotor control from internally generated and relatively automatic regulation toward externally guided, attentionally mediated control. In Parkinson's disease, cues may compensate for impaired basal ganglia function by

recruiting alternative cortical and cerebellar networks involved in sensorimotor synchronization (Grahn and Brett, 2007; Tosserams, Weerdesteyn, et al. 2022). The resulting anti-persistent fluctuations have therefore been interpreted as signatures of enhanced stride-to-stride error correction and tighter voluntary regulation of gait timing. Many studies are still underway to improve our understanding of neural and biomechanical mechanisms behind the use of cues in rehabilitation setting (Albers et al. 2026). In this context, because different cueing designs exert distinct effects on gait temporal structure, measures of LRA could be a valuable tool for probing the mechanisms underlying gait control.

1.2.4 Modeling approach

Several models have been proposed over the years to interpret the presence of persistence in stride-to-stride variability during free walking and its alteration in various pathologies and contexts. These modeling efforts complement clinical and behavioral findings presented in Section 1.2.1 and 1.2.2 by providing mechanistic hypotheses about the origin of statistical persistence. In particular, an ongoing debate revolves around whether LRA primarily emerges from supra-spinal neural dynamics, from spinal and peripheral pattern-generating circuits, or from biomechanical and task-level interactions within the musculoskeletal system.

One of the earliest frameworks proposed to explain the presence of LRA in gait variability originated from Hausdorff, Peng, et al. (1995), which both demonstrated the presence of LRA in gait and introduced a modeling approach to account for these observations. Further developments of this framework later culminated in the Super Central Pattern Generator (SCPG) model. Central Pattern Generators (CPGs) are neural circuits capable of producing rhythmic output in the absence of rhythmic input, and are widely considered a foundational component of locomotor control. SCPG model extends this concept by embedding stochastic structure into the parameters governing oscillatory activity, thereby aiming to reproduce the statistical properties of stride interval fluctuations observed experimentally.

The basic building block of these models is a nonlinear oscillator producing periodic output, whose intrinsic frequency varies over time. Early attempts to generate stride series with LRA include the *noisy CPG model* introduced by Hausdorff, Peng, et al. (1995). In this formulation, the oscillator frequency is perturbed at each stride by uncorrelated Gaussian noise around a fixed mean value. Although this model reproduces short-term variability, it fails to generate the observed scale-invariant correlation structure of human gait. In the same work, the authors proposed an alternative formulation, the *correlated CPG model*, in which frequency fluctuations are no longer independent but follow a structured stochastic process. In this case, only certain transitions between discrete frequency states are allowed, with specified transition probabilities, effectively introducing memory into the system. However, while this approach successfully reproduces persistence in free walking, it does not explicitly address how pathological conditions or aging modify the correlation structure.

This limitation was partially addressed by the *Neural Hopping Model* introduced by Ashkenazy et al. (2002). In this framework, the system is conceptualized as a random walk over a

discrete set of neural centers, each associated with a characteristic intrinsic frequency. At each stride, the system "hops" from one neural center to another, with jump sizes drawn from a Gaussian distribution with standard deviation σ. This parameter plays a critical role in shaping the temporal structure of variability: larger values of σ allow broader exploration of the neural state space, thereby increasing the degree of long-range dependence in the resulting stride interval series. Conversely, smaller values lead to more localized transitions and reduced persistence. A small additive noise term was also included at each selected node to capture intra-state variability.

A further development was proposed by West and Scafetta (2003). This formulation coupled a stochastic generator of intrinsic frequencies to a non-linear Van der Pol oscillator, which acts as a biomechanical proxy for lower limb dynamics. The key distinction of this approach is that the stochastic process does not directly generate stride intervals. Instead, it drives the parameters of a nonlinear dynamical system whose output represents gait kinematics. In this sense, the model separated neural timing variability from biomechanical execution. The sequence of frequencies generated by the correlated CPG was used as a forcing input to the oscillator, and the resulting output exhibited a fractal pattern under appropriate parameter regimes. This new version also allowed to reproduce the fractal properties of gait under several conditions, i.e., at slow, normal and fast speeds, and while following the rhythm of a metronome.

While the SCPG provided an interpretation involving supra-spinal and spinal structures, alternative hypotheses have proposed that statistical persistence may emerge from biomechanical and task-level interactions. The approach of Gates, Su, and Dingwell (2007) was based on a simplified 2D model of passive dynamic walking (Garcia et al. 1998). The system consisted of a two-legged mechanism with point masses located at the feet and hip. To sustain locomotion, an impulsive push-off force was applied at each step to compensate for energy losses. This force was subject to both motor and sensory noise and was modulated by a proportional feedback controller. Importantly, stride-to-stride variability arose not from neural timing fluctuations, but from the interaction between stochastic actuation and feedback stabilization within the mechanical system. By varying noise amplitude and feedback gain, the model reproduced a range of correlation structures, including both persistent and weakly correlated dynamics. The authors therefore demonstrated that complex central nervous system control mechanisms are not required to generate persistent gait dynamics. They nevertheless emphasized that the interaction between biomechanical and neural control processes warrants further investigation.

Indeed, converging evidence indicates that supra-spinal control plays a crucial role in shaping the temporal structure of gait variability, given the impact of several contextual constraints and neurological disorders. In light of these limitations, Dingwell, John, and Cusumano (2010) proposed a more abstract formulation based on optimal control, in which locomotor output is represented as time series of stride durations and stride lengths. Within this framework, stride-to-stride variability is interpreted as the byproduct of error correction processes, with a controller primarily regulating task-relevant variables. During treadmill walking, humans do not systematically correct deviations in stride duration and length, as these parameters are not directly relevant to the main task goal, namely maintaining a constant walking speed. As

a result, errors are allowed to *persist*. In contrast, the model predicted that over-correction of deviations in stride speed induced slight anti-persistence in stride velocity time series, which was observable in empirical data. Taken together, this formulation implies that the structure of LRA is fundamentally determined by the nature and strength of the corrective mechanisms applied. This idea forms a central motivation for the present thesis. In particular, the flexibility of the stochastic optimal control framework, and its potential to account for diverse task constraints within a unified formulation, motivates its use as the principal modeling approach adopted herein.

1.3 Aim of this work

The overarching aim of this thesis is to investigate how gait regulation shapes the temporal organization of stride-to-stride fluctuations and to determine what information these fluctuations can provide about locomotor control in both healthy individuals and patients with Parkinson's disease. A central hypothesis, based on the work of Dingwell, John, and Cusumano (2010) is that the temporal structure of gait variability emerges from the selective and coordinated regulation of gait parameters on a stride-by-stride basis. In this context, alterations in control strategies would be reflected in changes in variability patterns.

Before presenting the original contributions of this thesis, a dedicated methodological chapter introduces the mathematical concepts and analytical tools used throughout this work to characterize the temporal structure of gait variability. This chapter provides a formal definition of long-range autocorrelations, reviews their fundamental properties, and discusses the methodological approaches available for their quantification.

In Chapter 3, we first examine the alteration of gait variability in Parkinson's disease. We use simulations to explore how changes in stride-to-stride regulation influence the emergence of LRA, while also examining the potential effects of robotic gait assistance on these dynamics. In particular, Chapter 3 addresses the following research questions:

Can the framework proposed by Dingwell, John, and Cusumano (2010) account for the alterations in gait variability observed in Parkinson's disease, and could robotic assistance help restore healthy patterns of variability ?

Building on the premise that LRA reflects ongoing gait regulation, Chapter 4 extend the model to reproduce the anti-persistent pattern observed when walking with rhythmic cues. By studying transitions between self-paced walking and synchronization with an isochronous metronome, we characterize the dynamics through which healthy individuals adapt their control policies to changing task demands. Because LRA are typically estimated over relatively long time scales, direct observation of these adaptation processes is inherently limited in temporal resolution, and the model offers a way to test different hypotheses regarding the evolution of control parameters at a finer time scale than experimental observation alone allows. These analyses allow us to investigate the following question:

How does the temporal structure of gait variability evolve when healthy individuals transition between self-paced and externally cued walking, and what can this reveal about the underlying dynamics of gait control adjustments?

Together, the first two chapters point to three distinct regulatory strategies. Chapter 5 explore whether geometric characterization of stride-by-stride adjustments, derived from the interpretation of the model, can provide a complementary and potentially more practical assessment of gait regulation than conventional measures of LRA. The question behind this idea is the following:

Can geometric indicators of stride-by-stride adjustments reliably distinguish between different gait regulatory strategies, and do they offer a robust alternative to conventional LRA measures for shorter, clinically relevant recordings?

Finally, in Chapter 6, we apply the methodological framework developed in Chapter 4 to investigate the ability to modulate gait regulation in Parkinson's disease. Building on contemporary theories of motor control, which propose that the basal ganglia contribute to the estimation of motor costs and rewards underlying movement selection, we hypothesize that basal ganglia dysfunction in PD could impair the ability to efficiently modulate gait control policies when task demands change. To test this hypothesis, we examine transitions between free walking and synchronization with rhythmic auditory cues and compare the dynamics of these adjustments with those observed in healthy controls. By leveraging the high sensitivity of LRA to the regulatory changes induced by rhythmic cueing, we use their evolution during transitions as a window into the mechanisms responsible for adjusting gait control to changing task demands. This chapter thus aims to provide new insights into the neural mechanisms underlying behavioral flexibility and the contribution of the basal ganglia to the modulation of locomotor control. Overall, this chapter addresses the following questions:

Is the ability to modulate gait control policies in response to changing task demands impaired in Parkinson's disease, and could this impairment reflect basal ganglia dysfunction in the estimation of motor costs and rewards?

Finally, Chapter 7 concludes this thesis with a general discussion that synthesizes the main contributions of the preceding chapters and revisits the research questions outlined above in light of the results obtained, discussing to what extent each has been addressed and where open issues remain. This chapter also outlines potential extensions of the proposed framework and directions for future research.

1.4 Publications and communications

Published

- **Otlet V., Vandamme C., Warlop T., Crevecoeur F., and Ronsse R.** Effects of overground gait training assisted by a wearable exoskeleton in patients with Parkinson's disease. *Journal of neuroengineering and rehabilitation* 20(1), 156, 2023.

- **Vandamme C., Otlet V., Ronsse R., and Crevecoeur F.** Model of gait control in Parkinson's disease and prediction of robotic assistance. *IEEE Transactions on Neural Systems and Rehabilitation Engineering* 31, 1374-1383, 2023.

- **Vandamme C., Otlet V., Ronsse R., and Crevecoeur F.** Measured and modeled transitions between self-paced walking and synchronization with rhythmic auditory cues. *Journal of Neurophysiology* 134(6), 1939-1952, 2025.

In preparation

- **Vandamme C.*, Doyen A.*, De Comité A., Warlop T., Ronsse R., Lefèvre P., and Crevecoeur F** Preserved behavioral flexibility during locomotion and reaching in Parkinson's disease
**equal contribution*

- **Vandamme C., Ronsse R., and Crevecoeur F.** Assessing gait control from short time series using a geometric characterization of stride-by-stride corrections

Proceedings

- **Vandamme C., Otlet V., Ronsse R., and Crevecoeur F.** Model of gait control in Parkinson's disease and prediction of robotic assistance. *Annual meeting of the Neural Control of Movement Society*, Dublin, 2022 [Poster]

- **Vandamme C., Otlet V., Ronsse R., and Crevecoeur F.** Flexible and rapid modulation of gait control assessed by long-range autocorrelations. 52*nd Annual Meeting of the Society fro Neurosciences*, Whashington, DC, 2023 [Poster]

- **Vandamme C., Otlet V., Ronsse R., and Crevecoeur F.** Flexible and rapid modulation of gait control assessed by long-range autocorrelations. *Annual meeting of the Neural Control of Movement Society*, Dubrovnik, 2024 [Poster]

- **Vandamme C., Otlet V., Ronsse R., and Crevecoeur F.** Modulation of gait control under metronomic constraints assessed by long-range autocorrelations in healthy population and in Parkinson's disease. *International Society for Posture and Gait Research World Congress*, Maastricht, 2025 [Poster]

2

Long-Range Autocorrelations: Mathematical foundations

As introduced in Chapter 1, series of stride durations and length exhibit long-range autocorrelations (LRA). Long-range autocorrelations are potentially important for fundamental research, as the neural and biomechanical mechanisms generating these correlations remain unknown. This property is also of particular interest due to its clinical implications, notably its association with fall risk and disease progression. This chapter sets out the formal definition of LRA and their properties. On this basis, the methodological aspects related to the analysis of LRA will be discussed.

2.1 Definition

Consider a centered, stationary time series x_n, of mean $\mu = 0$ and constant variance σ^2. The autocorrelation function $C(\tau)$ is defined as:

$$C(\tau) = Corr(x_n, x_{n+\tau}), \tag{2.1}$$

which corresponds to the correlation between two samples separated by a time lag τ. A process is said to exhibit long-range dependence (or long memory) if its autocorrelation function decays asymptotically as a power law:

$$C(\tau) \sim \tau^{-\beta}, \quad \text{as } \tau \to \infty, \quad \text{with } 0 < \beta < 1. \tag{2.2}$$

This type of autocorrelation function is illustrated in Fig. 2.1, for three different β parameters (orange traces). In this case, the process memory, defined as the sum of $C(\tau)$, is infinite, hence the term *long-memory process*. This slow, power-law decay is the hallmark of long-range dependence. It implies that correlations persist over large time scales: each observation remains statistically dependent on distant past values, with a strength that gradually decreases as the temporal distance increases. Smaller values of β correspond to a slower decay and thus

stronger persistence.

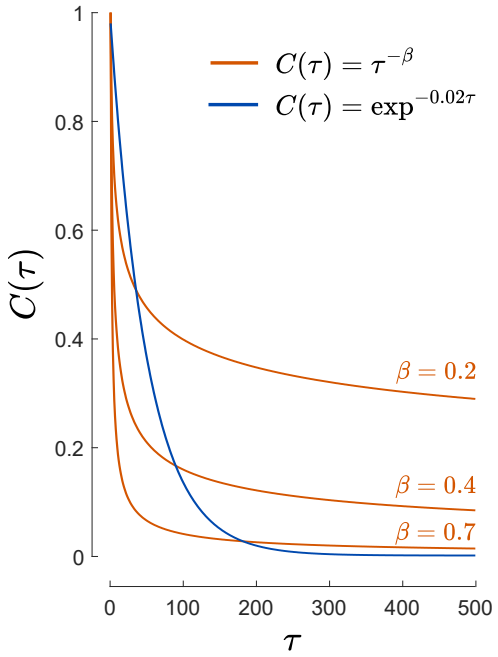


Figure 2.1 Example of autocorrelation functions characterizing processes exhibiting long-range autocorrelation (orange traces) and short-range autocorrelation (blue traces).

In contrast, in short-memory processes (typically $\beta > 1$, or exponential decay, corresponding to the blue trace in Fig. 2.1), a fixed number of preceding values influence the next value in the time series. These processes may exhibit local persistence, but its correlations vanish rapidly and do not extend over long time scales. Consequently, the sum of the autocorrelation function converges to a finite value.

In this context, it is therefore useful to distinguish between *persistence* as a qualitative notion and long-range autocorrelation as a precise mathematical property. Persistence refers to the tendency of a signal to maintain its behavior: large values tend to be followed by large values, and small values by small ones, resulting in "visible" clustering or trends. Long-range autocorrelation, on the other hand, specifies *how* correlations decay across time lags. Whilst long-range dependence induces persistence, persistence alone does not necessarily imply long-range structure.

2.2 Self-similarity and fractal structure

Long-range autocorrelated processes are closely related to the concept of fractals (Mandelbrot, 1967). A fractal object possesses the property of self-similarity, meaning that it is composed of an infinitely repeating pattern across several geometric scales. This concept of self-similarity is extended to time series, calling the latter a self-affine time series (Mandelbrot and Van Ness, 1968). In a self-affine series, the patterns of fluctuations at faster time scales mimics the pat-

terns of fluctuations at slower time scales, with a scaling factor. Intuitively, smaller time scales of the time series resemble the whole series. Due to this absence of a characteristic time scale, long-range correlated signals are therefore frequently described as exhibiting fractal or scale-free organization.

Building on this property, *fractional Brownian motion (fBm)* is one of the canonical models used to represent long-range autocorrelated processes (Mandelbrot and Van Ness, 1968). It is characterized by the Hurst exponent H. Its increments form a stationary process called *fractional Gaussian noise (fGn)* whose autocorelation function behaves like $Cov(\tau) \sim \tau^{2H-2}$. We have therefore the relationship $2H - 2 = -\beta$, with $H = 0.5$ meaning that the process is uncorrelated, $0.5 < H < 1$ implying long-range correlations and $0 < H < 0.5$ long-range anticorrelations. The Hurst exponent also governs the scaling of fluctuations across time scales. Mathematically, a fBm is characterized by the following scaling law :

$$\langle x^2 \rangle \sim \Delta\tau^{2H}, \tag{2.3}$$

which means that the expected squared displacement is power function of the time interval ($\Delta\tau$) over which it was observed (Delignières, Ramdani, et al. 2006).

2.3 Spectral representation

A key property of long-range dependent processes can be derived from the Wiener-Kintchine theorem, which states that the power spectral density of a time series is the Fourier transform of its auto-correlation function (Papoulis and Pillai, 2002). Consequently, the Power Spectral Density (PSD) $S(f)$ of long-memory processes scales asymptotically as a power law :

$$S(f) \sim f^{-\alpha} \text{ as } f \to 0, \tag{2.4}$$

with (Rangarajan and Ding, 2000):

$$\alpha = 1 - \beta \quad \text{and} \quad \alpha = 2H - 1. \tag{2.5}$$

Thus, long-range dependence manifests as increased power at low frequencies, often referred to as $1/f^{\alpha}$ noise. This provides a frequency-domain characterization equivalent to the time-domain definition.

2.4 Methods to assess LRA in a time series

Numerous methods have been described in the literature to assess whether a given time series exhibits long-range autocorrelations, and, if appropriate, to provide an estimate of the scaling parameter β (or equivalently, α or H) . This can be particularly challenging as the mathematical properties of such processes are asymptotic, whereas real-world data are finite and noisy. This section reviews commonly used methods.

2.4.1 Frequency domain method

As explained above, the PSD of long-range autocorrelated processes scales as a power-law (Eq. 2.4). Therefore, a rapid analysis of the PSD of the time series under study provides an estimate of the α exponent. The PSD is first computed as $S(f) = |X(f)|^2$, with $X(f)$ the Fourier transform of the series x_n. From Equation 2.4, we have :

$$\log S(f) \sim -\alpha \log f \tag{2.6}$$

The slope of the linear regression between $\log S(f)$ and $\log f$ gives the parameter $-\alpha = \beta - 1$. This method presents the advantage to be computationally cheap but does not prevent misleading conclusions about the presence of LRA, in particular if the parameters used to calculate the PSD (window type, smoothing) are inappropriate (Rangarajan and Ding, 2000). In this line of though, (Eke et al. 2000) and (Roume et al. 2019) proposed an improved version of this algorithm, adding some pre-processing to diminish the emphasis on the data at its ends, and excluding high-frequencies from the linear regression estimate.

2.4.2 Time domain methods

Other methods have been developed to estimate LRA from the self-similarity properties of fBm (see Section 2.2). These approaches rely on the way a measure of variability scales with the size of the time window over which it is computed. The scaling relationship provides an estimate of the Hurst exponent, H, which characterizes the self-similarity of the signal.

Rescaled Range Analysis (RRA) Originally introduced by Hurst (1951) and later adapted by Bassingthwaighte and Raymond (1994), RRA is one of the earliest methods developed to estimate scaling exponents. The method begins by partitioning the time series into non-overlapping intervals of length w. Within each interval, the series is integrated, and the range R of the resulting integrated series is calculated. This range is then normalized by the corresponding standard deviation S, yielding the rescaled range R/S. The rescaled ranges are averaged across all intervals of size w. This procedure is repeated for multiple interval lengths, typically ranging from 4 to $N/4$, where N denotes the total length of the time series. The Hurst exponent is estimated as the slope of the linear relationship between $\log(R/S)$ and $\log(w)$. In a refined version proposed by Caccia et al. (1997), a linear or higher-order polynomial trend is fitted to the integrated series within each interval, and the rescaled range R/S is computed from the resulting residuals.

Detrended Fluctuation Analysis (DFA) Introduced by Peng, Buldyrev, et al. (1994), DFA is currently the most widely used method for estimating scaling exponent. Compared to RRA, the time series is first integrated then divided into non-overlapping intervals of length w. Within each interval, a linear (or higher-order polynomial) trend is fitted, as illustrated in Fig. 2.2A for $w = 75$. The trends over all intervals are subtracted and the root-mean-square fluctuation $F(w)$ of the resulting residuals is calculated. The procedure is repeated for different interval sizes,

and the scaling exponent is estimated as the slope of the linear relationship between $\log F(w)$ and $\log w$.

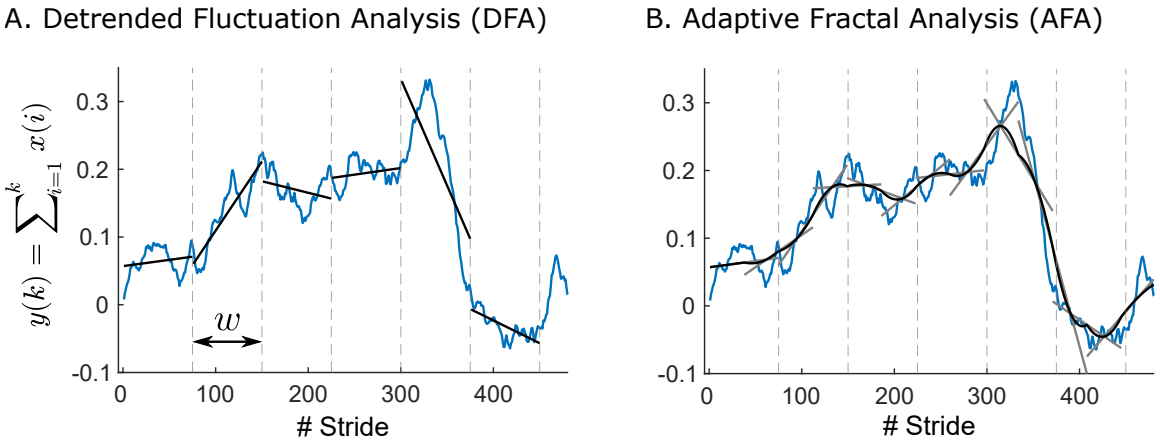


Figure 2.2 Detrending process for a window size of 75 strides in Detrended Fluctuation Analysis (A) and in Adaptive Fractal Analysis (B). The integrated series under study is shown in blue, and the identified trend is shown in black. In AFA, an intermediate local detrending is shown in gray.

Adaptive Fractal Analysis (AFA) AFA (Gao, Hu, and Tung, 2011; Riley et al. 2012) is a more recent approach, that has been recommended because of its reduced sensitivity to non-stationarities and improved robustness for shorter time series (Hollman, Lee, et al. 2022). For these reasons, AFA was selected for the present work and is described in detail below.

As in DFA, the first step consists of integrating the signal to construct a random-walk representation:

$$y(k) = \sum_{i=1}^{k} (x(i) - \bar{x}) \tag{2.7}$$

Unlike DFA, which relies on independent local detrending procedures, AFA constructs a continuous global trend function, denoted u^c and illustrated in Fig. 2.2B. To do so, local linear fits u^i are first estimated over overlapping windows at different time scales. For a given window size $w = 2n + 1$, adjacent windows overlap by $n + 1$ points. Within the overlap region, the global trend is obtained as a weighted average of two neighboring local fits :

$$u(l) = \omega_1 u^i(l + n) + \omega_2 u^{i+1}(l) \quad \text{with } l = 1, 2, 3, ..., n + 1 \tag{2.8}$$

where:

$$\omega_1 = (1 - \frac{l-1}{n}), \qquad \omega_2 = (\frac{l-1}{n}) \tag{2.9}$$

According to this scheme, the weights vary linearly with the distance from the center of the neighboring segments, ensuring continuity at the boundaries between adjacent regions. The resulting global trend is shown in black in Fig. 2.2B. Once this trend has been estimated, the

fluctuation function is computed as:

$$F(w) = \sqrt{\frac{1}{N}\sum_{k=1}^{N}(y(k) - u^c(k))^2} \tag{2.10}$$

This procedure is repeated for window sizes ranging from 11 to $N/2$. Because the fluctuation function follows the scaling relation:

$$F(w) \sim w^H, \tag{2.11}$$

the Hurst exponent is estimated as the slope of the linear relationship between $\log F(w)$ and $\log w$ across the analyzed scales.

2.4.3 Evenly-spacing

In the conventional implementation of RRA, DFA and AFA, the use of a logarithmic scale results in an over-representation of larger timescales in the linear regression (Fig. 2.3A). In addition, this region presents more variability around the linear trend, because the fluctuation function is computed from a smaller number of intervals. In order to increase the accuracy of DFA, Almurad and Delignières (2016) introduced the concept of evenly-spacing. The method remains essentially the same, but differs in the choice of interval sizes to ensure a linear spacing in the diffusion plot. In practice, the logarithmic x-axis is divided into k bins of equal width b:

$$b = \frac{1}{k}\log\frac{w_{max}}{w_{min}} \tag{2.12}$$

The fluctuation function $F(w)$ is first computed for all window sizes w ranging from w_{min} to w_{max}. Then, within each bin, the average values of $\log w$ $\log F(w)$ are computed, yielding k evenly spaced points from which the scaling exponent is estimated. This is illustrated in Fig. 2.3B, where the green dot corresponds to the average of all values contained within the green region in Fig. 2.3A. The method was initially applied to DFA but generalizes to all methods exploiting power laws, including PSD analysis, RRA and AFA.

2.4.4 Integrated methods

A limitation of individual methods is that they estimate scaling exponents without formally testing for the presence of long-range dependence. Indeed, Rangarajan and Ding (2000) have shown that RRA and PSD analyses, when used independently, may lead to the erroneous conclusion that a time series exhibits long-range dependence. To address this issue, an integrated approach was introduced by Rangarajan and Ding (2000) and later validated on physiological time series by Crevecoeur et al. (2010). This framework combines estimates obtained from multiple domains using this relationship :

$$H = \frac{1+\alpha}{2} \tag{2.13}$$

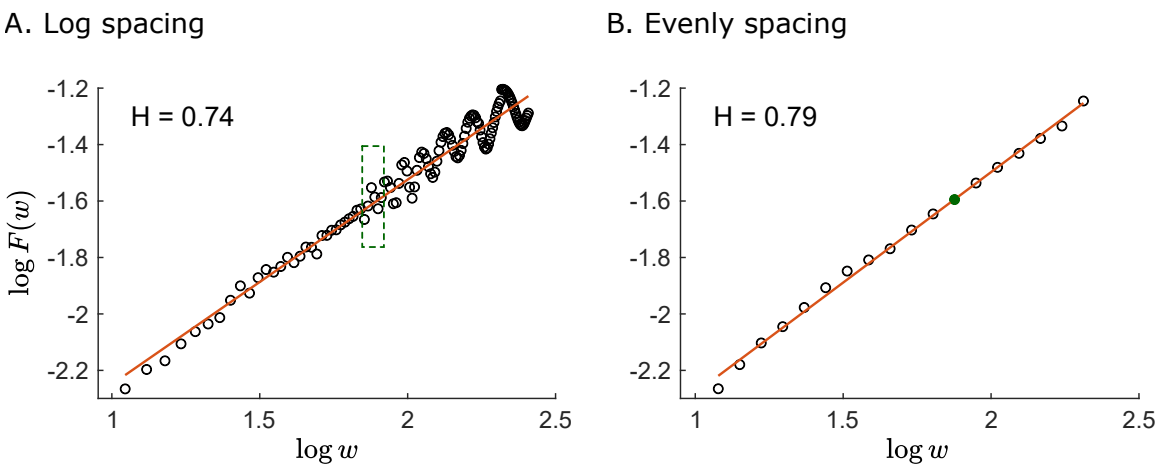


Figure 2.3 Illustration of the evenly spaced approach proposed by Almurad and Delignières (2016). Black circles represent the fluctuation function $F(w)$ for different window sizes, and the orange line the linear regression used to estimate the Hurst exponent. The true Hurst exponent of the series is $H = 0.8$. (A) Logarithmic spacing, all window size are represented, resulting in a higher density of points at larger scales and a disproportionate influence of these scales on the regression. (B) Evenly spacing, in which values are averaged within equally spaced bins on the logarithmic axis. The green point corresponds to the average of the values contained within the green region in panel A.

Accordingly, the estimates derived from PSD (α) and RRA (H) should satisfy Eq. 2.13. To account for inaccuracies arising from the asymptotic nature of long-range dependence, a tolerance criterion was introduced such that $d = |H - \frac{1+\alpha}{2}| < 0.1$. Nevertheless, Rangarajan and Ding (2000) emphasize that this method is not foolproof: the relation may hold for processes that do not exhibit long-range dependence, and conversely, it may fail for processes that do.

2.5 Discussion

As described in Section 2.1, LRA is fundamentally defined by its asymptotic behavior: correlations decay according to a power law and therefore remain significant across large time scales. This makes LRA particularly difficult to characterize in practice. Although several methods have been proposed, there is no consensus regarding which methods should be used, which parameters are most appropriate, or what series length is required for reliable estimation. This section reviews the literature related to these challenges and discusses the methodological choices made in this thesis.

First, estimates based on the PSD present the advantage of requiring low computational cost. However, the choice of parameters, such as windowing, depends on the series under consideration (Rangarajan and Ding, 2000). In addition, the α exponent tends to be overestimated in non-stationary signals (fBm) and the methods has been shown to yield more variability in the estimates (Roume et al. 2019). Still, the method can be useful when combined with an estimate of the Hurst exponent (Rangarajan and Ding, 2000) or for a quick classification of a signal (stationnay vs non-stationnay) (Delignières, Ramdani, et al. 2006; Roume et al. 2019). Next, RRA is theoretically only appropriate for stationary long-memory noise (fGn), not for

already integrated non-stationary processes (fBm). Therefore, an output above 1 cannot be properly interpreted. In contrast, for DFA and AFA, an output between 1 and 2 indicates that the series under study is non-stationnary (fBm) and that the output must interpreted as equal to $H + 1$ (Delignières, Ramdani, et al. 2006; Roume et al. 2019). This natural ability to accomodate non-stationary scaling regime is an important advantage. Those methods are then preferred, in particular with evenly-spacing. Finally, Hollman, Lee, et al. (2022) showed that AFA was more sensitive than DFA to conditions that influence fractal dynamics in gait. For those reasons, we chose to apply AFA, with evenly-spacing, in this work.

In AFA, a smooth trend is fitted to an integrated series and residual fluctuations are measured across different window sizes w. Theoretically, there should be a strict linear relationship between $\log F(w)$ and $\log w$. In practice, however, deviations from linearity can occur, particularly for smaller and larger window sizes. To mitigate these effects, this method is commonly performed over a restricted range of window sizes, where the linear relationship is most stable. In the literature applying DFA for stride series analyses, a variety of window ranges have been used, and choices were mostly made on a subjective basis. Damouras et al. (2010) analyzed the region of linearity for experimental stride series in different conditions and recommended the range ($w_{min} = 16, w_{max} = \frac{N}{9}$), later adopted by Ravi et al. (2020) in their guidelines for DFA. For AFA, Kirchner et al. (2014) and Hollman, Lee, et al. (2022) used $w_{min} = 5$ and $w_{max} = \frac{N}{2}$, suggesting that linearity might be more stable in AFA. In order to strike a balance between minimizing information loss and ensuring a precise fit, we used $w_{min} = 11$ and $w_{max} = \frac{N}{2}$ in the present thesis, as slight deviations from linearity were observed at the smallest scales. However, we systematically verified that our main results remained consistent under alternative parameter choices. In Chapter 5, we used $w_{min} = 5$ to increase the number of data points, as series under consideration were shorter.

A widely discussed aspect is then the required length of the series. Several authors have analyzed the performance of DFA according to the series length. Indeed, sufficiently long time series are required to reliably capture their scaling properties and both biases and variability can arise if series are too short (Delignières, Ramdani, et al. 2006). When the objective is merely to detect differences between groups, some degree of bias may be acceptable, if systematic. For example, Kuznetsov and Rhea (2017) suggested that series of approximately 250 strides can be sufficient for this purpose. Likewise, Kirchner et al. (2014) demonstrated that stitching together five trials of 25 strides into longer series enabled discrimination between people with Parkinson's disease and healthy controls using both AFA and DFA. However, the authors emphasized that, from a theoretical perspective, this stitching procedure contradicts the core assumption underlying long-range autocorrelation, according to which correlations should arise from consecutive strides. Nevertheless, DFA and AFA quantify scale-free fluctuations in variance across temporal scales rather than directly testing for long-range autocorrelation. The intact short-timescale structure within individual trials may retain sufficient group-specific information to yield discrimination and the stitching procedure may produce artificial scale-free structure at higher timescales. Still, while these measures may be discriminative, they cannot be interpreted as direct measures of LRA. In agreement with this view, Marmelat, Reynolds, and Hellman (2018) reported that stitching together short gait trials produced fractal fluctua-

tion properties that differed from those obtained from continuous longer trials.

When the goal is to accurately estimate the scaling exponent characterizing the system, bias should be minimized as much as possible. Accordingly, several studies conducted in diverse populations have recommended using series of approximately 500–600 strides for reliable estimation of scaling properties (Damouras et al. 2010; Delignières, Ramdani, et al. 2006; Marmelat and Meidinger, 2019). Other work has suggested that shorter series may still be acceptable provided that several trials are averaged (Pierrynowski et al. 2005). Evenly spacing, described in Section 2.4.3, would allow analyses to be performed on series around 250 strides whether applied to DFA (Almurad and Delignières, 2016; Warlop, Bollens, Detrembleur, et al. 2017) or AFA (Gao, Hu, and Tung, 2011). These considerations will guide the methodological choices made in this thesis, particularly when determining the experimental acquisition durations.

Methodological manipulations of gait time series may also substantially alter scaling behavior. Removing segments, adding random spikes, or mixing signals with different local properties (e.g., distinct values of H) can distort scaling estimates (Chen, Ivanov, et al. 2002). Removing segments in the middle of a series and reassembling the remaining subsets have a particularly strong effect in anti-correlated signals, depending on both the initial H value and the proportion of removed strides. No such manipulations were carried out in this thesis, as the potential segments removed were located either at the beginning or the end of the series. Random spikes, however, may be present in experimental gait data, and were shown to affect both correlated and anti-correlated signals. A common approach to dealing with these spikes is to apply a median filter locally (Ravi et al. 2020). Finally, mixing signals with different local behaviors also altered scaling properties. Terrier (2020) showed a nonlinear sensitivity when correlated and anti-correlated segments were combined: introducing a small proportion of correlated segments into an anti-correlated signal produced a stronger effect than the reverse situation.

3

Model of gait control in Parkinson's disease and prediction of robotic assistance

---

Published as : Vandamme, C., Otlet V., Ronsse R., Crevecoeur F. Model of gait control in Parkinson's disease and prediction of robotic assistance. *IEEE Transactions on Neural Systems and Rehabilitation Engineering* 2023, 31, 1374-1383

Minor changes have been made to ensure consistency in the notation used across the thesis. In addition, Section 3.2.3 has been extended to provide a more detailed description of the model

---

GAIT variability of healthy adults exhibits Long-Range Autocorrelations (LRA), meaning that the stride interval at any time statistically depends on previous gait cycles; and this dependency spans over several hundreds of strides. Previous works have shown that this property is altered in patients with Parkinson's disease, such that their gait pattern corresponds to a more random process. Here, we adapted a model of gait control to interpret the reduction in LRA that characterized patients in a computational framework. Gait regulation was modeled as a Linear-Quadratic-Gaussian control problem where the objective was to maintain a fixed velocity through the coordinated regulation of stride duration and length. This objective offers a degree of redundancy in the way the controller can maintain a given velocity, resulting in the emergence of LRA. In this framework, the model suggested that patients exploited less the task redundancy, likely to compensate for an increased stride-to-stride variability. Furthermore, we used this model to predict the potential benefit of an active orthosis on the gait pattern of patients. The orthosis was embedded in the model as a low-pass filter on the series of stride parameters. We show in simulations that, with a suitable level of assistance, the orthosis could help patients recovering a gait pattern with LRA comparable to that of healthy controls. Assuming that the presence of LRA in a stride series is a marker of healthy gait control, our study provides a rationale for developing gait assistance technology

to reduce the fall risk associated with Parkinson's disease.

3.1 Introduction

Gait, as many other physiologic signals, possesses a complex temporal organization. Indeed, the fluctuations from one stride to another, originally considered as random noise, display Long-Range Autocorrelations (LRA) (Hausdorff, Peng, et al. 1995). It means that the fluctuation at any time statistically depends on remote previous cycles with a power-law relationship, revealing the existence of a long-term dependency in the locomotor system. The presence of a temporal correlation across consecutive strides is characterized by the Hurst exponent, a metric directly linked to the autocorrelation function and reflecting the degree of this autocorrelation (Rangarajan and Ding, 2000).

This feature is considered to indicate the flexibility and adaptability of the locomotor system to external events. Clinically, its presence is often considered as a marker of health, while its alteration has been associated with different pathological conditions (Stergiou and Decker, 2011). In particular, it has been shown that the presence of LRA in the series of consecutive stride durations of patients with Parkinson's Disease (PD) is decreased compared to healthy individuals (Bartsch et al. 2007; Hausdorff, 2009), and that this decrease becomes more pronounced as the disease progresses (Warlop, Detrembleur, Bollens, et al. 2016). This indicates that these patients have a more random temporal organization of the stride series, which is associated with an increased risk of falling (Dierick et al. 2021), and therefore decreases their quality of life.

The physiological origins of LRA in gait variability of a healthy population, as well as the reasons why these LRA are impacted in the PD population, remain unclear. Several models have been developed to understand the mechanisms governing the presence of LRA in interstride interval time series (Dingwell, John, and Cusumano, 2010; Gates, Su, and Dingwell, 2007; Sarbaz et al. 2011; West and Scafetta, 2003). Among those, some authors attribute the presence of LRA to the biomechanics of walking while others argue for a neural origin. Some studies demonstrated that LRA are partly under volitional control and evidenced the supra-spinal influence on the correlation structure, since gait (Hausdorff, Ashkenazy, et al. 2001) or cycling patterns (Warlop, Bollens, Crevecoeur, et al. 2013) become less correlated when guided with a metronome. Likewise, the early stages of PD are associated with a decline in LRA while biomechanics at this stage can be considered unaltered. Therefore, we assumed here a neural origin for the presence of LRA. The present paper looked specifically at the model of Dingwell, John, and Cusumano (2010), which reproduced gait variability in a healthy young population within the framework of stochastic optimal control, in a way that is independent of the biomechanical system. This model suggested that LRA emerge from the fact that humans exploit the task redundancy to regulate their velocity while walking.

Based on this model, we addressed the two following questions. First, we investigated whether and how the model could be adapted to simulate gait impairments experienced by

PD patients for different stages of the disease. Second, the model was used to investigate the impact of a robotic device and, more specifically on the possibility of restoring the presence of LRA in the series of stride parameters. Indeed, robot-assisted gait training has shown promising effects on the gait of PD patients. Some studies showed improvements of gait parameters such as velocity, endurance, stride length and duration, cadence, and balance (Capecci et al. 2019). Other advances in the development of assisted gait include studies on the effect of oscillator-based walking assistance on the presence of LRA (Otlet and Ronsse, 2022), based on the Super Central Pattern Generator model described in West and Scafetta (2003).

In this paper, we demonstrate that gait parameters in Parkinson's disease can result from an augmentation of stride-to-stride regulation used to mitigate the impact of noise. Moreover, the decline in LRA in patients could be a consequence of a relative inability to exploit the task redundancy. It is also demonstrated that an oscillator-based robotic assistance, included in the model as a low-pass filter, could restore the presence of LRA in simulated time series of stride durations. These results provide theoretical support for developing gait assistance technology for patients with a view towards reducing the risk associated with falling as the disease progresses.

3.2 Materials and Methods

3.2.1 Data

The experimental stride series of healthy subjects from Dingwell, John, and Cusumano (2010) were re-used to validate the model. The dataset was composed of 34 stride sequences characterized by the stride duration (T), length (L) and velocity (S). The experiment involved 17 healthy young adults. Each participant was asked to walk on a treadmill for 5 minutes at a self-selected speed. Each participant completed two trials with a 2-minute break in between. Series length ranged from 248 to 309 strides. Mean values, standard deviation and Hurst exponent of all series (T, L and S) were averaged across participants and the 95% confidence intervals were computed, assuming a normal distribution ($CI = Mean \pm 1.96 * SD$).

In addition, data of PD patients were collected by Warlop, Detrembleur, Bollens, et al. (2016) and also incorporated in the present analyses. This study included 20 patients with PD, who were asked to walk overground for 10 minutes at a self-selected speed. For each patient, stride durations (T) were extracted from series of 512 strides. The dataset included the stage of the disease of each patient, assessed using the modified Hoehn & Yahr scale (H&Y), here ranging from 1 to 3. These scores monitor the progression of the disease based on a clinical evaluation of motor performance. The H&Y evaluation includes a balance assessment, the severity of tremor, bradykinesia and rigidity, and whether symptoms are unilateral or bilateral. Unlike healthy participants' data, this dataset only contained the series of stride durations, and not stride lengths. Again, the mean, standard deviation, and Hurst exponent were computed. Then, a standard least-square regression line was drawn to model the evolution of each variable (standard deviation and Hurst exponent) as a function of the disease progression, captured by the H&Y index. The Spearman's correlation coefficient was used to assess the relationship

between this index and both the stride variability and the stride persistence. The level of significance was set to $p < 0.05$.

3.2.2 Assessment of the Long-range autocorrelation

The Hurst exponents, noted H, were computed with the Adaptive Fractal Analysis (AFA), a method described by Riley et al. (2012) and recently recommended for stride time fractal exponents (Hollman, Lee, et al. 2022). Briefly, the AFA consists in identifying smooth trends signals from a time series. The process is repeated for trends of different timescales and the residuals of each fit are reported against the corresponding timescale. The analysis of the scaling of the residuals as a function of the timescales gives the Hurst exponent of the time series. If $0 \leq H < 0.5$, the series is said to be anti-persistent, meaning that it exhibits negative LRA. If $H = 0.5$, the series corresponds to random fluctuations around its mean (white noise). If $0.5 < H \leq 1$, the series is persistent, or has positive LRA. The Hurst exponent relates to the fractional Brownian motion model and is by definition restricted within the interval]0,1[(Mandelbrot and Van Ness, 1968). Other notations exist, like the scaling exponent α, which simply extends the definition of H to values larger than 1 (Roume et al. 2019). This refers to non-stationary series, a case that was not encountered in this paper.

The AFA is similar to the Detrended Fluctuation Analysis (DFA) (Peng, Buldyrev, et al. 1994), more commonly used in the evaluation of LRA, as both algorithms quantify the residuals of fits computed with different sizes of time window. The main difference is that AFA identifies globally smooth fits by combining overlapping windows and is therefore more robust to non-stationarities (Gao, Hu, and Tung, 2011).

3.2.3 Gait model for young and healthy population

The model developed to reproduce gait variability of PD patients and predict the impact of a robotic assistance was based on the model previously published by Dingwell, John, and Cusumano (2010), capturing gait variability in a healthy and young population. The model aimed at describing the inter-stride dynamics resulting from a regulation derived in the context of Linear-Quadratic-Gaussian (LQG) control. Strides were fully characterized by their length (L) and duration (T) from which the speed (S) was derived ($S = \frac{L}{T}$). Through a discrete system, these stride features were updated iteratively:

$$x_{n+1} = x_n + u(x_n) + N_n u(x_n) + \eta_n \tag{3.1}$$

where x_n is the state vector, composed of the duration T_n and length L_n of stride n. The term $u(x_n)$ is the motor command and $N_n u(x_n)$ represents a command-dependent noise, with N being a diagonal matrix. Finally, η is an additive noise vector. Both η and the diagonal of N are zero-mean, gaussian random variables with covariance matrix equal to $\text{diag}[\sigma_1^2\ \sigma_2^2]$.

The command was determined by a controller, which regulated stride variability resulting from internal and external sources of noise according to a behavioral goal, i.e. keeping a constant velocity v (either strictly fixed by a treadmill or intrinsically selected by the walker based

on their own preference). This means that the following equation should hold at each step: $L_n - vT_n = 0$. This task introduced redundancy as there is an infinite amount of combinations of T_n and L_n that satisfy this relationship. These combinations form a straight line in the plane T, L, called the Goal-Equivalent Manifold (GEM). Along this redundant dimension, one pair of T and L might be naturally preferred by the participant for biomechanical reasons (length of the legs, inertia, etc.). This pair was referred to as the Preferred Operating Point (POP), corresponding to $T_{POP}$and L_{POP}. When noise disturbances push the state away from the POP, it is possible that locally, the optimal correction is to drive the system towards the GEM and not necessarily to the POP. To capture this, the model used the following cost-function for each step:

$$C = \omega_v e^2 + \omega_{POP} p^2 + \omega_{u,1} u_1^2 + \omega_{u,2} u_2^2. \tag{3.2}$$

The first term penalizes the error on the velocity, with $e^2 = (L - vT)^2$. The second term concerns the distance from the POP, with $p^2 = (T - T_{POP})^2 + (L - L_{POP})^2$. Then, the last two terms penalize the effort made to reduce these errors; u_1 (resp. u_2) being relative to the correction applied to the stride duration (resp. stride length). The parameters ω_v, ω_{POP}, $\omega_{u,1}$, and $\omega_{u,2}$ reflect the relative importance of the cost of each error term. The weights ω_v and ω_{POP} correspond to the level of regulation applied respectively to the stride velocity and to the POP, with respect to the energetic cost that this regulation requires and that is quantified by the parameters $\omega_{u,1}$ and $\omega_{u,2}$.

Finding the optimal command is a classic LQG control problem. In this framework, the system follows a *Linear* dynamic (Eq. 3.1), with a *Quadratic* cost function (Eq. 3.2), and the system is subject to *Gaussian* noise. The general form of such a system and such a cost function is given by:

$$x_{n+1} = Ax_n + Bu_n + \epsilon_n C u_n + \eta_n \tag{3.3}$$

$$Cost_n = x_n^T Q_n x_n + u_n^T R u_n \tag{3.4}$$

In this case, we have:

$$x_n = \begin{bmatrix} T_n \\ L_n \\ T_{POP} \\ L_{POP} \end{bmatrix} \quad A = \begin{bmatrix} 1 & 0 & 0 & 0 \\ 0 & 1 & 0 & 0 \\ 0 & 0 & 1 & 0 \\ 0 & 0 & 0 & 1 \end{bmatrix} \quad B = \begin{bmatrix} 1 & 0 \\ 0 & 1 \\ 0 & 0 \\ 0 & 0 \end{bmatrix} \quad C = \begin{bmatrix} \sigma_1 & 0 \\ 0 & \sigma_2 \\ 0 & 0 \\ 0 & 0 \end{bmatrix}$$

And:

$$Q = \begin{bmatrix} \omega_v v^2 + \omega_{POP} & -\omega_v v & -\omega_{POP} & 0 \\ -\omega_v v & \omega_v + \omega_{POP} & 0 & -\omega_{POP} \\ -\omega_{POP} & 0 & \omega_{POP} & 0 \\ 0 & -\omega_{POP} & 0 & \omega_{POP} \end{bmatrix} \quad R = \begin{bmatrix} \omega_{u,1} & 0 \\ 0 & \omega_{u,2} \end{bmatrix}$$

The LQG framework provides a closed loop solution to the optimal control problem. The command is optimal in the sense that it minimizes the expected value of a quadratic cost criterion and is a linear function of the state:

$$u_n = -L_n x_n \tag{3.5}$$

where L_n is the feedback gain. As we aimed to model steady-state walking, both the system and the cost were time-invariant. Therefore, we used the infinite horizon formulation. The optimal state feedback gains were time-invariant and were obtained by solving the Algebraic Ricatti Equation (Åström, 1970) :

$$L = (R + B^T S B + C^T S C)^{-1} B^T S A \tag{3.6}$$
$$S = Q + A^T S A - (A^T S B)(R + B^T S B + C^T S C)^{-1} B^T S A \tag{3.7}$$

A schematic representation of the model is provided in Fig. 3.1 (top line). The first box is the controller, capturing the Central Nervous System. It takes as input the current state of the walker (i.e., the stride duration T and the stride length L) and their goal, in terms of stride length and stride duration (whose combination gives the targeted velocity). Considering these two inputs, the controller sends a command to the second box that captures the impact of the system, resulting in the next state.

We used a noise level of $\sigma_1 = 0.011$ (relative to T_n) and $\sigma_2 = 0.017$ (relative to L_n). The weights of the cost function were set to $\omega_v = 30$, $\omega_{POP} = 1$ and $\omega_{u,1} = \omega_{u,2} = 10$. The weights implicitly carried the units required to render each term of the cost function unitless. Finally, the target velocity was $v = 1.21$ [$\frac{m}{s}$], with $T_{POP} = 1.105$ [s] and $L_{POP} = vT_{POP}$ [m]. These parameters allow the simulation of walking series of an average participant but do not model the variability of speeds adopted by different participants.

To validate the model, a total of 34 series of 512 strides were simulated and their features were compared to the experimental data. Each stride series was described by three series of inter-stride durations, lengths and velocities. The mean, standard deviation, and Hurst exponent of each series were computed. These values were then averaged over the 34 strides simulations and 95% confidence intervals were computed, as defined above.

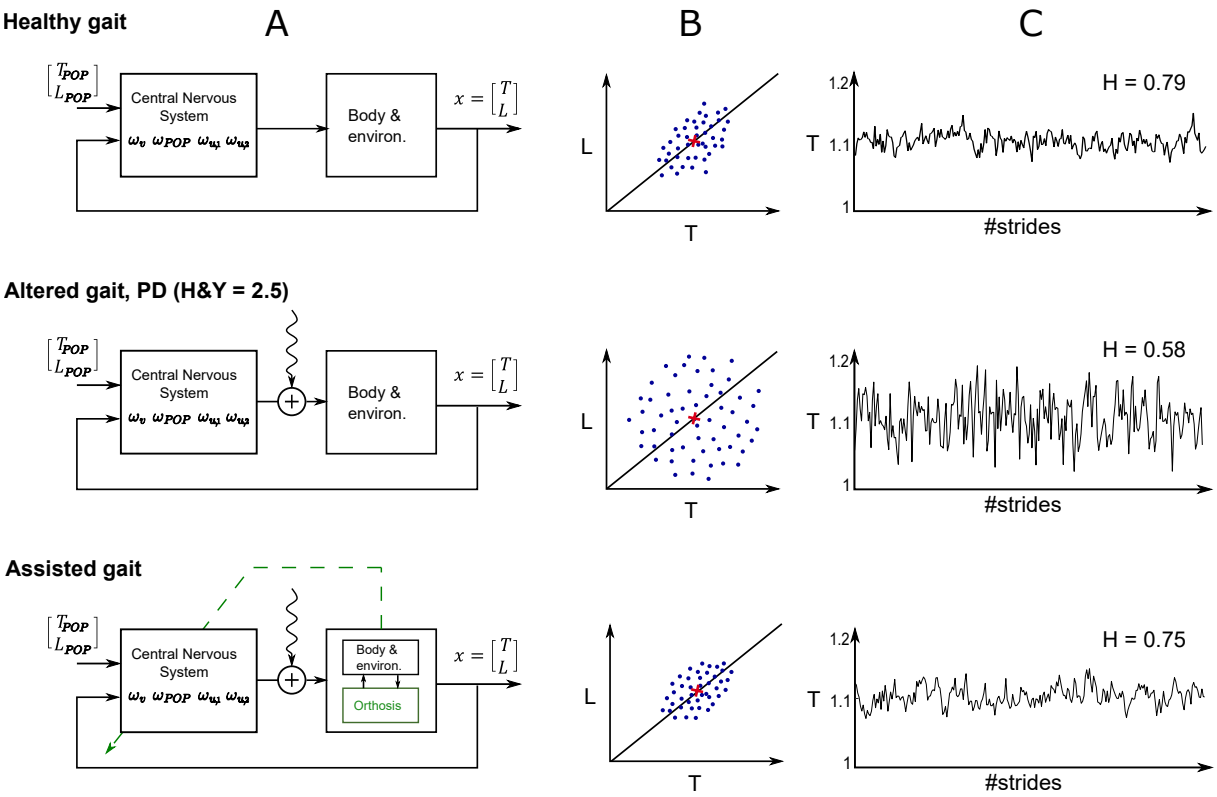


Figure 3.1 (A, top to bottom) Schematic representation of the model for healthy gait, gait altered by Parkinson's disease, and gait altered by Parkinson's disease assisted by an orthosis driven by low-pass dynamics. (B) Simulated stride distribution (stride length "L" versus stride duration "T") around the goal equivalent manifold (black straight line) and the preferred operating point (red cross). (C) Example of simulated series of stride durations for each population (healthy - patients) and condition (assisted - unassisted) and their corresponding Hurst exponent (H).

3.2.4 Model adaptations to Parkinson's disease and robotic assistance

Parkinson's disease

The model was adapted by tuning two parameters selected to reproduce the evolution of gait impairments with PD. To reproduce the increasing variability of inter-strides durations, the noise level of the system was increased (i.e. η in Eq. 3.1). The parameter σ_1, which is the variance of the noise impacting stride duration, was determined by fitting the experimental data. Then, assuming a similar variability increase of inter-stride length, σ_2 was multiplied by the same factor. To reflect the reduced Hurst exponent of patients, the weights of the cost function (Eq. 3.2) were also manipulated, in particular ω_{POP}, the weight penalizing deviations away from the POP. Again, this parameter was fitted to best reproduce the changes observed in the series of stride durations but impacted the persistence of the series of stride lengths as well. The tuning of parameters ω_{POP} and η was performed jointly because ω_{POP} affected both the variability and the persistence (i.e. the Hurst exponent) in the stride series. The model calibration was performed by testing all possible pairs of parameters ($1 < \omega_{POP} < 35$ and $0.011 < \sigma_1 < 0.044$) and by selecting the parameters that best fitted the Hurst exponent and the variability of the experimental series of stride durations of 20 PD patients, according to a least-square fitting.

In Fig. 3.1, these changes are illustrated by an increased noise signal added to the motor command. The change of control strategy occurred in the Central Nervous System, where the weight ω_{POP} was impacted, reflecting a more pronounced tendency to regulate stride variables around the POP.

Effects of a robotic assistance

Robot-assisted gait training has shown promising effects on gait of PD patients (Capecci et al. 2019). Current studies have used adaptive oscillators in assistance (Ronsse et al. 2011), which resulted in a net effect on the discrete time model comparable with a low-pass filter. Indeed, adaptive oscillators learn the feature of the user's gait and tend to maintain them equal to what they used to be during the preceding cycles, by means of a soft and adaptive robotic assistance. As this has not been tested on PD patients yet, this study aimed to model the impact of such an assistance on the LRA of patients. The assistance was added to the system dynamics as follows:

$$\begin{aligned} & x_{n+1} = x_n + u(x_n) + N_n u(x_n) + \eta_n - \lambda(x_{n+1} - x_n) \\ \Leftrightarrow\ & x_{n+1} = x_n + (1+\lambda)^{-1}(u(x_n) + N_n u(x_n) + \eta_n), \\ & \text{with } \lambda = \begin{bmatrix} \lambda_1 & 0 \\ 0 & \lambda_2 \end{bmatrix}. \end{aligned} \tag{3.8}$$

The matrix λ represents the filter coefficient, which plays the role of time constant in the discrete time filter. It can be interpreted as the level of assistance of the orthosis, with λ_1 (resp. λ_2) the filter coefficient on the state variable T (resp. L). Higher coefficients correspond to higher degrees of assistance. The filter coefficients were tuned for every stage of the disease to recover a level of variability similar to that of control subjects (numerical values from Fig. 3.2B). Then, the corresponding Hurst exponents were computed.

The orthosis and its controller thus intrinsically modify the dynamics of the user's "body", as it continuously interacts with it and affects stride generation accordingly. In Fig. 3.1, this is captured by embedding the orthosis in the "body + environment" block, i.e. the biomechanical system that is controlled by the central nervous system. However, it is unknown whether patients learn this new dynamic that includes the effect of the filter, i.e. of the assistive device. If they do, the controller uses Eq. 3.8 to derive the optimal motor command. This potential adaptation is captured by the green dashed line connecting both blocks, illustrating that the dynamic model is updated in the controller with knowledge of the filter. In contrast, patients who do not adapt their control will generate motor command considering Eq. 3.1 as a system model without the filter. Finally, a partial adaptation would consist in a controller that considers only a fraction of λ while computing the optimal command, resulting in a partial compensation for the filtering dynamics of the orthosis. The persistence of the time series from the two first conditions, referred as "adaptation" and "no adaptation", was compared across different values of λ used to lower the variability. The cost function remained unchanged (Eq.

3.2).

In addition, the model allows considering the possibility that the orthosis acts on the cadence only, on the stride length only, or on both. Three conditions were simulated: the orthosis filtered only the cadence ($\lambda_2 = 0$), only the stride length ($\lambda_1 = 0$) or both ($\lambda_1 = \lambda_2 > 0$), compared to no assistance at all ($\lambda_1 = \lambda_2 = 0$). For each situation, the Hurst exponents of the series of stride durations were reported.

Working code was made publicly available here: https://git.immc.ucl.ac.be/clevandamme/gait_model_pd.

3.3 Results

3.3.1 Healthy gait

Each stride series was composed of a series of inter-stride durations, lengths and speeds. Each of them was analyzed in terms of mean, standard deviation and auto-correlation structure assessed based on an estimate of the Hurst exponent. The average results across 34 healthy participants (data from Dingwell, John, and Cusumano (2010)) and simulations are reported in Fig. 3.2. For consistency with experimental data, the simulation results referred to series of 512 strides, but we verified that they were also valid for longer stride series (series of 1024 strides, data not shown). As expected, the means of simulated data matched exactly with values corresponding to the experimental series as they were used for calibrating the model. It can be reminded that the model did not intend to reproduce the inter-subjects' variability since all simulations were performed with the same velocity goal, and the same POP, whereas actual participants were asked to walk at their most natural speed, resulting in some variability across subjects. Note that for such standard parameter values, randomness in the time series produced higher levels of variability in the estimates of the Hurst exponents. The variability of the simulated series matched human data for T, L and S (Fig. 3.2B). While the variability of T and L could be directly manipulated through the parameters σ_1 and σ_2 (Eq. 3.1), the variability of S was a consequence of the combination of noise applied to T and L, as well as of the controller that regulated this velocity (ω_v). We observed a relatively strong persistence in the experimental series of stride durations and lengths with values similar to those observed in overground walking experiments (Terrier, Turner, and Schutz, 2005). The model succeeded in reproducing a comparable persistence of T and L series, with mean Hurst exponents between 0.5 and 1 for both. Experimental data further suggested that velocity was slightly anti-persistent ($H < 0.5$), while the model simulated velocity series characterized by a Hurst exponent of 0.5, which can be interpreted as white noise. The observation that velocity was slightly anti-persistent was accommodated in the model previously proposed by Dingwell, John, and Cusumano (2010) by considering a sub-optimal command to over-correct the errors on the velocity. We focused here on the formulation corresponding to the stochastic optimal control, which allowed capturing changes in the Hurst exponents of the series exhibiting changes in persistence, thus we do not model the anti-persistence explicitly. Furthermore, the anti-persistence of series of velocity may not generalize to overground walking since this has mostly been observed in treadmill studies

(Dingwell, John, and Cusumano, 2010; Terrier and Dériaz, 2012).

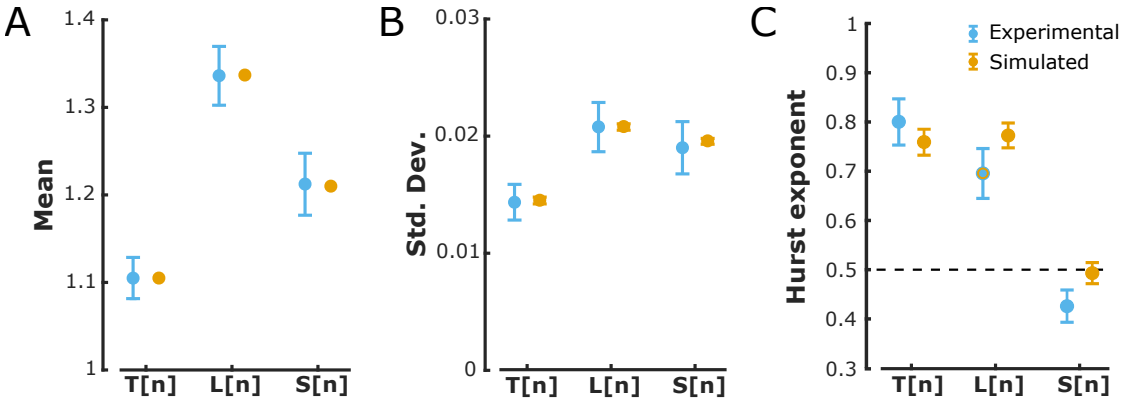


Figure 3.2 (A) Mean stride durations ($T[n]$), lengths ($L[n]$) and speed ($S[n]$) for healthy subjects' data and simulated series. (B) Standard deviations of stride series ($T[n]$, $L[n]$ and $S[n]$. (C) Hurst exponent for $T[n]$, $L[n]$ and $S[n]$. Reported values result from an average of 34 experimental stride series from (Dingwell, John, and Cusumano, 2010), compared to our simulations. Error bars represent the 95% confidence interval on these averages.

An example of simulated series of stride durations with characteristics as summarized in Fig. 3.2, is illustrated in Fig. 3.1 (top), as well as the strides distribution in the plane T, L. From Fig. 3.1B, we observe a narrow distribution along the GEM, meaning that each stride had a similar speed. In contrast, points were not constrained to remain in a close neighborhood of the POP, and had some freedom to move along the GEM.

3.3.2 Gait in Parkinson's Disease

The evolution of gait in PD patients according to disease severity is outlined in Fig. 3.3A. For each participant, the observed standard deviation and Hurst exponent of the series of inter-stride durations was plotted as a function of their clinical score obtained from the H&Y scale. Data of patients confirmed the previously observed significant increase in the standard deviation of series of strides durations (mean std $= 0.028 \pm 0.016$), compared to control subjects (0.014 ± 0.004, $t(50) = 4.62, p < 10^{-4}$). Experimental data also supported the decline of LRA in patients with PD ($H = 0.62 \pm 0.13$) compared to control subjects ($H = 0.8 \pm 0.13$, $t(50) = -4.71, p < 10^{-4}$).

Relating individual gait outcomes to disease severity illustrated the progressive impact of the disease on strides variability and persistence. The variability was correlated with the H&Y score with a Spearman's coefficient of 0.5. The regression was statistically significant ($R^2 = 0.22$, $F(1,18) = 4.93$, $p = 0.04$). Concerning the persistence, the Spearman's coefficient was equal to -0.68. Again, the regression was statistically significant ($R^2 = 0.52$, $F(1,18) = 19.86$, $p = 0.0003$). The disease stage was therefore clearly related to the variability of stride duration and to its temporal organization.

The linear regressions between the disease severity and the two variables of interest, namely the standard deviation and the Hurst exponent, were used as target values for the model simu-

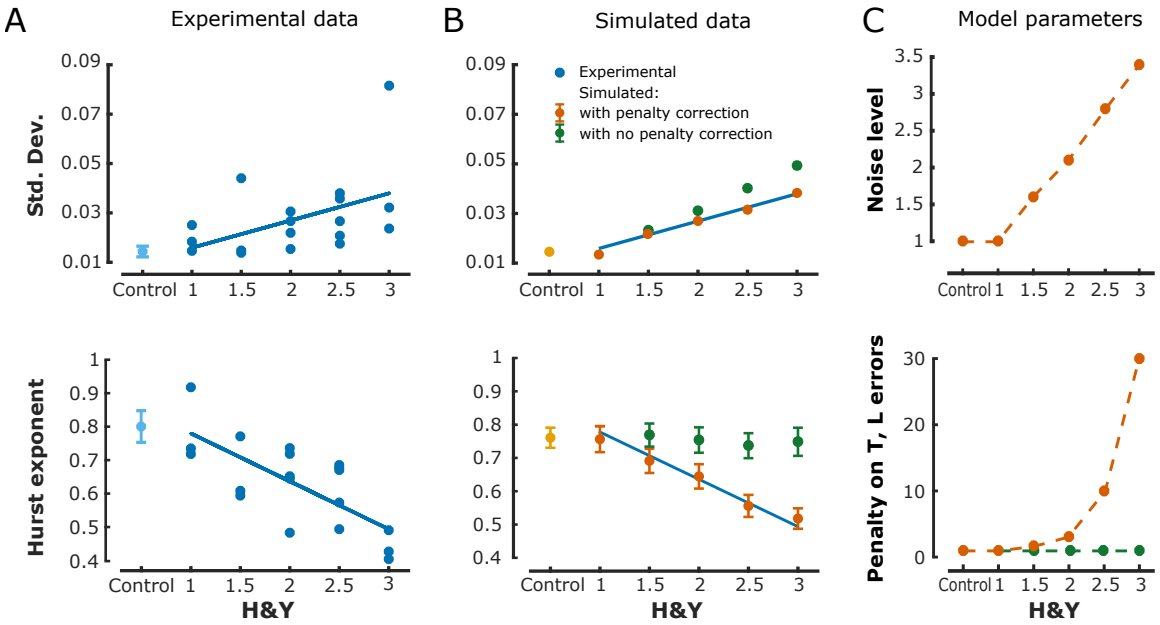


Figure 3.3 (A) Individual standard deviation and Hurst exponent of series of stride durations of Parkinson's patients according to disease severity (assessed with the H&Y scale), compared to control group (light blue), data taken from Warlop, Detrembleur, Bollens, et al. (2016). (B) Mean standard deviation and Hurst exponent of 20 simulated series of stride durations according to disease severity. (C) Model parameters used to fit the stride characteristics of each disease stage (orange trace). The increasing level of noise in the system accounts for the higher variability in stride durations while a higher penalty away from the POP (T_{POP} and L_{POP}) is directly linked to a reduced Hurst exponent. In green, alternative set of parameters to illustrate the impact of the regulation on the POP

lations. To that purpose, two manipulations on the model were made. The first one was motivated by the observation that PD patients displayed larger inter-stride variability as described by the data presented in Fig. 3.3A. The simulation results and associated noise are represented in Fig. 3.3B and C respectively (top panel). The noise level increased linearly with the disease severity, but remained unchanged for patients with a H&Y score of 1. The adaptation of the noise parameter was performed jointly with the adjustment of the cost parameter ω_{POP}, which determined the penalty applied on errors on the POP. This manipulation aimed to reproduce the reduced LRA observed as the disease progresses. The Hurst exponents of simulated series and the corresponding ω_{POP} are reported in Fig. 3.3B and C (orange traces). The penalty ω_{POP} gradually increased to 30, a level comparable to the penalty applied on the velocity (ω_v, Eq.3.2).

To illustrate the joint impact of the adaptation of noise and cost parameters, the green trace (Fig. 3.3B-C) represents an alternative set of parameters, where only the noise level was modified. It highlights that, when the control was not adapted in response to the increase in noise variance, the increase in variability of the output series was in consequence more dramatic. For a H&Y of 3, the standard deviation increased by 35% when ω_{POP} remained fixed.

These results could not be obtained by changing other parameters. For $\omega_{POP} = 1$, by dividing or multiplying ω_v by 2, the Hurst exponent of T did not change. The impact was rather

on the Hurst exponent of S, the series of stride velocities, which is not of interest here. Furthermore, the results of Fig. 3.3B were robust to small changes in the cost function. Changing ω_{POP} by $\pm 10\%$ had negligible effect on the standard deviation and the Hurst exponent. A typical simulated stride series and stride distribution matching the parameters of the empirical series obtained with PD patients is presented in Fig. 3.1B-C (middle). Strides were much more spread out, resulting from the increase in variability. The distribution otherwise aligned with the redundant axis of the task requirement became more circular around the POP, given that the weight on this part of the task increased.

3.3.3 Simulation of robotic assistance

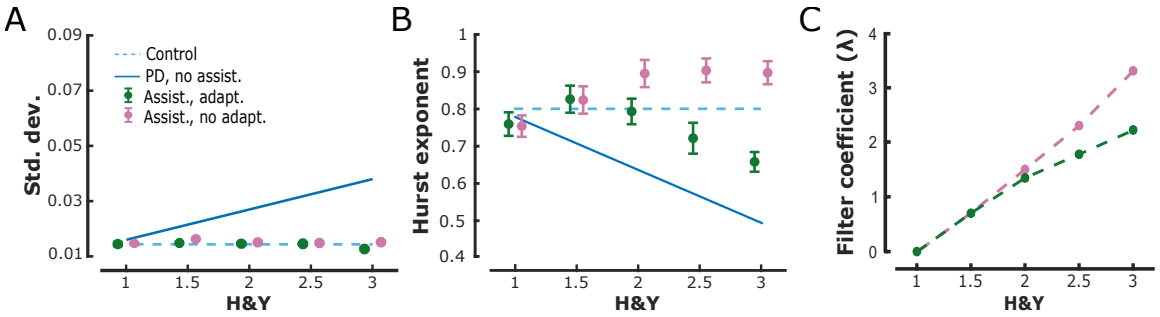


Figure 3.4 Simulation of the effect of an orthosis on patients' series of inter-stride durations, both with (green) and without (pink) adaptation to the orthosis. Comparison of (A) the standard deviation and (B) the Hurst exponent of the simulated data to non-assisted patients and healthy subjects. (C) Filter coefficient applied to T and L required in both cases to reach levels of variability corresponding to healthy patients.

To evaluate the potential impact of an orthosis, we simulated the same system and controller with the addition of a low-pass filter on the stride series as a first order model of the effect of a robotic device controlled by adaptive oscillators (Ronsse et al. 2011) on humans' gait dynamics. The impacts of the filter on the stride variability and on the LRA of the series are respectively described in Fig. 3.4A and 3.4B. Filter coefficients have been defined for each disease's stage to fit the variability of healthy gait. These are reported in Fig. 3.4C. Those coefficients differed depending on whether or not the patient had learned the new dynamics that included the effect of the filter (Eq. 3.8). In the first case, the patients adapted their control by considering the state transition dynamics as in Eq. 3.8, i.e. with the filter. In the second case, they acted as if there was no assistance and computed a command based on the system described in Eq. 3.1. The filter coefficients required to recover healthy levels of gait variability were higher if the patient did not adapt to the orthosis. Still, in both cases, the more the disease progresses (higher H&Y), the higher the level of assistance (higher λ). Lastly, in the model, it was not necessary to provide assistance for patients at the first stage of PD as their gait parameters matched those of the control group ($\lambda = 0$).

These values of λ produced strides series of mean standard deviations and mean Hurst exponents represented in Fig. 3.4A-B. Regardless of the simulated patient's adaptation, the robotic assistance reduced the stride variability and increased the Hurst exponent of series of stride durations, compared to non-assisted patients (solid blue line). The filter coefficients λ_1

and λ_2 were set in a way that the variability of assisted patients had the same value as that of healthy subjects. This is illustrated in Fig. 3.4A. As shown in Fig. 3.4B, the levels of persistence of patients adapting their control did not reach the reference value of control subjects for late stages of the disease (H&Y $\geq$ 2.5). In contrast, if patients did not take into account the filtering, the Hurst exponents went beyond those of healthy subjects.

The model allows the investigation of another potential strategy, which would be to adjust the filter coefficient to match levels of persistence corresponding to those of healthy participants (dashed blue line). If the patients adapt to the robotic assistance, the filter coefficients must be further increased for patients with a H&Y $>$ 2. The variability is consequently further reduced and drops to $0.01[s]$ (-30%) for H&Y $= 3$. In the other case, if patients do not adapt their control, the filter coefficients must be lowered for patients with a H&Y $>$ 1.5. As a result, the variability reached a value of $0.018[s]$ ($+22\%$), for H&Y $= 3$. One of the simulations characterized in Fig. 3.4 is presented in Fig. 3.1B-C (bottom), illustrating the capabilities of the filter to recover stride series and stride distribution similar to those of healthy participants.

The foregoing simulations were derived by applying a filter to both T and L. We now present a comparison of the Hurst exponents of T, obtained with filters applied either only to the cadence, only to the stride length or to both (Fig. 3.5A), considering a full adaptation of patients. It appears that the persistence of T was not significantly increased when the simulated orthosis only acted on the length of the strides, compared to the Hurst exponents of simulated non-assisted patients. The Hurst exponent of T was only increased if the robotic assistance acted directly on the cadence, regardless of whether L was filtered or not. To illustrate this, an example of stride distribution for each situation is shown in Fig. 3.5B. The light and dark blue distributions correspond to those presented in Fig. 3.1B, middle and bottom respectively. In red, the filter was only applied to T, resulting in a distribution more constrained along the line $T = T_{POP}$ with a small effect of the GEM, slightly tilting the distribution. In contrast, in green, it only filters L and strides are distributed along $L = L_{POP}$. From this figure, we observe that a simple filter on the stride duration was sufficient to recover LRA compatible with series of healthy participants. However, a filter on the stride length, in addition to that applied to the cadence, was necessary to have a stride distribution more aligned with the redundant axis, like the stride distributions of healthy participants. Moreover, the series of stride lengths is most likely to be impacted by the disease too. Therefore, a filter would be necessary to strengthen the LRA of the series of stride lengths.

3.4 Discussion

The purpose of this study was to develop a model capturing gait variability of PD patients to complement the current understanding of gait regulation in this population, with a particular emphasis on the decline of statistical persistence exhibited in stride-to-stride variability. A second objective was to study the effect of an oscillator-based robotic assistance on these patients' gait. For this purpose, we adapted the model capturing gait variability of healthy young adults, and added a low-pass filter representing the effect of the assistance on the time series of stride amplitudes and durations. According to the model developed in Dingwell,

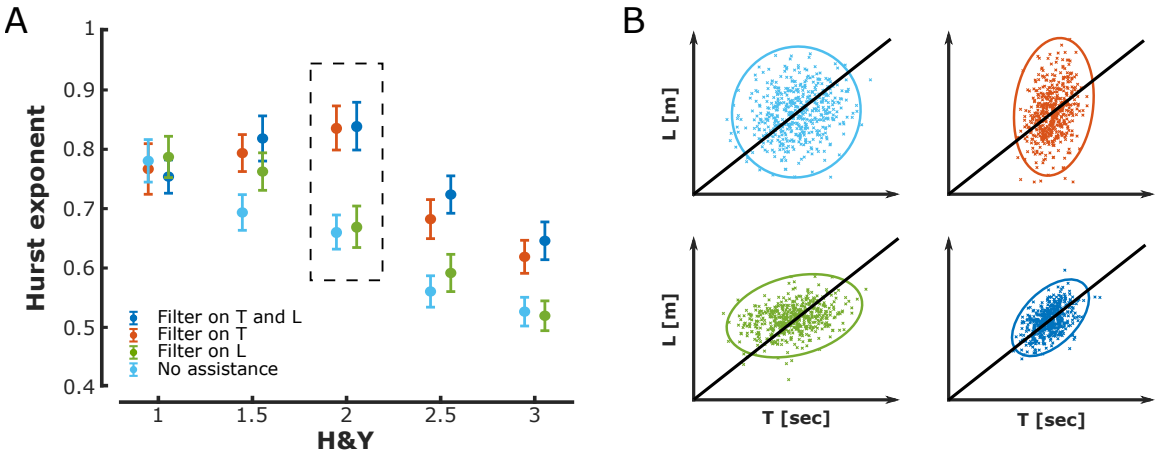


Figure 3.5 (A) Mean Hurst exponent of simulated series stride durations according to disease severity with different kind of robotic assistance. The robotic assistance filters the stride duration T (red), the stride length L (green), both (dark blue), none (light blue). (B) For a H&Y of 2, the resulting stride distribution along the goal equivalent manifold for these 4 scenarios.

John, and Cusumano (2010), the presence of LRA in gait variability emerged from a control strategy that first seeks to minimize velocity errors while only weakly limiting the deviations from the POP. In 2020, Kozlowska et al. (2020) further supported this model by highlighting the strong coupling between the trends appearing in the series of stride duration and stride length, which corresponded to movements along the GEM. To capture the behavior of PD patients, the model was adapted by manipulating two parameters: the noise in the process dynamics was increased to reproduce the increase in variability of the stride series; and the cost parameter ω_{POP} was increased to reduce the statistical persistence of the series of stride durations. Considering these parameters adjusted to pathological gait, we showed that the addition of a low-pass filter - capturing the effect of an adaptive oscillator-based robotic assistance - had a positive impact on both the variability and the statistical persistence of stride series, and could restore values comparable to healthy groups.

The model developed in this study offers a novel interpretation of gait deficits in the PD population and suggests that patients adopted a different control strategy than healthy subjects. A first phenomenon known to be associated with the progression of the disease is the increase in stride-to-stride variability (Hausdorff, Cudkowicz, et al. 1998) that was directly captured by increasing the process noise. Then, we demonstrated that this variability, which must be undesirable beyond a certain level, can be partially reduced by regulating gait parameters more strictly around the preferred operating point. This was achieved by increasing the cost of deviation from the POP captured in the model by the parameter ω_{POP} (Eq. 3.2). This regulation had a direct impact on the persistence of the series of stride durations. Not only gait parameters became more variable as a result of impairments in the sensorimotor system (Dierick et al. 2021; Takakusaki, 2017), but the series also became more random, which in this framework, reflected a compensation strategy for the increased variability.

This hypothesis is in accordance with the fact that patients recruit more attentional re-

sources while walking (Baker et al. 2008). It has been shown that patients rely more on frontal-cortical mechanisms to support gait movement execution, due to defective basal ganglia mechanisms ensuring movement automaticity (Morris, 2000). It is possible that patients recruit attentional resources to regulate not only the velocity, but also stride duration and stride length, which requires a conscious effort. The increased cognitive load associated with walking in PD patients is corroborated by the fact that strides variability is impacted when patients are instructed to execute another task while walking, such as a mental calculation (Yogev et al. 2005). A common interpretation of these findings is that the attentional resources are recruited for the dual task, and this impairs patients' control of gait. Our interpretation is in line with this idea and the model formalizes it in the context of stochastic optimal control. Our developments included an increased penalty on the deviation away from the POP, which is equivalent to assuming a more stringent regulation of inter-stride variability without exploiting the GEM. The latter likely incurs an attentional or cognitive load to control each individual stride.

This novel interpretation of gait deficits in PD patients is also in line with the use of therapies involving rhythmic cues. These therapies consist in providing external auditory cues adapting in real-time to the subject's gait rhythm so that the subject synchronizes their walking rhythm with this external rhythm. These studies showed an improvement in the presence of LRA to the level of healthy subjects (Hove et al. 2012; Uchitomi et al. 2013).

As an alternative to auditory stimulations, we explored potential benefits of robotic assistance based on adaptive oscillators with a net output on inter-stride time series comparable to a low-pass filter. We showed that such technology could restore healthy patterns of gait in PD patients, both in terms of standard deviation and statistical persistence. However, for a given set of parameters that one wishes to recover with the assistance, we found that the filter coefficients applied by the robot may depend on whether the patients adapt or not to the device. In practice, it is likely that patients partially learn the impact of the robotic assistance on their strides dynamic and adapt their control according to this newly acquired knowledge. Therefore, we expect that the true impact of the orthosis on the stride variability and persistence be between the results found with full adaptation and those found with no adaptation at all. Depending on the degree of adaptation of each patient, the level of assistance can be adjusted to obtain gait characteristics as close as possible to those of healthy population. Note that it is reasonable to assume that patients do adapt to the orthosis, at least partially, considering that Parkinson's patients adapt successfully their gait to split-belt treadmill (Roemmich et al. 2014). This adaptation occurred within the first 50 strides (Mohammadi et al. 2015). Further research is needed to investigate whether and how quickly they can adapt to a robotic device.

As for healthy population, the model simulated the behavior of an average patient, under the assumption that a specific H&Y corresponds to a specific gait impairment given by the regression. For clinical applications, the level of assistance must be individualized according to the actual needs of each patient and their personal ability to adapt to the robotic assistance. The level of assistance of an orthosis based on adaptive oscillators such as the Active Pelvis Orthosis presented in D'Elia et al. (2017) is set by a virtual stiffness parameter, which controls the torque to be provided to the user at the hip level. This parameter also accounts for the

patient's weight to guarantee a safe interaction.

The less flexible control strategy of patients could be ascribed in the model to a relative inability to exploit the GEM. This allows one to formulate the hypothesis that patients with PD might have an altered internal task formulation and fail to exploit the redundancy of the task, whereby a target velocity can be achieved with difference combination of stride timing and amplitude. Support for this interpretation is given by current theories associating movement related costs and the basal ganglia (Shadmehr and Krakauer, 2008). This idea was supported by the work of Mazzoni and colleagues (Mazzoni et al. 2007), who showed that movement slowing in PD could not be attributed to an inability to execute accurate movements. Indeed, patients demonstrated normal speed-accuracy tradeoffs compared to the performance of healthy subjects, but they were more reluctant to perform fast movements (i.e. they needed more trials to reach the correct velocity). It was suggested that patients may associate an abnormally high cost for movements that they are otherwise able to execute. Our present developments suggest that not only the value of the cost, but also its structure (in this case, the GEM) may not be well represented in this population.

The model provides a discrete characterization of gait in two different populations (healthy – patients) and conditions (assisted – unassisted). It is possible to connect this model with continuous time models (Gates, Su, and Dingwell, 2007; West and Scafetta, 2003) and to leverage frameworks recently developed to recover joint forces and muscles activation to build a comprehensive musculoskeletal model (De Groote et al. 2016; Eskinazi and Fregly, 2018). For exemple, as done in West and Scafetta (2003), the simulated series of stride frequency might be the input to a nonlinear forced Van der Pol oscillator whose output is the movement of the two legs. However, even if the resulting series of stride frequency slightly differ from the input frequencies, they keep the same fractal properties, mean and standard deviation.

One implicit hypothesis that motivated our investigation on the presence and recovery of statistical persistence in patients was the hope that restoring LRA could have a causal influence on fall risk. Indeed, the fractal exponent of strides series has been proposed to be a predictive marker of fall (Hausdorff, 2007), although this remains uncertain. Indeed, the loss of persistence might not be the cause of fall risk, but rather a marker of the compensatory mechanism, which is itself linked to disease severity and necessarily correlated with fall risk. We expect that future research will address this issue in details.

To summarise, the model developed to simulate gait variability of patients with Parkinson's disease suggested that these patients adopted a control strategy that sought to strictly regulate the deviation from the preferred target stride duration and length, in addition to the coordinated regulation of stride velocity. This strategy could be initiated to limit the increased stride variability that characterizes Parkinson's disease and makes patients' gait less stable. As a consequence of this less flexible control, the variability of their series of inter-stride durations displays a reduced level of autocorrelation, a marker of reduced adaptive capabilities and higher risk of falling. In addition, this study predicts an improvement in both the stride durations variability and statistical persistence for patients assisted with an oscillator-based robotic

device. We believe that our modelling work provides a strong theoretical ground for future investigations on the benefit of gait assistance technologies in clinical populations.

3.5 Complementary discussion

3.5.1 From computational predictions to experimental intervention

The computational framework developed in this work provides predictions regarding the effects of gait assistance that can be considered alongside the subsequent experimental study of Otlet, Vandamme, et al. (2023). The purpose of that study was to test whether a wearable hip orthosis, providing assistance through adaptive oscillators could improve gait performance and restore the LRA typically reduced in Parkinson's disease. Eight patients underwent overground gait training with the orthosis three times per week for four weeks, with gait assessed before and after training and again one month later. Following training, patients increased their hip range of motion, gait speed, and stride length, while decreasing stride duration. These improvements were maintained one month after training. In contrast, the LRA of stride duration was standardized towards values closer to those observed in healthy individuals immediately after training, but this normalization was not retained at the one-month follow-up.

The improvement in LRA observed after training is consistent with the model's prediction, namely that assistance may facilitate the re-emergence of a correlated gait pattern. However, several differences between the two studies should be considered. First, the computational predictions concerned the immediate effects of assistance, whereas the experimental study included a longitudinal follow-up and focused on the effects of four weeks of training. Second, while the study of Otlet, Vandamme, et al. (2023) investigated a broad range of gait parameters, the model primarily addresses the temporal organization of gait variability and provides limited insight into changes in their mean values.

Taken together, these two studies provide useful guidance for the design of future assistive devices. The model suggests that an assistance should not simply impose a preferred cadence or stride length, but should preserve the redundancy available to the locomotor system and allow the patient to select different combinations of stride duration and stride length to achieve the desired walking velocity. This principle is consistent with the adaptive strategy implemented by Otlet, Vandamme, et al. (2023), in which assistance was continuously synchronized with the patient's gait rather than prescribing a fixed temporal pattern. In addition, although the model explored different levels of assistance according to H&Y stage, the substantial inter-individual variability observed within a given stage suggests that the level of assistance may be better determined by the individual's actual walking capacity than solely by clinical classifications.

Finally, it is important to highlight again that restoration of LRA should not be interpreted as equivalent to a reduction in fall risk. Although reduced LRA has been associated with an increased risk of fall in Parkinson's disease, the presence of LRA alone does not establish that a patient is walking more safely. If reduced LRA reflects a diminished ability to exploit task

redundancy and to flexibly organize stride-to-stride fluctuations, then an effective intervention may not be one that directly imposes a more fractal gait pattern. Instead, it may be more beneficial to create an environment in which patients can safely explore a broader motor repertoire while progressively rediscovering the redundancy available in the walking task. Such an approach may ultimately provide a more natural route towards the recovery of long-range temporal organization than artificially enforcing a target level of LRA.

3.5.2 Impact of methodological heterogeneity between datasets

An important consideration is that the two datasets used in this study to develop the model were collected under different experimental conditions, in two separated studies. In particular, participants with Parkinson's disease walked overground, whereas healthy controls walked on a treadmill. Although treadmill walking has been reported to modify gait dynamics in people with Parkinson's disease (Hollman, Von Arb, et al. 2020; Warlop, Detrembleur, Stoquart, et al. 2018), previous work indicates that it does not significantly affect the AFA exponent in healthy controls (Hollman, Watkins, et al. 2016). Thus, in the present comparison, the treadmill condition of the control dataset is unlikely to account for the observed difference in AFA exponent. This would have been a more substantial concern had the experimental conditions been reversed, with patients walking on a treadmill and controls overground.

A second limitation is the absence of age matching between groups. Aging itself can affect both the AFA exponent and gait variability, and may therefore contribute to the observed differences. However, the effects of aging and Parkinson's disease on gait dynamics are generally reported in the same direction, with Parkinson's disease tending to exacerbate the alterations associated with aging (Hausdorff, Cudkowicz, et al. 1998).

Finally, the datasets were acquired using different sensing modalities (IMUs versus contact sensors) and with different or incompletely reported sampling frequencies. Nevertheless, both datasets were specifically collected to investigate long-range autocorrelations in gait, suggesting that their temporal resolution was adequate for the intended analysis. In that regard, the 512-Hz sampling frequency used by Warlop and colleagues is well above the generally recommended 120 Hz threshold (Ravi et al. 2020).

Importantly, however, the objective of the present study was not to establish a difference in LRA between Parkinson's disease and healthy aging, but rather to investigate the mechanisms underlying a difference that has already been consistently reported in the literature using appropriately controlled protocols. The present datasets therefore served to develop and evaluate a mechanistic explanation of an established phenomenon, rather than to provide a definitive direct comparison between the two populations. Future studies using age-matched participants and identical acquisition and walking conditions would nevertheless be valuable to confirm that the proposed mechanisms hold when population differences are assessed under a common experimental protocol.

4

Measured and modeled transitions between self-paced walking and synchronization with rhythmic auditory cues

Published as : Vandamme, C., Otlet V., Ronsse R., Crevecoeur F. Measured and modeled transitions between self-paced walking and synchronization with rhythmic auditory cues. *Journal of Neurophysiology* 2025 134:6, 1939-1952

Minor changes have been made to ensure consistency in the notation used across the thesis

CONSTRAINING gait rhythm with a metronome has been shown to influence gait pattern in many different ways. While rhythmic cues can improve a number of parameters in some clinical populations, they do alter the long-range autocorrelations naturally exhibited in series of stride durations. However, transitions between walking with and without a metronome (and vice-versa) have not been measured, it is therefore unclear how people adapt to such a change in task. To address this gap, a total of 21 healthy volunteers were asked to walk overground during three conditions: one unconstrained control condition, followed by two conditions in which a metronome was activated during either the first or second half of the session to test both transitions. The long-range autocorrelations were assessed over a sliding window on the stride series to measure their evolution. Our observations were reproduced with a computational model allowing us to relate sudden changes in movement parameters to the long-range autocorrelations, which are typically measured over longer timescales. The results showed a clear transition in both conditions involving a metronome, with long-range autocorrelations of the series of stride durations gradually reduced when the metronome was turned on and recovered when it was turned off. In these two conditions, the change in long-range autocorrelations could be reproduced in the model by an instantaneous switching of

the control policy associated with the presence or not of the metronome, suggesting that long-range autocorrelations emerge from a flexible control strategy that rapidly regulates timing and amplitude parameters according to task requirements.

4.1 Introduction

In natural walking conditions, humans seem to have a remarkable ability to finely tune their stride-to-stride fluctuations. Despite an infinite number of pairs of stride length and duration enabling them to reach a given desired velocity, the coefficient of variation of those gait parameters is on the order of just a few percent (Terrier and Schutz, 2003). This variability has been extensively studied because it holds significant potential as a sensitive parameter for assessing mobility and fall risk in clinical settings, and gaining insights into stride-to-stride control across different contexts (Hausdorff, 2005). However, to fully understand how humans regulate their strides, it is necessary to analyze not only the average magnitude of the stride-to-stride variability but also the temporal structure of these fluctuations.

Indeed, gait variability in healthy adults exhibits Long-Range Autocorrelations (LRA), or statistical persistence, meaning that the fluctuation at any time statistically depends on remote previous cycles with a power-law relationship, revealing the existence of a long-term dependency in the locomotor system (Hausdorff, Peng, et al. 1995). This pattern has been found in a variety of biological signals such as heartbeat (Peng, Havlin, et al. 1995), breathing (Fadel et al. 2004), neural activity (Bédard et al. 2006) and finger tapping (Gilden et al. 1995), but its interpretation remains debated. In gait, statistical persistence has been associated with the flexibility and the adaptability of the locomotor system while its loss has been correlated with a higher risk of falling in some pathologies such as Parkinson's disease (Hausdorff, 2009; Warlop, Detrembleur, Bollens, et al. 2016). This metric is also highly sensitive to context, as evidenced by its alteration in various conditions such as cautious gait (Herman et al. 2005), forced marching in military populations and load carrying (Krajewski et al. 2020), walking at non-preferred velocity (Jordan et al. 2007), and synchronization to external cues (Delignières and Torre, 2009). In particular, several authors have shown that constraining gait rhythm with a metronome resulted in series of stride duration exhibiting anti-persistence, with little or no impact on the magnitude of this variability (Delignières and Torre, 2009; Jordão et al. 2022; Kaipust, McGrath, et al. 2013; Marmelat, Torre, et al. 2014; Sejdić, Fu, et al. 2012; Terrier and Dériaz, 2012; Vaz, Groff, et al. 2019). In contrast to statistical persistence, which indicates that deviations from the mean are statistically more likely to be followed by deviations in the same direction, anti-persistence means that deviations in one direction are statistically more likely to be followed by deviations in the opposite direction (Terrier and Dériaz, 2012).

Several models have been proposed over the years to interpret the presence of persistence in stride-to-stride variability when walking freely, and the emergence of anti-persistence in these same series when synchronizing with a metronome. While many authors consider that LRA in stride interval naturally arise from the complex interaction between different structures acting at different time scales (Wagenmakers et al. 2004), others suggested that it might be due instead to the inherent biomechanics of walking and may not require complex central nervous system

control mechanisms (Gates, Su, and Dingwell, 2007). It has also been argued that LRA might simply be a predictable consequence of partial error correction (Pressing and Jolley-Rogers, 1997). In that sense, Dingwell, John, and Cusumano (2010) demonstrated that, when walking on a treadmill, humans do not immediately correct deviations in stride duration and length, as these two parameters are irrelevant to the main objective of the task, namely maintaining a stable velocity. In contrast, they showed that humans would slightly over-correct small deviations in stride speed, resulting in slight anti-persistence in series of stride velocity.

Finally, the use of rhythmic cues has also been extensively studied in populations suffering from gait impairments, such as Parkinson's disease, especially for rehabilitation purposes. It has been hypothesized that a metronome effectively improves stride length, cadence and speed, and reduces stride-to-stride variability (Spaulding et al. 2013). However, as stated earlier, invariant cueing disrupts the natural statistical persistence of stride-to-stride fluctuations. To address this limitation, there is a growing interest in fractal metronomes, which would reinstate a pattern of variability similar to that of healthy individuals (Lheureux et al. 2020). In this context, few authors investigated whether the benefits of rhythmic cues, either visual or auditory, isochronous or fractal, could be retained, with promising results in the elderly and in patients with Parkinson's disease (Hove et al. 2012; Rhea et al. 2014; Vaz, Knarr, and Stergiou, 2020). Nevertheless, in these studies, the temporal characterization of the retention remained poor, consisting of a single measurement of the Hurst exponent over a post-synchronization phase. There is therefore a need for new methods to analyze the transition between phases with and without rhythmic cueing and to better understand the effect of the metronome.

To address this gap, we investigated the impact of the sudden activation or deactivation of an isochronous metronome, by measuring the evolution of the (anti-)persistence of new experimental stride series over a sliding window. Under the model linking the presence of persistence to goal-directed correction (Dingwell, John, and Cusumano, 2010), we reproduced in theory the effect of the metronome and test different changes in control policies at the transitions. Our observations were compatible with an instantaneous adjustment of the control policy in the model, resulting in a modulation of LRA associated with the synchronization of the cadence with the metronome. Together, our results highlight a functional link between statistical persistence and a flexible modulation of gait control, and suggest that healthy adults rapidly and efficiently adapted their gait to task requirements.

4.2 Material and Methods

4.2.1 Experimental procedure

A total of 21 young adults (9 females, age: 25.4 ± 1.5 yrs; height: 175.3 ± 11.8 cm; mass: 75.2 ± 14.3 kg) were enrolled in this study and performed the three conditions described below. The target sample size was based on previous studies reporting a significant effect of an isochronous cueing on statistical persistence (Delignières and Torre, 2009; Marmelat, Torre, et al. 2014; Sejdić, Fu, et al. 2012; Terrier and Dériaz, 2012; Vaz, Groff, et al. 2019). Partici-

pants were naive to the purpose of the experiment and had no known neurologic, muscular or orthopedic disorder that could alter their gait. The ethics committee of the host institution (UCLouvain) approved the experimental procedures and participants provided written informed consent before the experiment following usual procedures.

Each participant walked along a 34-meters-long rectangular track with rounded corners for 15 minutes in three conditions: a first control condition without metronome to measure their spontaneous cadence, followed by two conditions involving a transition between a phase without a metronome, and a phase with a metronome imposing the cadence of their gait (Fig. 4.1A), or vice-versa. In these two conditions, the metronome was activated either during the first half of the session (Cued→Free condition), or during the second half of the session (Free→Cued condition). Participants were instructed to synchronize one foot to the metronome beat. The order of the conditions involving a metronome was randomly attributed to the participants. The metronome was set at the frequency corresponding to the participants' spontaneous cadence, recorded as the average cadence during the control condition. The cueing was isochronous, meaning that the inter-beat intervals did not display any variability. During a training lap with the metronome, this frequency was tested and adapted, with a maximum adjustment of ±5% when requested by the participant. Participants were asked to maintain a constant speed within each session and were specifically instructed not to interrupt their walk when the metronome was switched on or off.

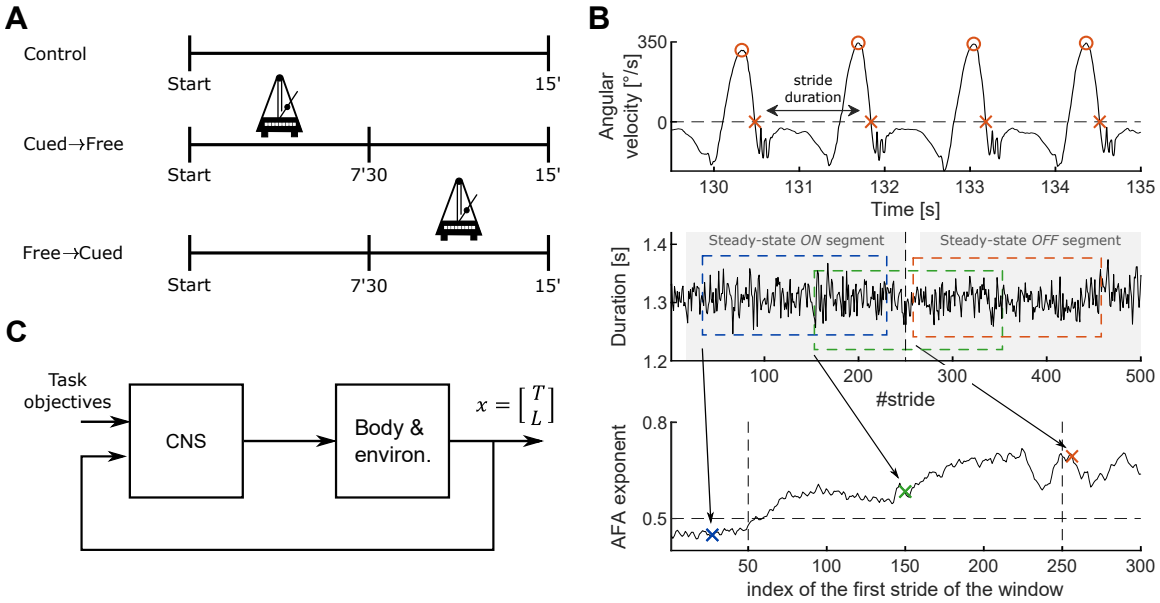


Figure 4.1 Experimental paradigm, data processing, and model of stride-to-stride regulation. A: overview of the three conditions completed by the participants, with durations and periods when the metronome was on. B, top to bottom: illustration of stride duration derivation from the sagittal angular velocity recorded by an inertial measurement unit (IMU) placed on the participant's ankle, example of series of stride durations in Cued→Free condition and evaluation of the evolution of the adaptive fractal analysis (AFA) exponent over a sliding window of 200 strides. By convention, the AFA exponent of the i^{th} window includes strides i to $i + 200$. C: schematic representation of the model of gait control.

4.2.2 Data acquisition and processing

Data were collected using NGIMU (x-io Technologies, Bristol, UK), and MATLAB R2021a (The MathWorks, Natick, MA, USA) was used for data processing, analysis, and statistics ("Statistics and Machine Learning Toolbox"). Participants wore four Inertial Measurement Units (IMUs), placed on both ankles (just above the lateral malleolus) and on top of both feet. These IMUs were used to obtain the sagittal angular velocities at a sample rate of 400Hz, and derive series of stride durations. Stride durations were defined as the time between two consecutive heel strikes of the same foot, calculated from the detection of the zero crossings following each peak in the sagittal angular velocity (Fig. 4.1B, top panel) (Otlet and Ronsse, 2023). By default, the IMU used to extract the stride durations was the one attached to the left ankle. However, due to connection losses between the IMUs and the computer, some sessions displayed gaps in the recorded data. In those cases, we used the IMU attached to the right ankle or those placed on the feet. When IMUs from different sides could be used to reconstruct stride series, the properties of the resulting stride series were similar (mean, standard deviation and autocorrelation functions). Therefore, the IMU used for analysis had no impact on the results. For some sessions, connection losses of the two IMUs did not allow us to reconstruct the stride series with sufficient accuracy (more than 10% missing strides). Such a number of missing strides could be critical for characterizing the temporal structure of the variability and could prevent a proper computation of the AFA exponent. Four sessions of different participants were therefore discarded from the analyses (three sessions in the control condition and one session in the Cued→Free condition). The remaining sessions had a maximum of 2% missing strides, which should have no impact on the evaluation of the statistical persistence, according to several studies (Chen, Ivanov, et al. 2002; Ma et al. 2010). All sessions in the control conditions included enough strides to estimate the average pace of the participants and determine the metronome frequency.

In addition, four more sessions were discarded due to a clear inability of these participants to perform the task, i.e. to synchronize one foot with the metronome beat. Besides the difficulties reported by these participants themselves during the experiment, these series exhibited large oscillations around the instructed pace. These oscillations were of a similar or even greater magnitude than in the non-paced condition, showing that they were unable to adapt their cadence to the target value and follow the instruction. To determine which sessions needed to be excluded, we plotted a moving average with a window of 50 data points in the Cued part of the series (Cued→Free and Free→Cued sessions) and calculated the Root Mean Square Error (RMSE) from the metronome instruction. Outliers were defined as sessions with RMSE 1.5 times the interquartile range above the third quartile (RMSE$> Q_3 + 1.5\times$ IQR). The four series that were removed based on this criterion were the two sessions with metronome of one participant, and the Free→Cued condition of two other participants. These series had a RMSE greater than 0.0085 s, while the series kept for the analysis had a RMSE below 0.0041 s. In sum, 55 series out of the 63 recorded ones were kept for the analysis.

To confirm that participants adopted a stable speed, we derived an estimate of stride lengths in the control condition, based on the method described in Trojaniello et al. (2014). We com-

puted the stride velocities by dividing these lengths by the corresponding stride durations and computed the range of variation of each series of stride velocities smoothed with a moving average of 10 strides. We reported a maximum range of variation of 15% across all the participants in the control condition.

4.2.3 Data analysis

In the Cued→Free and Free→Cued condition, we decomposed the stride series into two parts to compare the series with and without the metronome in time window that did not involve the transition. The first 15 strides of the pre-switch and post-switch series were discarded in order to restrict our analysis to steady-state behavior and avoid biases that may arise from non-stationarities. These steady-state segments are highlighted by the shaded areas in Fig. 4.1B, middle panel. These resulting series ranged from 340 to 420 strides according to each participant's pace. We estimated the standard deviation and the level of LRA of these series to assess the behavioral changes induced by the metronome.

The level of LRA was computed with the Adaptive Fractal Analysis (AFA), a method described in Riley et al. (2012) and recommended to estimate fractal exponents of stride time series for its robustness to non-stationarities (Gao, Hu, and Tung, 2011; Hollman, Lee, et al. 2022). Briefly, the AFA consists in identifying smooth trends signals from a time series. These signals are derived from a linear combination of local polynomial fits applied to overlapping windows of a fixed size. The process is repeated for window size ranging from 11 strides to half the length of the series, evenly spaced on a logarithmic scale. The residuals of each fit are reported against the corresponding timescale and the analysis of the scaling of the residuals as a function of the timescales gives the AFA exponent of the time series. This exponent estimates the same quantity as the exponent obtained with the Detrended Fluctuation Analysis (DFA), also called α exponent or Hurst exponent (H), capturing randomness or (anti-) persistence in the time series. When $0 < H < 0.5$, the series is anti-persistent. When $H = 0.5$, the series corresponds to random fluctuations around its mean (white noise), and when $H > 0.5$, the series displays statistical persistence associated with LRA. The Hurst exponent is by definition restricted within the interval $]0, 1[$ while the AFA can yield values higher than 1. This corresponds to non-stationary series, a case that was not encountered in the present experiment.

To characterise the behavioral response following the change in task instruction set by turning on or off the metronome, we then analyzed the evolution of the AFA exponent by applying the AFA over a sliding window of 200 strides involving the transition (Fig. 4.1B). All strides were considered for this analysis, strides excluded from the steady-state segment analysis were re-integrated to interpret the transition correctly. We aimed to use the smallest possible windows to characterize the transitions over the shortest time scale. However, windows of size below 200 strides resulted in noisy profiles, altering the interpretability of the results. While numerous studies recommended using DFA on series of at least 500 strides (Damouras et al. 2010; Delignières, Ramdani, et al. 2006; Marmelat and Meidinger, 2019), evenly-spaced regressions as employed in this study allow reducing the required number of strides to approximately

250 by reducing the sensitivity of the slope estimation to variability in the data (Warlop, Bollens, Detrembleur, et al. 2017). Other authors suggested that the AFA allows to estimate the Hurst exponent on time series of approximately 200 strides (Gao, Hu, Mao, and Perc, 2012), further supporting this choice of window size in the present study.

In the conditions involving a metronome, some series displayed a discontinuity at the transition, i.e. a sudden increase or decrease in the mean stride durations, likely resulting from short-term adjustments to the introduction or removal of the metronome. Such an abrupt change could artificially increase the AFA exponent as long as the discontinuity falls within the sliding window, as it introduces an artificial transient effect potentially leading to erroneous conclusions about changes in LRA. To address this potential confounding factor, we applied a correction to remove this discontinuity for all sessions in Cued→Free and Free→Cued conditions, and then compared the evolution of the AFA exponents with and without the correction. This correction consisted in subtracting from the second part of the series an offset corresponding to the difference between the average value of the 15 first strides after the switch and the average value of the 15 last strides before the switch. In addition, the same offset measured in each session was used to build surrogate data to perform a control analysis as explained in the following. Surrogate data are often used in gait analysis to assess whether observed variability patterns truly reflect non-linear dynamics (Theiler et al. 1992) We adapted this technique to distinguish the effect of a potential change in average pace from a change in experimental constraints. For each session in Cued→Free condition, we extracted the Cued part of the series and duplicated it. We then added the offset to the duplicated series and concatenated it with the other, thus obtaining artificial "Cued-Cued" series reproducing the same discontinuity encountered experimentally, but which did not feature any change of task. For each session in Free→Cued condition, we followed the same procedure to obtain "Free-Free" series. In both cases, the surrogate series allowed us assessing the effect of a short-term change in the mean of stride series, which could be dissociated from the change in gait pattern corresponding to the metronome.

4.2.4 Model

Stride series with similar evolution of LRA as those obtained experimentally were then reproduced within the framework of stochastic optimal control (Åström, 1970). This framework offers an interpretation of the transitions as a task-dependent change in gait control mediated by the introduction or removal of the metronome. The model developed here was based on the study by Dingwell, John, and Cusumano (2010) and Vandamme et al. (2023), and adapted to reproduce a broader range of behavior such as the anti-persistence emerging from metronome-guided walking, as well as transitions between these two tasks. A schematic representation of the model is provided in Fig. 4.1C. Briefly, each stride was generated iteratively from the previous one according to the following discrete time system:

$$x_{(n+1)} = x_n + u(x_n) + N_n u(x_n) + \eta_n \tag{4.1}$$

Each stride was characterized by a state vector, x_n, composed of two state variables defined

as the stride duration and length ($x_n = [T_n, L_n]^T$). The noise was composed of an additive noise vector η_n and a command-dependent noise $N_n u(x_n)$. The vector η and the diagonal of the matrix N were zero-mean, gaussian random variables with covariance matrix equal to $diag[\sigma_1^2, \sigma_2^2]$, off diagonal terms being equal to 0. The command $u(x_n)$ can be seen as the stride-by-stride regulation of length and cadence against noise disturbances according to the behavioral goal.

The initial formulation of the model was designed to reproduce treadmill walking, without a metronome (Dingwell, John, and Cusumano, 2010). Therefore, the overall objective was to maintain a constant velocity. As an infinite amount of $[T_n, L_n]^T$ allow maintaining a constant velocity, there is one degree of freedom in the set of state variables allowing to maintain a constant speed, making the task redundant. However, along this redundant axis, one pair, called the Preferred Operating Point (POP) and noted $[T_{POP}, L_{POP}]$ might be naturally preferred, likely due to biomechanical constraints on the achievable range of cadence and length modulation. A secondary objective was then to limit deviations from this preferred pair of stride length and duration. These two objectives were balanced with the energetic cost that this regulation required. The cost function (Eq. 4.2) used to compute the motor command captures these objectives, each one weighted with a factor ($\omega_v, \omega_{POP}, \omega_u$) reflecting their relative importance:

$$Cost = \omega_v(L_n - v_{TAR}T_n)^2 + \omega_{POP}[(T_n - T_{POP})^2 + (L_n - L_{POP})^2] + \omega_u(u_1^2 + u_2^2) \tag{4.2}$$

The first term penalizes deviations from the targeted velocity v_{TAR}, the second term weighted by ω_{POP} penalize deviations away from the POP, the last term weights the cost of the command. Finding the optimal command is a classical Linear-Quadratic-Gaussian (LQG) control problem, the derivation of which is described in details in Todorov (2005). The command is optimal in the sense that it minimizes the expected value of the quadratic cost criterion defined by Eq. 4.2, and the solution is a linear function of the state (optimal feedback gains). As we aimed to model steady-state walking, both the system and the cost were time-invariant. Therefore, we used the infinite horizon formulation. The optimal state feedback gains were time-invariant and were obtained by solving the Algebraic Ricatti Equation (Åström, 1970).

The parameters of this model were adjusted to match the level of variability of the series of stride durations and its temporal structure. In the control condition, i.e. to model overground walking without a metronome, the weights of the cost function were set to $\omega_v = \omega_{POP} = 2.5$ and $\omega_u = 10$. The penalty applied to deviations from T_{POP} and L_{POP} was therefore relatively small compared to the weight applied to the cost of the motor command, allowing deviations away from the POP to persist, and the series of stride durations and lengths to exhibit fractal-like fluctuations, i.e. LRA. Here, the penalty applied on deviations from the velocity v_{TAR} was also set to 2.5 to account for the fact that the velocity was not strictly regulated since our participants were not walking on a treadmill. To simulate treadmill walking, this parameter would be considerably higher. The target velocity was $v_{TAR} = 1.21[m/s]$, with $T_{POP} = 1.189[s]$ and $L_{POP} = v_{TAR}T_{POP}[m]$, which was set to the mean velocity and stride duration adopted by the participants.

The model was then adapted to reproduce the properties of stride series when participants

were asked to synchronize with a metronome. Our initial approach was based on the modulation of the parameter ω_{POP} to simulate a stronger regulation around the POP. However, we observed that the behaviour was not fully explained by this approach. In fact, to synchronize with a metronome, participants needed to regulate the asynchronies between heel strike of one foot and the metronome beat, or in other words, adapt the stride duration they targeted at each stride. If one stride felt behind the metronome, the following stride needed to be shorter to catch up with the metronome. In the model, a target duration T_n^* was iteratively computed as the duration between two beats of the metronome (fixed, noted T_{met}) added to the previous stride error. The initial system dynamics (Eq. 4.1) was augmented to include this supplementary state variable:

$$\begin{cases} T_{n+1} = T_n + (1 + N_{1,n})u_{1,n} + \eta_{1,n} \\ L_{n+1} = L_n + (1 + N_{2,n})u_{2,n} + \eta_{2,n} \\ T^*_{n+1} = T_{met} + (T^*_n - T_n) \end{cases} \tag{4.3}$$

The cost function was also adapted to include a term penalizing errors on the target stride duration T_n^* at each time step:

$$\begin{aligned} Cost =& \omega_v(L_n - v_{TAR}T_n)^2 + \omega_{POP}[(T_n - T_{POP})^2 + (L_n - L_{POP})^2] \\ &+ \omega_u(u_1^2 + u_2^2) + \omega_{met}(T_n - T_n^*)^2 \end{aligned} \tag{4.4}$$

The parameter weighting the synchronization to the metronome was set to $\omega_{met} = 0.35$ in order to fit the average AFA exponent observed experimentally when the metronome was turned on. The duration of the metronome T_{met} was set to $T_{POP} = 1.189[s]$, as the metronome was set at the frequency corresponding to the participants' spontaneous average cadence in the experimental setting.

Different transitions from $\omega_{met} = 0$ to $\omega_{met} = 0.35$ (and vice-versa) were tested. The transitions were initiated at different rates: infinite slope, corresponding to instantaneous transitions; or slopes set to $\pm\frac{\omega_{met}}{50}$, or $\pm\frac{\omega_{met}}{100}$). Negative (resp. positive) slopes correspond to a decrease (resp. increase) of the regulation to the metronome beat and therefore refers to the Cued→Free (resp. Free→Cued) condition. The controller was then recomputed following changes in ω_{met} to adapt the feedback gains. Each set of parameters was used to generate 100 series in the Cued→Free and Free→Cued condition. We used the onset of change in LRA to identify the change in ω_{met} that matched the experimental observations.

We also varied the initial asynchrony by manipulating T^* at the transition of the Free→Cued condition. The initial value of T^* could be set to T_{met}, capturing a perfect synchronization of the first beat of the metronome with the corresponding stride. To match the experimental settings more realistically, the initial asynchrony was also randomly drawn from a uniform distribution $T^* \sim U(T_{met} - \frac{T_{met}}{2}, T_{met} + \frac{Tmet}{2})$. These boundaries were chosen to match the worse initial asynchrony that participants could experience, which corresponds to the case where the metronome beat occurred exactly between two strides. In the Cued→Free condition, the metronome was activated before gait initiation. We therefore assumed an initial asynchrony of zero ($T^* = T_{met}$).

The parameters (transition rate and initial condition) were selected to reproduce the evolution of the AFA exponents observed experimentally. All the statistical analyses were then applied on a sample of 20 series generated with the selected parameters, similarly to the experimental data. All model parameters, and the criteria for choosing their values, are summarized in Table 4.1.

Parameters	Criteria
$v_{TAR} = 1.21\ m/s$ $T_{POP} = 1.189\ s$ $L_{POP} = v_{TAR}.T_{POP}\ m$	Average values obtained from the control condition.
$\sigma_1 = 0.017\ s$ $\sigma_2 = 0.021\ m$	Values from Dingwell, John, and Cusumano (2010).
$\omega_v = \omega_{POP} = 2.5$ $\omega_u = 10$	Fit to AFA exponent of series of stride durations in control condition.
$\omega_{met} = 0$ if metronome off $\omega_{met} = 0.35$ if metronome on	Fit to AFA exponent of series of stride durations in cued condition.
$T_{met} = T_{POP}$ $T^*_{init} \sim U(T_{met} - \frac{T_{met}}{2}, T_{met} + \frac{T_{met}}{2})$	Experimental protocol.
Transition rates from $\omega_{met} = 0$ to $\omega_{met} = 0.35$ (and vice-versa)	Fit to the onset of change in AFA exponent.

Table 4.1 Model parameters

Finally, even though this variable was not measured in the protocol, the model allowed to extract the series of synchronization errors, or asynchronies, defined as the time interval between heel strikes and metronome beats, when activated. This series was noted A_n and computed as follow: $A_n = \sum_{k=1}^{n}(T_k - T_{met})$, with T_k the duration of stride k and T_{met} a constant denoting the duration between two beats of the metronome. We computed the average AFA exponent and standard deviation of these series, to compare them with values previously reported in the literature (Delignières and Torre, 2009; Vaz, Groff, et al. 2019).

4.2.5 Statistical analyses

We performed one-tailed paired t-tests to test the specific hypothesis, derived from prior work (Delignières and Torre, 2009; Marmelat, Torre, et al. 2014; Sejdić, Fu, et al. 2012; Terrier and Dériaz, 2012; Vaz, Groff, et al. 2019), that both the AFA exponent and the standard deviation of series of stride durations would be lower during the Cued parts than during the Free parts of the series. Effect sizes were characterized with Cohen's d, defined as the difference between the means divided by the pooled standard deviation.

4.3 Results

4.3.1 Behavioural experiments

We first analyzed separately the Cued and Free steady-state segments of the strides series and reported the AFA exponents and standard deviations of all participants in both conditions including the metronome in Fig. 4.2. As expected, we observed lower AFA exponents when participants were guided by the metronome (Fig. 4.2A). The strides series exhibited anti-persistence with an average AFA exponent significantly lower than 0.5 (AFA exponent $= 0.42 \pm 0.11$, $p = 0.003$, in the Cued→Free condition). In contrast, the average AFA exponent of the Free parts of the series was equal to 0.79 ± 0.10, which is commonly reported in the literature regarding free walking in healthy adults (Bollens, Crevecoeur, Nguyen, et al. 2010; Hausdorff, Peng, et al. 1995). We also observed an effect of the metronome on the standard deviation of series of stride durations, associated with a decrease when the metronome was turned on (Fig. 4.2B). We performed one-tail paired t-test to evaluate whether the observed differences were significant. Standard deviation of stride series significantly increased when the metronome was muted compared to series of strides set to the rhythm of the metronome in the Cued→Free condition ($\Delta std = 8.3 \times 10^{-4} \pm 0.0019[s]$, $t(18) = 1.95$, $p = 0.033$). A statistical difference was also observed in the Free→Cued condition, where the standard deviation decreased after turning on the metronome ($\Delta std = -0.0015 \pm 0.0035[s]$, $t(17) = -1.79$, $p = 0.045$). Although the p-values were just below 0.05, this indicated a clear trend. The effect size, as measured by Cohen's d, was $d = 0.22$ in the Cued→Free condition and $d = -0.38$ in the Free→Cued condition, indicating a small effect. Regarding the autocorrelation functions, the AFA exponent of series of stride durations significantly increased when the metronome was not activated in both conditions (Cued→Free: $\Delta AFA = 0.34 \pm 0.15$, $t(18) = 9.97$, $p < 10^{-4}$; Free→Cued: $\Delta AFA = -0.33 \pm 0.17$, $t(17) = -7.93$, $p < 10^{-4}$). In contrast to the standard deviation, the effect was very strong, with $d = 3$ in the Cued→Free condition and $d = -2.3$ in the Free→Cued condition (Fig 4.2).

We then investigated how participants switched from one task to another. Fig. 4.3A shows an example of a series of stride duration for each condition, all from the same participant. In the middle (resp. right) panel, the vertical dotted line represents the stride at which the metronome was switched off (resp. switched on). The evolution of the AFA exponent of each series was estimated by applying the AFA over a sliding window of 200 strides (see Section 4.2). On average, participants took 765 ± 57 strides per condition depending on the pace that they chose to adopt. Therefore, to compare and average the evolution of LRA of all participants, the series were all aligned to the stride at which the metronome was turned off or on, and truncated to the same length. The evolution of the AFA exponent of the stride series of each participant are represented in Fig. 4.3B, with one highlighted series corresponding to the representative participant presented in Fig. 4.3A. In the conditions involving a transition, the two vertical lines indicate the interval of AFA exponents measured on windows containing strides on either side of the transition. In the control condition, the AFA exponent remained relatively stable, despite clear fluctuations. Regarding the exemplar participant, we observed in the Cued→Free condition a clear increase of the AFA exponent from a level corresponding to a white noise (AFA

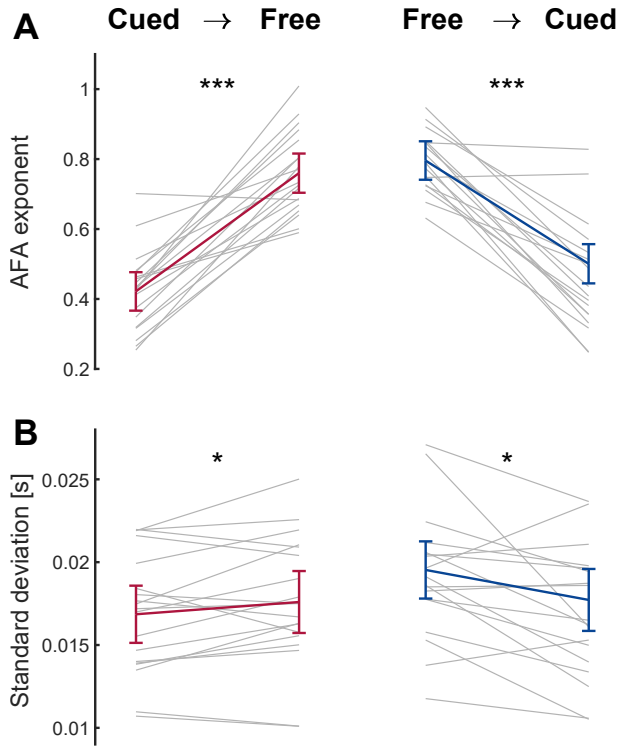


Figure 4.2 Analysis of differences between Cued and Free stride series in behavioral data. Adaptive fractal analysis (AFA) exponent (A) and standard deviation (B) of series of stride durations before and after the switch of the metronome (shaded areas in Fig. 4.1B), in Cued→Free condition (left) and Free→Cued condition (right). Group average and 95% confidence interval are shown in color and individual participants data are shown in gray lines (Cued→Free condition: $n = 19$; Free→Cued condition: $n = 18$). Stars indicate significant differences determined using paired, one-tail t test: $^{*}P < 0.05$,$^{***}P < 0.001$.

exponent $= 0.5$) to a level similar to the control condition (AFA exponent > 0.5). It can be observed already that the AFA exponent started increasing directly after the first dotted line (i.e. as soon as the time window included the first stride from the free walking condition), suggesting that the participant recovered LRA quickly after the metronome was turned off. Conversely, the AFA exponent was gradually reduced after switching on the metronome in the Free→Cued condition, and reached a level lower than 0.5, corresponding to anti-persistence. The presence of a high variability across the participants and intrinsic fluctuations of the AFA exponent of each participant can be observed from the gray curves that represent each individual participant. Although there was variability across participants, the average trend among all participants was reliable and similar to the one of the representative participant (Fig. 4.3C).

On average, the AFA exponent of series of stride durations in control condition displayed consistent trend and stabilized around a value of 0.67 (Fig. 4.3C, left panel). The standard deviation of individual traces ranged from 0.05 to 0.18. In the Cued→Free condition, the mean level of LRA of the series of stride durations evolved from a stable AFA exponent of 0.5 (with individual SD from 0.017 to 0.096) to a level similar to the control condition (i.e. AFA exponent $\cong 0.69$, range of individual $SD = [0.024, 0.10]$). The differences in AFA exponents between

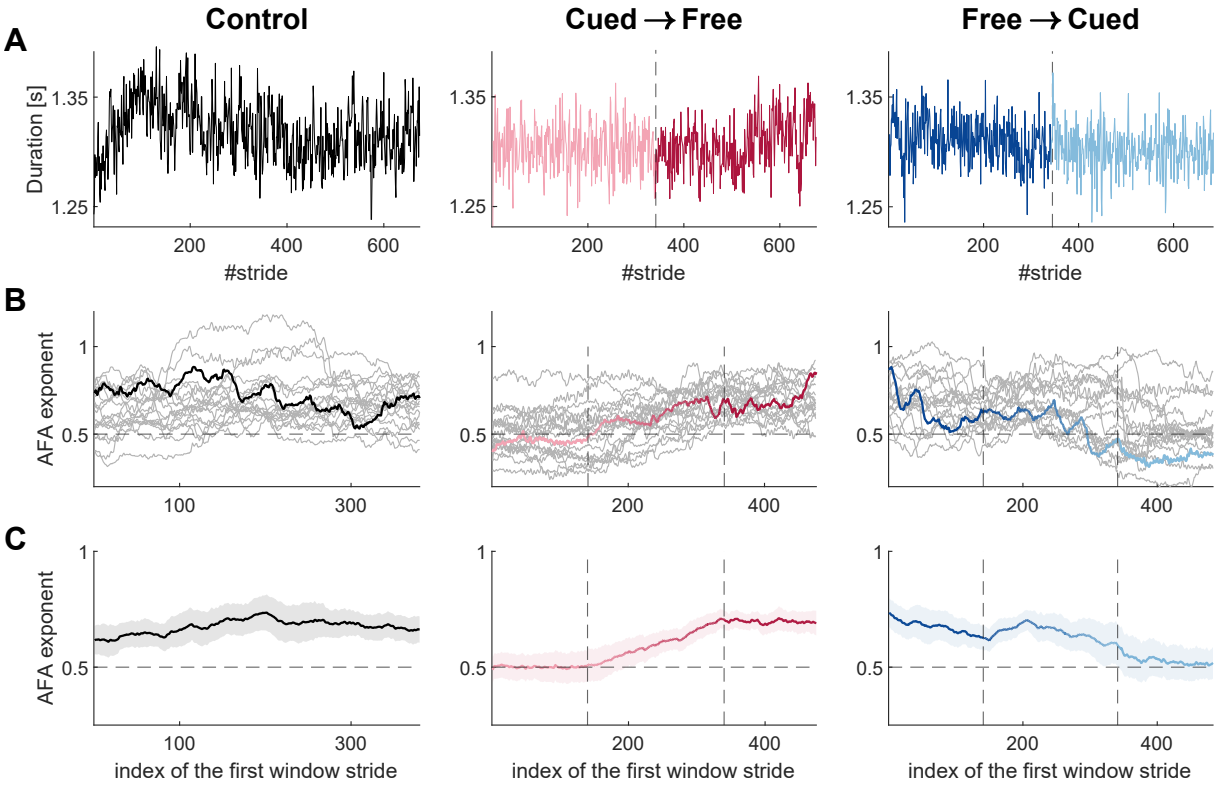


Figure 4.3 Transition analysis in behavioral data. A: series of stride duration for one exemplar participant in three conditions: control (left), Cued→Free (middle), and Free→Cued (right). Data in light shades (resp. dark shades) correspond to strides performed with (resp. without) the metronome, the dotted vertical line corresponds to the metronome switch. B: evolution of the AFA exponent of the stride series of each participant ($n = 18$) estimated by applying the AFA over a sliding window of 200 strides. Traces in color correspond to the series of the exemplar participant presented earlier. The two vertical lines indicate the interval of AFA exponents measured on windows containing strides on either side of the transition. C: same as B averaged over all participants with 95% confidence interval (shaded area).

the *Cued* and *Free* parts were smaller than those shown in Fig. 4.3A, likely due to a bias in the AFA when applied on shorter stride series corresponding to the moving window. Regarding the transition, the AFA exponent increased linearly as the AFA was applied to windows advancing after the switching off, such that the series contained increasingly more strides from the free walking phase. To determine the onset of this increase, we performed a segmented linear regression (Weiler et al. 2015). The first segment fitted data from the first AFA exponent of the average trace (x_1) to the sample x_i, restricted to a slope of 0. The second segment fitted data from x_i to x_{200}, corresponding to the stride window with an AFA exponent significantly larger than 0.5, according to the following criteria: $mean(\text{AFA exponent}) - 2 * SE > 0.5$. We then selected x_i such that the sum of the residuals of both fits was minimized. This analysis confirmed that the AFA exponent started to increase as soon as the window contained only three strides of the free walking phase, i.e. three points after the first vertical line on Fig. 4.3C, middle panel.

Similar to the Cued→Free condition, we observed a transition between two steady states in

the Free→Cued conditions, from a level of LRA corresponding to the control condition (AFA exponent= 0.67, range of individual $SD = [0.017, 0.12]$), to a level of LRA corresponding to a white noise (AFA exponent= 0.53, range of individual $SD = [0.021, 0.16]$). In contrast to the Cued→Free condition, the AFA exponent did not decrease instantaneously after switching off the metronome and even slightly increased just after the transition before decreasing.

To ensure a proper interpretation of these transitions, we considered the possibility that the discontinuity in the series, occurring when the metronome was switched on or off, artificially increased the AFA exponent. An upper bound of this increase was estimated using surrogate series featuring an abrupt change of mean value of the same magnitude as the experimental data (see Section 4.2). The AFA exponent of the surrogate Cued-Cued series reached an average value of 0.547 ± 0.014 when the AFA was applied to stride windows containing the discontinuity (Fig. 4.4A, yellow trace, between the vertical bars), while the value was on average 0.501 ± 0.004 otherwise. Regarding the *Free→Free* series, we also observed an increase in the AFA exponent for windows including the transition (mean AFA exponent $= 0.789 \pm 0.044$) compared to stride windows without any transition (0.673 ± 0.026), of even greater magnitude (Fig. 4.4B, yellow). This was explained by more pronounced discontinuities in the Free→Cued condition due to the nature of the task. The sudden need to synchronize with the rhythm of the metronome required an abrupt change if the pace adopted before the transition was different from the pace of the metronome. In contrast, if the metronome's cadence did not precisely align with the participant's natural rhythm, they could recover that natural cadence more gradually once the metronome was turned off. These results motivated the application of an adjustable offset to the second part of each series of stride duration (after metronome transition) to mitigate these discontinuities. The average evolutions of the AFA exponent of these series (i.e., after correction) were already presented in Fig 4.3C and are represented in Fig. 4.4A-B (black traces) together with the evolution of AFA exponent of the initial series (gray traces). Together, these results further refined the interpretation of a rapid increase after the transition, particularly in the case of the Cued→Free transition where the onset of the AFA exponent increase is crucial. While the AFA exponent was indeed impacted by the presence of discontinuities, Cued-Cued surrogates revealed that this effect remained limited in this condition. In addition, we still observed a rapid increase of the AFA exponent after correction, consolidating the assumption that this rapid increase reflected a genuine change in control strategy.

Collectively the behavioural results highlighted a rapid transition of the AFA exponent between the values corresponding to Cued and Free conditions measured separately. These transitions were more pronounced when measured based on the AFA in comparison with the series standard deviation (and after controlling for average offsets), suggesting that LRA capture subtle changes in gait regulation that may be more difficult to identify based on standard metrics. However, since the AFA exponents were evaluated on series of 200 strides, it was difficult to precisely establish the number of strides required to adapt to the removal/addition of the metronome. The seemingly gradual change in the AFA exponent was in fact a consequence of the method used, consisting of applying the AFA to windows gradually containing more and more strides occurring after the switch of the metronome. To assess the transition in more

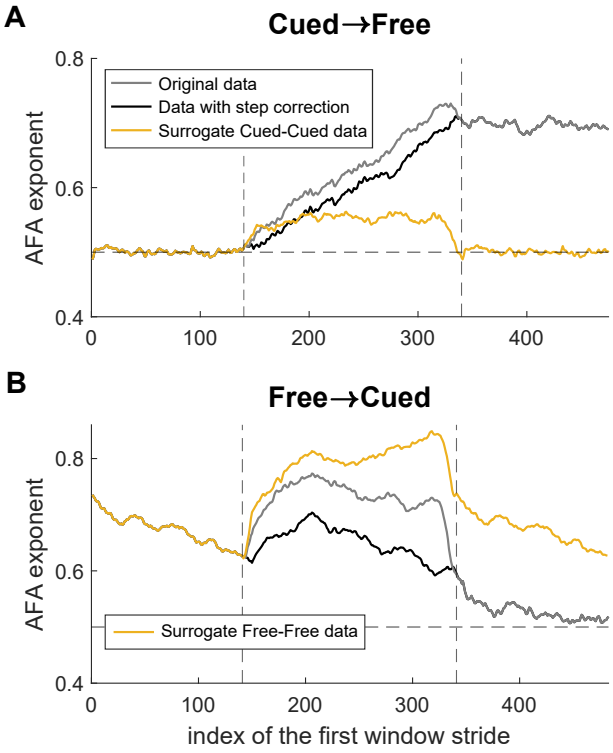


Figure 4.4 Analysis of the impact of discontinuities in stride series on the adaptive fractal analysis (AFA) exponent in Cued→Free (A) and Free→Cued (B) conditions. Mean evolution of the AFA exponent of stride series before (gray) and after (black) applying an offset to the second part of the series to reduce the discontinuities (i.e., difference in mean value at the metronome shift). In yellow, mean evolution of the AFA exponent of surrogate data built to reproduce the discontinuities without any change of task (Cued→Cued and Free→Free series).

detail, it was necessary to replicate them in a computational model in which we could simulate and test different hypotheses. Indeed, the almost instantaneous increase observed during the transition from Cued to Free condition, as soon as the time window included data from the free walking conditions, suggested that participants' sensorimotor control of gait could change rapidly. Our modeling work confirmed this hypothesis.

4.3.2 Model

With the model, we tested different transitions in the control policy and assessed their consequences on the measured AFA exponents applied similarly to simulated and recorded series. We simulated strides series using different candidate parameters to investigate how we could reproduce participants' behavior. Our basic premise was that gait features were flexibly regulated, allowing for fluctuations in stride duration and length in the absence of a metronome, whereas a control strategy with stricter regulation of stride duration was applied with a metronome to comply with the task instruction. A target duration (T^*) was iteratively computed for each stride to synchronize with the beat of the metronome (see Section 4.2, Eq. 4.3) and errors on this evolving target were penalized in the cost function, weighted by the parameter ω_{met} (Eq. 4.4). To match the average AFA exponent reported in the experimental

data (Fig. 4.2), this parameter was set to 0.35 when gait was guided by a metronome. When walking freely, without any imposed cadence, this parameter was set to 0.

In the simulations presented below, the transition between these two values was linear and had a rise time of 1, 50 or 100 strides (Fig. 4.5A, green, yellow and red respectively). For each of these scenarios, we simulated 100 series of 700 strides and reported the mean evolution of the AFA exponent of all these series on Fig. 4.5B with the same sliding-window analysis as for the experimental data. In the Cued→Free condition, only an instantaneous transition between $\omega_{met} = 0.35$ and $\omega_{met} = 0$ allowed to reproduce the evolution of LRA observed experimentally, i.e., an immediate increase of the AFA exponent after the switching of the metronome. We performed the same segmented linear fit analysis as for the experimental data and found that the green trace, corresponding to an instantaneous switch of the control, started to increase seven strides after the first vertical line, as compared with three strides for the experimental data. Thus, the instantaneous increase observed experimentally likely reflected an instantaneous change in the control strategy when the metronome was turned off.

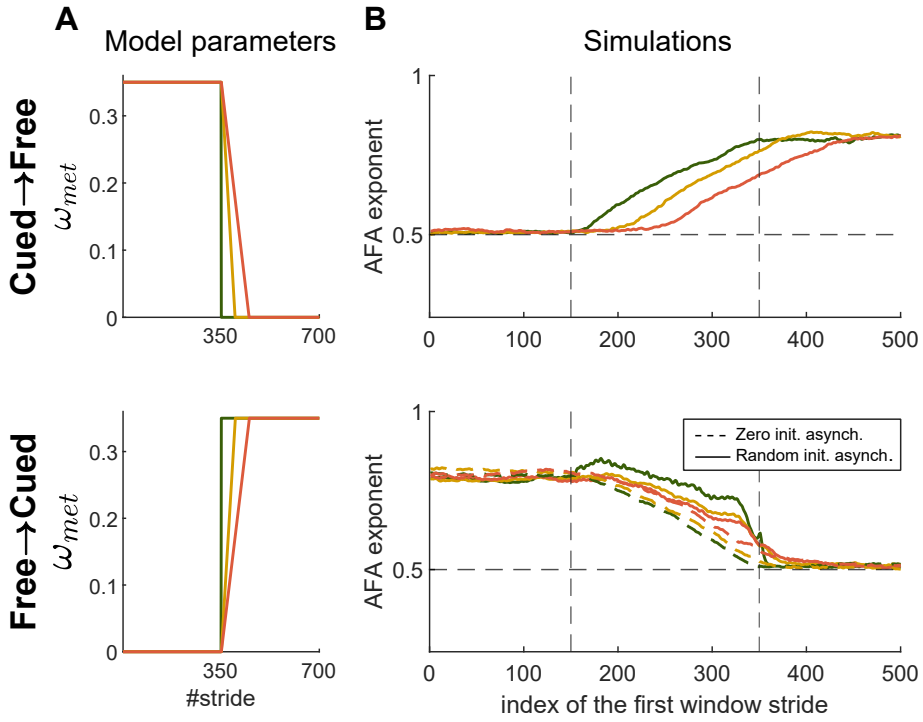


Figure 4.5 Transition analysis in simulations. A: value of parameter ω_{met} at each stride for three transition rates under study in Cued→Free (top) and Free→Cued (bottom) conditions. B: evolution of the AFA exponent averaged over 100 simulated series. The colors indicate the parameters used to generate the stride series. In Free→Cued condition (bottom), the colored dotted traces correspond to an asynchrony with the metronome at the transition set to zero, solid lines correspond to a random initial asynchrony.

In the Free→Cued condition, we also manipulated the asynchrony at the transition when the metronome was turned on. The three solid lines correspond to a random initial asynchrony, while the dotted lines correspond to an initial asynchrony of zero, i.e. perfect synchronization

from the first stride. It appeared that a non-zero initial asynchrony, consistent with the experimental conditions, with an instantaneous transition in the parameter ω_{met} reproduced all features of the data. Among simulations including a random initial asynchrony, transitions at 3 different rates were tested. These three transitions exhibited an AFA exponent greater than 0.5 at the second vertical line, all three similar to experimental data (AFA exponent $= 0.59 \pm 0.046$). Finally, only an instantaneous transition between $\omega_{met} = 0$ and $\omega_{met} = 0.35$ with initial random asynchrony reproduced the local increase in the AFA exponent occurring directly after the transition in the experimental data. To further understand the origin of this increase, we analyzed each simulation separately. We computed the difference between the maximum AFA exponent following the transition and the AFA exponent at the transition, and found a correlation coefficient of 0.57 between this variable and the initial asynchrony. The model thus suggested the following explanation for the transient increase reported in the Free→Cued transition: a random initial asynchrony, combined with immediate strong regulation, induced important deviations from the average pace for a few strides to synchronize with the metronome. This would yield locally changes in the time series and transient variations in the AFA, similarly to the effect of a sudden shift in mean value on the AFA exponent (Fig. 4.4).

We selected the parameters that best fitted the behavior observed experimentally, i.e. an instantaneous shift right after the switch in both conditions, and a random initial asynchrony in the Free→Cued condition. With these parameters, we simulated 20 new series for each condition. As we did with the participants data, we divided the series into two parts at the moment when the metronome was turned on/off (exactly in the middle of the series for the simulations) and compared their AFA exponents and standard deviations (Fig. 4.6).

The simulated series exhibited an average AFA exponent below 0.5 in Cued parts of the series (0.42 ± 0.05 in Cued→Free condition), reproducing the anti-persistent stride series that appeared only when applying the AFA to longer series (here 350 strides), similarly to experimental data. The AFA exponent of the simulated series of stride duration was significantly impacted by the metronome (Cued→Free: $\Delta AFA = 0.34 \pm 0.10$, $t(19) = 15.23$, $p < 10^{-4}$; Free→Cued: $\Delta AFA = -0.26 \pm 0.09$, $t(19) = -13.14$, $p < 10^{-4}$), in a comparable way to the participants' stride series (Fig. 4.6A). The effect sizes were $d = 9.3$ in the Cued→Free condition and $d = -4.7$ in the Free→Cued condition. We also observed a decrease in standard deviation when the metronome was activated in both conditions as shown in Fig. 4.6B (Cued→Free: $\Delta std = -0.0018 \pm 0.0014[s]$, $t(19) = -7.11$, $p < 10^{-4}$; Free→Cued: $\Delta std = 1.15 * 10^{-3} \pm 0.0016[s]$, $t(19) = 3.46$, $p = 0.0026$). The effect sizes were $d = 5.2$ in the Cued→Free condition and $d = -1.2$ in the Free→Cued condition. Effect size on simulated data (both SD and AFA exponent) were larger than on experimental data, due to the fact that inter-subject variability was not included in the model. However, the magnitudes of the differences between Cued and Free walking was similar and the effect was greater on the AFA exponent than on the SD both in simulated and experimental data.

From the same 20 simulations, we extracted the series of asynchronies between heel strikes and metronome beats in the Cued parts of the series. In accordance with the literature, theses series displayed a strong persistence, with an average AFA exponent equal to 0.91 ± 0.059

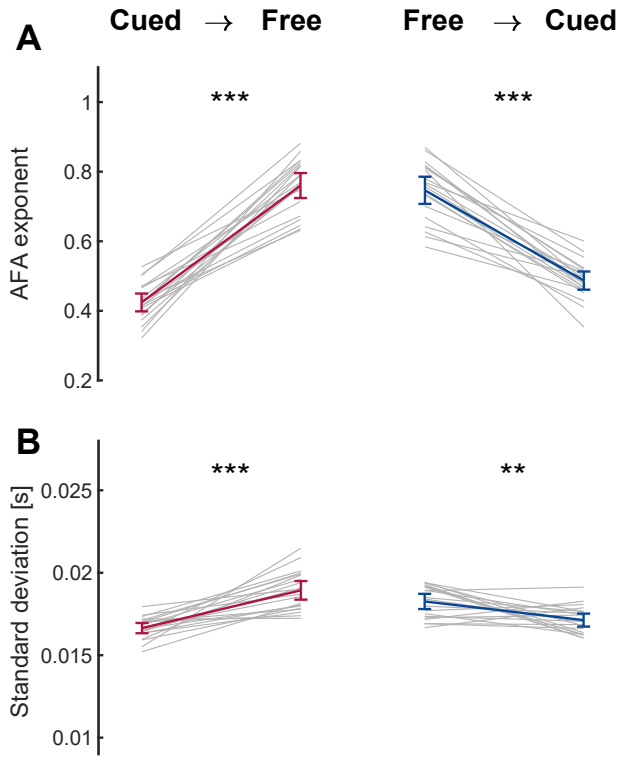


Figure 4.6 Analysis of differences between *Cued* and *Free* stride series in simulations. Adaptive fractal analysis (AFA) exponent (A) and standard deviation (B) of simulated series of stride durations before and after the switch of the metronome in Cued→Free condition (left) and Free→Cued condition (right). Group average and 95% confidence interval are shown in color and individual simulations' data ($n = 20$) are shown in gray lines. Stars indicate significant differences determined using paired, one-tail t test: $^{**}P < 0.01$,$^{***}P < 0.001$.

(Delignières and Torre, 2009; Vaz, Groff, et al. 2019). The mean asynchrony was below $10^{-4}[s](\cong 0)$ and the standard deviation of the series was 0.0392 ± 0034 [s]. Since this variable was not measured in the protocol, we were unable to compare these values to experimental data. While the expected temporal structure of variability seemed successfully reproduced by the model, some authors demonstrated that people tend to adopt anticipatory strategies and strike before the tone (Jordão et al. 2022; Vaz, Groff, et al. 2019). They therefore displayed a negative mean asynchrony, something that we did not capture in our simulations.

We performed a sensitivity analysis to explore the impact of changes in the parameters. For $\omega_v = \omega_{POP} = 2.5$, dividing or multiplying ω_{met} by 2 had a significantly impact on the AFA exponent compared to $\omega_{met} = 0.35$ but not on the standard deviation. When increasing this parameter, the regulation of the asynchrony was strengthened and the series of stride durations became more anti-persistent, with lower value of AFA exponent. In contrast, a decrease of this parameter resulted in an increase of the AFA exponent with values above 0.5. Dividing ω_{POP} by 2 ($\omega_{POP} = 1.25$) significantly increased the standard deviation of series of stride durations for $\omega_v = 2.5$ and $\omega_v a = 0.35$, but multiplying it ($\omega_{POP} = 5$) had no impact both on the standard deviation and AFA exponent. By multiplying and dividing ω_v by 2, the AFA exponent and standard deviation of stride durations did not change significantly, the effect was rather

on the stride velocity, which is not of interest here. In addition, we assessed the impact of smaller changes in ω_{met}. Changing ω_{met} by $\pm 10\%$ had negligible effect on the standard deviation and the AFA exponent. Results were therefore robust to small changes in the cost function.

To summarize, the series of stride durations of participants exhibited anti-persistence and a slight decrease in standard deviation when synchronizing their gait with an isochronous metronome. When turning off the metronome in a Cued→Free condition, the AFA exponent rapidly increased to stabilize around a value similar to the self-paced condition, indicating the presence of LRA. In contrast, in the Free→Cued condition, the AFA exponent slightly increased shortly after the transition then linearly decreased. These transitions were then reproduced in the model by an instantaneous change in the cost function for both conditions, provided that a random initial asynchrony was included in the model for the Free→Cued condition.

4.4 Discussion

We investigated the time course of behavioral changes induced by synchronizing walking with a metronome. Indeed, we and other authors observed that synchronization of gait to an auditory stimulation profoundly modifies the statistical persistence of series of stride duration, with little effect on the mean and standard deviation of the same series. To characterize the transition from walking with to without a metronome and vice versa, 21 healthy young participants were asked to walk overground in three conditions each lasting 15 minutes. The first condition was a control condition, with no constraints, to measure the participants' natural pace. In the following two conditions, the metronome was activated during either the first or second half of the session. We measured the evolution of the AFA exponents of these series over a sliding window and reproduced these traces in the framework of stochastic optimal control. In the natural walking conditions (i.e. without metronome), the model suggested that statistical persistence resulted from a selective and coordinated regulation of stride length and duration while maintaining a constant target speed. Conversely, gait control when guided by a metronome was modeled by adding a cost regulating the asynchronies between the metronome beat and heel strike, resulting in anti-persistent stride series and accounting for the observed changes of standard deviation. This model allowed to test several transitions between these two control modes and compare the resulting trends of AFA exponents with the experimental data. The results of the experiments were compatible with the simulations involving instantaneous switching of the control policy in both conditions, including an initial random asynchrony in the Free→Cued transition consistent with the experimental setting.

The model showed here that the emergence of anti-persistence in series of stride duration arises as a direct consequence of the presence of persistence in the series of asynchronies, which represent the integration of stride intervals. Although not directly measured in the experimental data, data from previous synchronization studies and simulated data consistently exhibited statistical persistence in asynchronies (Chen, Ding, and Kelso, 1997; Delignières and Torre, 2009). In the model, this was attributed to a flexible control mechanism (i.e., characterized by low control gains) acting on this variable, in a similar way to previous studies which at-

tributed these statistical properties to a partial correction of asynchronies (Mates, 1994; Pressing and Jolley-Rogers, 1997). This is also analogous to the role of flexible control in the regulation of stride duration and length when walking freely on a treadmill in Dingwell, John, and Cusumano (2010). In this study, they demonstrated that the level of control strongly determines the statistical persistence of the associated gait parameter. In particular, they showed that reducing control gains increased the level of persistence in series of stride durations whereas over-correcting the errors in velocity resulted in anti-persistent series. In a recent study, higher control gains were associated with Parkinson's disease, as this population often exhibits altered persistence, suggesting they were unable to exploit the task redundancy introduced when only a speed constraint is applied (Vandamme et al. 2023). Here we showed that anti-persistent series of stride durations arose not from over-correction of this gait parameter, but from partial correction of the integral of these series.

Furthermore, we suggest that humans rapidly adjusted the control policy, potentially within a single stride, to comply with the task requirements, which was followed by a gradual change in LRA. This conclusion is supported by the fact that the observed changes in the AFA exponent were consistent with simulations involving a rapid task-dependent control adjustment. This is all the more striking given that the two transitions tested here were very different in nature. They showed distinct patterns of change in the average AFA exponent, which could nevertheless both be attributed to a rapid change in control in the model. In particular, we observed an unexpected increase in the AFA exponent at the activation of the metronome, then followed by a gradual decrease (Fig. 4.3C). This observation did not directly follow from a symmetrical switch in control strategy (simulations not shown). Yet, it was reproduced in the model by considering the fact that the initial asynchrony at the transition was random. This suggests that variations in LRA, both in amplitude and timing, could be fully explained by a very rapid task-dependent modulation of gait control.

Our interpretation emphasizes the role of rapid changes in control strategy without considering the effect of non-linear interactions that occur during gait control. While non-linearities inherent to the biomechanics of walking are not necessary to explain the transitions, this does not reject the possibility that they may contribute to the presence of persistence and anti-persistence. In that sense, Gates, Su, and Dingwell (2007) showed that non-linearities were sufficient to explain LRA. We believe that both task-dependent control and complex biomechanics likely participate in the selection of efficient control strategies across individuals, and that the interaction between these factors remains to be investigated in more detail. It is possible to connect this model with continuous-time approaches (Gates, Su, and Dingwell, 2007; West and Scafetta, 2003) and integrate it with musculoskeletal frameworks (De Groote et al. 2016; Eskinazi and Fregly, 2018). Such extensions would be valuable for characterizing the underlying neurophysiological mechanisms of cued walking in greater detail while taking biomechanical constraints into account.

The minimalistic model presented here, designed with a high level of abstraction, does not specify how different neural substrates implement or switch between control policies. Synchronizing movement with rhythmic auditory cues likely requires distributed processing across

a large network, including sensorimotor cortex, supplementary motor area, premotor cortex, basal ganglia, and cerebellum (Grahn and Brett, 2007; Repp and Su, 2013). The mobilization of these supraspinal structures may either supplement or override the automated regulation of free walking. Some authors argued that the disappearance of correlations under metronomic conditions could be interpreted as a complete overriding of the locomotor system's dynamics by supraspinal influences (Hausdorff, Purdon, et al. 1996). Conversely, others emphasized the fact that LRA were still present under metronomic conditions in the series of asynchronies, suggesting that the source of LRA was still at work but expressed differently (Delignières and Torre, 2009). Regarding the transitions, our framework enforces abrupt transitions on a timescale corresponding to a stride (i.e., about 1s) to capture the observed behaviour. However, it does not specify how the nervous system detects a task change or triggers a switch in control policy. We hypothesize that the detection and triggering occur at a shorter timescale. For instance, the typical mean reaction time to the onset of an auditory stimulus is approximately $140 - 150$ ms (Welford et al. 1980). Here, we hypothesized that the introduction or removal of the metronome was perceived and used to change the control strategy almost instantaneously. Although evaluating the metronome frequency may require at least a couple of strides, our assumption is based on the fact that the auditory stimulus was salient and that the transition from Cued to Free walking required in the model a rapid switch. However, future extensions of the model could incorporate an additional module that estimates the transition less directly.

One of the main limitations of this study was the lack of assessment of the synchronization performance of participants through the measure of the asynchronies between the heel strikes and metronome beats. The critical impact of these asynchronies on the evolution of LRA at the Free$\rightarrow$Cued transition was unexpected, explaining why they were not included in the experimental design. Since this metric seems to play a central role in the control mechanisms, investigating its evolution in detail at the transitions could improve the interpretation of the evolution of AFA exponents. Synchronization performance might also directly impact the stride-to-stride variability (Moumdjian, Buhmann, et al. 2018), which would explain the slightly different results in the effect of the metronome on the standard deviation from one study to another.

It also remains unclear how the metronome interacts with the regulation toward the preferred pair of stride length and duration. This pair is partially defined by the biomechanics constraint of each subject, and was associated with the gait parameters that minimizes the energetic cost associated to the stride itself (Kuo, 2001; O'Connor et al. 2012). In free walking (without a metronome), there is a balance between the cost of the regulation (represented in the model by the term weighted by ω_u in Eq. 4.4) and the additional cost of a suboptimal pair (weighted here by ω_{POP}). Indeed, although this pair may be preferable in terms of energetic cost, it can also lead to significant changes from stride to stride, which are potentially costly from the perspective of task-dependent modulation. In this context, the metronome constraint often requires the adoption of different gait parameters from the preferred pair, thus introducing a conflict between these two terms of the cost function. The sensitivity analysis, used to test the impact of the parameter ω_{POP} did not allow to determine whether a reduction of this

parameter occurred when the metronome was activated to mitigate this conflict, this parameter having no impact on the statistical persistence of the stride duration under metronomic constraints (i.e., when $\omega_{met} = 0.35$). However, it did have an impact on the variability of these same series. Participants may adopt different strategies in this regard, explaining the variation in synchronization performance and in the effect of the metronome on the stride-to-stride variability.

In this paper, we chose to study the impact of the synchronization to rhythmic auditory cues with no variability. However, there is a growing body of literature advocating the use of fractal-structured cues, as they do not impact the level of persistence in gait variability of healthy adults (Marmelat, Torre, et al. 2014). This type of cues could also restore healthy gait patterns in population exhibiting a loss of complexity, such as older adults and patients with Parkinson's disease (Hove et al. 2012; Lheureux et al. 2020; Rhea et al. 2014; Vaz, Knarr, and Stergiou, 2020). Although this could improve some biomarkers of gait control, there is no evidence that the mechanism underlying the recovery of statistical persistence of gait variability with fractal cues is equivalent to the natural emergence of these patterns. In particular, in the model presented here, the persistence arose from the regulation of variability which from assumptions originated in sensorimotor noise, which in principle is not correlated with an internal fractal timer. Therefore, although lower levels of persistence have been associated with an increased risk of falling (Dierick et al. 2021; Hausdorff, 2007), the mechanism by which persistence levels restored artificially could improve gait control requires careful investigations. In addition, walking with invariant cues does not result in loss of complexity but rather in a shift of this complexity towards series of asynchronies. The model presented here offers an opportunity to investigate the use of fractal cues in the future. Like the type of cues (fractal-like, invariant or random), two sensory modalities – auditory or visual – in synchronization task can also affect gait parameters differently. In finger tapping synchronization task, it has been shown that the strength of persistence in the series of asynchronies depended on the sensory modality (Chen, Repp, and Patel, 2002). These results seem to generalize to gait synchronization since a study from Vaz and colleagues (Vaz, Rand, et al. 2020) showed that visual cues improved synchronization and had a different impact on step length persistence than auditory cues. Again, the model presented here provides an opportunity to investigate this further.

To conclude, this study highlights that transitions from self-paced walking to synchronization could result from instantaneous switches in control strategy dictated by a cost-function that exploits task redundancy when possible, and regulates asynchronies when constrained. Our study offers a novel interpretation to the emergence of anti-persistence in series of stride duration when gait is guided with a metronome as the result of regulation of strides to minimize asynchronies. Finally, this study proposes a new methodological framework that could be applied in future research to explore the use of cues in gait rehabilitation and its influence on gait control.

7

Conclusion and perspectives

THIS thesis is grounded in several decades of research on the temporal structure of gait variability, initiated by the seminal observations of Hausdorff, Peng, et al. (1995), who demonstrated that stride-to-stride fluctuations exhibit long-range autocorrelations (LRA). Since then, extensive work has shown that this gait pattern is altered in aging, neurological disorders, and experimentally constrained walking, highlighting its potential clinical relevance as markers of locomotor control. Despite this growing body of evidence, the origin and functional significance of LRA remain debated. The present thesis aimed to extend the model proposed by Dingwell, John, and Cusumano (2010), who interpreted the presence of LRA within an optimal control framework. In this framework, LRA emerge from the flexible and coordinated regulation of stride duration and stride length, allowing errors to persist within a task-relevant manifold for which walking speed remains invariant. The flexibility of the stochastic optimal control framework, along with its ability to incorporate a wide range of task constraints within a single unified formulation, motivates its adoption as the primary modeling approach in this work.

7.1 Main contributions

In Chapter 3, we first investigated whether and how the framework proposed by Dingwell, John, and Cusumano (2010) could be adapted to simulate gait impairments experienced by patients suffering from Parkinson's disease and demonstrated that the reduction of LRA commonly observed in patients could emerge from stronger stride-to-stride corrections implemented to mitigate the impact of noise. We also highlighted that this loss of persistence may reflect a reduced ability or willingness to exploit task redundancy, resulting in a tighter regulation around a preferred pair of gait parameters. We then explored the effect of robotic gait assistance and showed that an oscillator-based assistance, modeled as a low-pass filter acting on gait dynamics, could restore the presence of LRA in simulated stride duration series. Together, these findings provided theoretical support for developing gait assistance technology for patients with a view towards reducing the risk associated with falling as the disease pro-

gresses.

In Chapter 4, building on the idea that LRA emerge from the continuous regulation of gait on a stride-by-stride basis, we investigated how these statistical properties evolve when gait control is abruptly modified by external constraints. Specifically, we examined the transitions between self-paced walking and walking synchronized to an isochronous metronome. We evaluated the LRA over a sliding window and reproduced the observed evolutions using simulations. We further extended the framework developped in Chapter 3: gait control when guided by a metronome was modeled by adding a cost regulating the asynchronies between the cue and heel strike, resulting in anti-persistent stride series and accounting for the observed changes of standard deviation. The model then allowed us to test different changes in control policies at the transitions, and we showed that experimental data were compatible with an almost instantaneous adjustment of the control policy. These results reinforced the link between the statistical structure of gait variability and gait regulation and suggested that healthy adults rapidly and efficiently adapted their gait to task requirements, while providing a novel framework for studying the mechanisms underlying rhythmic cueing and its potential applications in gait rehabilitation.

In Chapter 3 and Chapter 4, we therefore identified three distinct gait regulatory strategies, each associated with a characteristic variability signature (persistent, random, and anti-persistent fluctuations). Based on these interpretations, in Chapter 5, we hypothesized that geometric descriptors of stride-by-stride adjustments could complement, and potentially overcome some limitations of conventional LRA measures, which typically require long recordings. Using both simulations and experimental data, we compared the AFA exponent with two geometric indicators: the correlation between stride length and stride duration, and the magnitude of stride-by-stride corrections along a goal-equivalent manifold (GEM), defined as the set of stride length–duration combinations yielding the same walking speed. The results demonstrated that corrections along the GEM reliably discriminated between free and cued walking and maintained a strong discriminatory power even for shorter stride series. Furthermore, this geometric framework accurately reproduced the influence of synchronization errors during transitions to cued walking, providing further support for the proposed control models. Overall, these findings strengthened the view that LRA arise from the flexible regulation of a redundant locomotor system, but also opened new perspectives for the assessment of gait regulation in both experimental and clinical contexts.

Finally, in Chapter 6, we applied the methodology developed in Chapter 4 to investigate whether patients with Parkinson's disease could rapidly and efficiently modulate gait regulation despite basal ganglia dysfunction. We examined transitions between free walking and synchronization with rhythmic cues and hypothesized, and interpreted the results in light of current theories associating basal ganglia and the evaluation of motor cost. The results revealed that the amplitude of the modulation in gait control was comparable between patients with PD and age-matched controls. However, the dynamics these adjustments during condition transitions were partially altered in the PD group, showing a tendency towards slower changes following the metronome onset. The interpretation of these results was strengthened

by similar results observed in two reaching tasks, making it unlikely that the effects reflected task-specific characteristics and instead supporting the notion of preserved of behavioral flexibility. These findings suggest that the transformation of internal representations of movement costs and rewards into efficient control policies does not rely exclusively on the basal ganglia, at least within the context of our paradigm. Rather, the neural mechanisms responsible for modulating control policies may remain functionally preserved in PD, or compensatory mechanisms within alternative circuits may support these functions.

7.2 Future work

7.2.1 LRA and gait adaptability

The presence of LRA has been often interpreted as a marker of adaptability in biological systems. According to several authors, gait complexity would emerge from the interactions among numerous subsystems, which operate at different timescales. In such systems, a perturbation of one sub-component is less likely to affect the system globally. Therefore, complexity has been associated with a greater capacity to cope with internal and external perturbations. Similarly, other authors suggest that variability in general contribute to robustness by distributing mechanical loads across tissues and muscle fibers. Within this framework, LRA are often considered as a signature of "healthy" variability arising from fluctuations that are largely task-irrelevant and therefore do not need continuous corrections. More recently, it was suggested that distinct types of fractal properties in sensorimotor behaviour characterize, on the one hand impaired functional ability, and on the other hand internal adaptations for maintaining performance despite the imposed constraints (Torre et al. 2019). Within the framework developped in this thesis, strong stride-to-stride corrections emerge when gait is regulated toward a highly specific target, leading to random or anti-persistent fluctuations. Conversely, when the control objective is less restrictive, deviations can persist over longer timescales, producing LRA while reducing the need for continuous corrective actions. Such a strategy may allow the system to accommodate perturbations at a lower energetic cost.

Still, the relationship between LRA and adaptability remains largely theoretical, as relatively few studies have directly examined whether fractal gait dynamics predict adaptive performance (Torre et al. 2019). Notably, Ducharme, Liddy, et al. (2018) and Ducharme, Kent, and Van Emmerik (2019) found no association between LRA measured during unperturbed walking and subsequent locomotor adaptation on a split-belt treadmill in both young and older adults. Further work is therefore needed to determine which aspects of adaptability, if any, are captured by fractal gait measures.

7.2.2 Foot placement

The present framework is primarily focused on temporal and spatial parameters of forward progression, namely stride duration and stride length. An important direction for future work would therefore be to extend the framework to include variables related to foot-placement

control. Foot placement plays an important role in the regulation of the walking pattern and is influenced by the dynamics of the center of mass, particularly in the mediolateral direction. Previous work suggests that foot placement and step-width regulation are controlled, at least partly, independently from stride duration and stride length (Collins and Kuo, 2013). Interestingly, step-width variability has also been shown to exhibit LRA (Franz et al. 2017; Stout et al. 2016). Extending the current model to include foot placement, based on existing models such as Dingwell and Cusumano (2019), could therefore provide an opportunity to investigate how the temporal organization of variability differs across gait parameters and how these parameters are coordinated. In particular, it could be examined whether the emergence of LRA in step width can be explained by the same balance between corrective actions and tolerance of deviations proposed in the present framework for stride duration and stride length. Alternatively, foot-placement variables may require distinct control policies because they are subject to different biomechanical and sensory constraints. Such an extension could also provide a more comprehensive account of how multiple gait parameters are regulated simultaneously. This may be particularly relevant in clinical populations, where alterations in the coordination between center-of-mass dynamics and foot placement have been reported (Lang et al. 2026). More generally, incorporating foot placement would allow future work to move beyond the regulation of forward progression and investigate whether the temporal organization of variability reflects common or parameter-specific principles of locomotor control.

7.2.3 Fractal cueing

The present framework may also have important implications for the study of fractal cueing strategies in gait rehabilitation. By explicitly linking the statistical structure of gait variability to the underlying regulation processes, it provides a useful tool for investigating how different external cues modulate gait control and, in turns, shapes the structure of gait variability. A growing body of work has suggested that fractal auditory cues can restore the LRA, which are typically reduced in several pathological populations (Lheureux et al. 2020; Rhea et al. 2014). This line of work is partly motivated by the observation that isochronous cueing tends to disrupt the natural fractal structure of gait variability. Because reduced LRA have been associated with increased fall risk in several clinical populations (Hausdorff, 2007), this cue-induced alteration of gait dynamics was initially interpreted as potentially maladaptive, reflecting an "unnatural" pattern of locomotor control. However, the reduction of LRA observed during synchronization with an isochronous metronome should not automatically be interpreted as a loss of stability, as rhythmic auditory stimulation has been shown to improve gait outcomes and reduce falls in Parkinson's disease (Thaut, Rice, et al. 2019).

In addition, the clinical significance of an artificial restoration of LRA through fractal cueing remains uncertain. Indeed, the mechanisms responsible for the reappearance of LRA under fractal cueing may differ fundamentally from those responsible for their spontaneous emergence during natural walking, which has been attributed to a flexible and coordinate regulation of gait parameters (Dingwell, John, and Cusumano, 2010). Future studies should therefore determine whether cue-induced restoration of LRA translates into clinically meaningful outcomes, such as improved balance, enhanced adaptability to environmental perturbations, or

reduced risk of falls. From a rehabilitation perspective, these functional outcomes may ultimately be more relevant than the restoration of a specific statistical signature.

7.2.4 State estimation

Beyond the extensions discussed above, another promising direction would be to explicitly incorporate a state-estimation process. The current framework assumes that the state of the locomotor system is perfectly known, whereas gait regulation relies on noisy sensory information that must be integrated across multiple modalities. Introducing a state estimator, as proposed in previous models of foot placement (Maeda et al. 2017), could help distinguish between changes in the control policy itself and changes arising from an imperfect estimation of the current gait state. Such an extension may prove particularly relevant for understanding differences between cueing modalities such as auditory and visual, which are known to induce distinct adaptation dynamics and likely rely on partly different neural pathways and sensory processing mechanisms (Vaz, Rand, et al. 2020). It would also provide a framework for investigating the role of proprioceptive deficits, which are frequently reported in Parkinson's disease (Konczak et al. 2009).

7.2.5 Selection of preferred gait parameters

Finally, a potential extension of the current model concerns the selection of preferred gait parameters. At present, the preferred stride duration and stride length are imposed rather than emerging from an optimization process. Future developments could therefore incorporate mechanisms governing the selection and adaptation of these preferred values. Such an approach would provide a closer link with theories proposing that locomotor behavior results, at least in part, from the optimization of energetic expenditure, consistent with (Kuo, 2001; Kuo et al. 2005) In these models, preferred gait emerges from the selection of coordinated step length and cadence combinations that minimize metabolic cost for a given speed, reflecting trade-offs between step-to-step transition costs (push-off work) and swing-limb dynamics. Other frameworks extend this perspective by modeling gait selection at a more mechanistic level, where muscle activations, tendon dynamics, and joint-level coordination are explicitly represented. In this context, preferred gait emerges as the solution of a high-dimensional optimal control problem in which muscle-driven simulations reproduce experimentally observed walking patterns by minimizing physiological cost functions such as metabolic energy, muscle effort, or activation squared terms (Falisse et al. 2019). Importantly, energy minimization alone is unlikely to fully explain gait choices, as factors such as stability, comfort, sensory feedback, and environmental and task constraints also contribute to the selection of walking patterns (Antos et al. 2022). Still, integrating these complementary approaches would allow to address not only how gait is regulated around a preferred state, but also how this preferred state itself emerges and adapts in response to external cues, environmental constraints, or pathology.

7.3 Concluding words

Overall, this thesis demonstrates that a relatively simple framework, grounded in the regulation of gait variability, can account for a broad range of observations. Starting from a parsimonious model of stride-to-stride regulation, the framework was progressively extended to explain alterations associated with Parkinson's disease, the effects of rhythmic cueing, the dynamics of transitions between control strategies, and the geometric organization of gait variability. The model repeatedly reproduced experimental findings obtained in different populations, under different task constraints, and across independent studies. This convergence supports the idea that the seemingly complex dynamics of human movement may emerge from a small number of fundamental control principles governing how variability, redundancy, and task goals are balanced. Beyond providing new insights into gait regulation and behavioral flexibility, the work presented here illustrates the value of parsimonious models as tools for integrating experimental observations, generating testable predictions, and guiding future developments in both basic motor control research and clinical rehabilitation.

Bibliography

Albers, C., Mirelman, A., Avanzino, L., Bloem, B. R., Botta, A., van der Cruijsen, J., de Lange, E., Maidan, I., Nieuwboer, A., Pelosin, E., Tosserams, A., Weerdesteyn, V., Gilat, M., & Nonnekes, J. (2026). Understanding cueing strategies for gait impairments in parkinson's disease: Protocol of the multicenter unite-pd study [e70382 EJN-2025-09-33228.R1]. *European Journal of Neuroscience*, *63*(2), e70382.

Almurad, Z. M., & Delignières, D. (2016). Evenly spacing in detrended fluctuation analysis. *Physica A: Statistical Mechanics and its Applications*, *451*, 63–69.

Almurad, Z. M., Roume, C., Blain, H., & Delignières, D. (2018). Complexity matching: Restoring the complexity of locomotion in older people through arm-in-arm walking. *Frontiers in Physiology*, *9*, 1766.

Almurad, Z. M., Roume, C., & Delignières, D. (2017). Complexity matching in side-by-side walking. *Human movement science*, *54*, 125–136.

Antos, S. A., Kording, K. P., & Gordon, K. E. (2022). Energy expenditure does not solely explain step length–width choices during walking. *Journal of Experimental Biology*, *225*(6), jeb243104.

Asci, F., Falletti, M., Zampogna, A., Patera, M., Hallett, M., Rothwell, J., & Suppa, A. (2023). Rigidity in Parkinson's disease: evidence from biomechanical and neurophysiological measures. *Brain*.

Ashkenazy, Y., Hausdorff, J. M., Ivanov, P. C., & Stanley, H. E. (2002). A stochastic model of human gait dynamics. *Physica A: Statistical Mechanics and its Applications*, *316*(1-4), 662–670.

Åström, K. J. (1970). *Introduction to stochastic control theory*. Academic Press.

Azulay, J.-P., Mesure, S., & Blin, O. (2006). Influence of visual cues on gait in parkinson's disease: Contribution to attention or sensory dependence? *Journal of the neurological sciences*, *248*(1-2), 192–195.

Baker, K., Rochester, L., & Nieuwboer, A. (2008). The effect of cues on gait variability—reducing the attentional cost of walking in people with parkinson's disease. *Parkinsonism & related disorders*, *14*(4), 314–320.

Bartsch, R., Plotnik, M., Kantelhardt, J. W., Havlin, S., Giladi, N., & Hausdorff, J. M. (2007). Fluctuation and synchronization of gait intervals and gait force profiles distinguish stages of Parkinson's disease. *Physica A: Statistical Mechanics and its Applications*, *383*(2), 455–465.

Bassingthwaighte, J. B., & Raymond, G. M. (1994). Evaluating rescaled range analysis for time series. *Annals of biomedical engineering*, *22*(4), 432–444.

Beauchet, O., Allali, G., Sekhon, H., Verghese, J., Guilain, S., Steinmetz, J.-P., Kressig, R. W., Barden, J. M., Szturm, T., Launay, C. P., et al. (2017). Guidelines for assessment of gait and reference values for spatiotemporal gait parameters in older adults: The biomathics and canadian gait consortiums initiative. *Frontiers in human neuroscience*, *11*, 353.

Bédard, C., Kröger, H., & Destexhe, A. (2006). Does the 1/f frequency scaling of brain signals reflect self-organized critical states? *Physical Review Letters*, *97*(11), 118102.

Bello, O., & Fernandez-Del-Olmo, M. (2012). How does the treadmill affect gait in parkinson's disease? *Current aging science*, *5*(1), 28–34.

Berardelli, A., Dick, J. P., Rothwell, J. C., Day, B. L., & Marsden, C. D. (1986). Scaling of the size of the first agonist EMG burst during rapid wrist movements in patients with Parkinson's disease. *Journal of Neurology, Neurosurgery & Psychiatry*, *49*(11), 1273–1279.

Bloem, B. R., Grimbergen, Y. A., Cramer, M., Willemsen, M., & Zwinderman, A. H. (2001). Prospective assessment of falls in parkinson's disease. *Journal of neurology*, *248*(11), 950–958.

Bollens, B., Crevecoeur, F., Detrembleur, C., Warlop, T., & Lejeune, T. M. (2014). Variability of human gait: Effect of backward walking and dual-tasking on the presence of long-range autocorrelations. *Annals of biomedical engineering*, *42*(4), 742–750.

Bollens, B., Crevecoeur, F., Nguyen, V., Detrembleur, C., & Lejeune, T. (2010). Does human gait exhibit comparable and reproducible long-range autocorrelations on level ground and on treadmill? *Gait and Posture*, *32*(3), 369–373.

Braun Janzen, T., Koshimori, Y., Richard, N. M., & Thaut, M. H. (2022). Rhythm and music-based interventions in motor rehabilitation: Current evidence and future perspectives. *Frontiers in human neuroscience*, *15*, 789467.

Brisswalter, J., & Mottet, D. (1996). Energy cost and stride duration variability at preferred transition gait speed between walking and running. *Canadian Journal of Applied Physiology*, *21*(6), 471–480.

Bryant, M. S., Rintala, D. H., Hou, J., Collins, R. L., & Protas, E. J. (2016). Gait variability in parkinson's disease: Levodopa and walking direction. *Acta Neurologica Scandinavica*, *134*(1), 83–86.

Caccia, D. C., Percival, D., Cannon, M. J., Raymond, G., & Bassingthwaighte, J. B. (1997). Analyzing exact fractal time series: Evaluating dispersional analysis and rescaled range methods. *Physica A: Statistical Mechanics and its Applications*, *246*(3-4), 609–632.

Calabresi, P., Picconi, B., Tozzi, A., Ghiglieri, V., & Di Filippo, M. (2014). Direct and indirect pathways of basal ganglia: A critical reappraisal. *Nature neuroscience*, *17*(8), 1022–1030.

Camarda, R., Camarda, C., Grimaldi, S., Camarda, L. K., Monastero, R., & Gangitano, M. (2005). Effects of levodopa oral bolus on the kinematics of the pointing movements in Parkinson's disease patients. *Journal of Neurology 2005 252:9*, *252*(9), 1074–1081.

Capecci, M., Pournajaf, S., Galafate, D., Sale, P., Le Pera, D., Goffredo, M., De Pandis, M. F., Andrenelli, E., Pennacchioni, M., Ceravolo, M. G., & Franceschini, M. (2019). Clinical effects of robot-assisted gait training and treadmill training for Parkinson's disease. A randomized controlled trial. *Annals of Physical and Rehabilitation Medicine*, *62*(5), 303–312.

Cavanaugh, J. T., Kochi, N., & Stergiou, N. (2010). Nonlinear analysis of ambulatory activity patterns in community-dwelling older adults. *Journals of Gerontology Series A: Biomedical Sciences and Medical Sciences*, *65*(2), 197–203.

Chang, M. D., Shaikh, S., & Chau, T. (2009). Effect of treadmill walking on the stride interval dynamics of human gait. *Gait & posture*, *30*(4), 431–435.

Chen, Y., Ding, M., & Kelso, J. A. S. (1997). *Long Memory Processes (1 f a Type) in Human Coordination* (tech. rep.).

Chen, Y., Repp, B. H., & Patel, A. D. (2002). Spectral decomposition of variability in synchronization and continuation tapping: Comparisons between auditory and visual pacing and feedback conditions. *Human movement science*, *21*(4), 515–532.

Chen, Z., Ivanov, P. C., Hu, K., & Stanley, H. E. (2002). Effect of nonstationarities on detrended fluctuation analysis. *Physical review E*, *65*(4), 041107.

Chien, J., Yentes, J., Stergiou, N., & Siu, K. (2015). The effect of walking speed on gait variability in healthy young, middle-aged and elderly individuals. *Journal of physical activity, nutrition and rehabilitation*, *2015*, http–www.

Cody, F. W., Macdermott, N., Matthews, P. B., & Richardson, H. C. (1986). Observations on the genesis of the stretch reflex in Parkinson's disease. *Brain : a journal of neurology*, *109 (Pt 2)*(2), 229–249.

Collins, S. H., & Kuo, A. D. (2013). Two independent contributions to step variability during over-ground human walking. *PloS one*, *8*(8), e73597.

Crevecoeur, F., Bollens, B., Detrembleur, C., & Lejeune, T. (2010). Towards a "gold-standard" approach to address the presence of long-range auto-correlation in physiological time series. *Journal of neuroscience methods*, *192*(1), 163–172.

Damouras, S., Chang, M. D., Sejdić, E., & Chau, T. (2010). An empirical examination of detrended fluctuation analysis for gait data. *Gait & posture*, *31*(3), 336–340.

De Comite, A., Crevecoeur, F., & Lefèvre, P. (2021). Online modification of goal-directed control in human reaching movements. *Journal of neurophysiology*, *125*(5), 1883–1898.

De Comite, A., Crevecoeur, F., & Lefèvre, P. (2022). Reward-Dependent Selection of Feedback Gains Impacts Rapid Motor Decisions. *eNeuro*, *9*(2).

De Groote, F., Kinney, A. L., Rao, A. V., & Fregly, B. J. (2016). Evaluation of Direct Collocation Optimal Control Problem Formulations for Solving the Muscle Redundancy Problem. *Annals of Biomedical Engineering*, *44*(10), 2922–2936.

Decker, L. M., Cignetti, F., & Stergiou, N. (2013). Executive function orchestrates regulation of task-relevant gait fluctuations. *Gait & posture*, *38*(3), 537–540.

D'Elia, N., Vanetti, F., Cempini, M., Pasquini, G., Parri, A., Rabuffetti, M., Ferrarin, M., Molino Lova, R., & Vitiello, N. (2017). Physical human-robot interaction of an active pelvis orthosis: Toward ergonomic assessment of wearable robots. *Journal of NeuroEngineering and Rehabilitation*, *14*(1), 1–14.

Delignières, D., Ramdani, S., Lemoine, L., Torre, K., Fortes, M., & Ninot, G. (2006). Fractal analyses for 'short' time series: A re-assessment of classical methods. *Journal of Mathematical Psychology*, *50*(6), 525–544.

Delignières, D., & Torre, K. (2009). Fractal dynamics of human gait: A reassessment of the 1996 data of Hausdorff et al. *Journal of Applied Physiology*, *106*(4), 1272–1279.

Desmurget, M., Gaveau, V., Vindras, P., Turner, R. S., Broussolle, E., & Thobois, S. (2004). Online motor control in patients with Parkinson's disease. *Brain*, *127*(8), 1755–1773.

Dierick, F., Vandevoorde, C., Chantraine, F., White, O., & Buisseret, F. (2021). Benefits of nonlinear analysis indices of walking stride interval in the evaluation of neurodegenerative diseases. *Human Movement Science*, *75*.

Dingwell, J. B., & Cusumano, J. P. (2019). Humans use multi-objective control to regulate lateral foot placement when walking. *PLoS computational biology*, *15*(3), e1006850.

Dingwell, J. B., John, J., & Cusumano, J. P. (2010). Do humans optimally exploit redundancy to control step variability in walking? *PLoS Computational Biology*, *6*(7), 14.

Dingwell, J. B., Salinas, M. M., & Cusumano, J. P. (2017). Increased gait variability may not imply impaired stride-to-stride control of walking in healthy older adults: Winner: 2013 gait and clinical movement analysis society best paper award. *Gait & posture*, *55*, 131–137.

Dotov, D., Bayard, S., De Cock, V. C., Geny, C., Driss, V., Garrigue, G., Bardy, B., & Dalla Bella, S. (2017). Biologically-variable rhythmic auditory cues are superior to isochronous cues in fostering natural gait variability in parkinson's disease. *Gait & posture*, *51*, 64–69.

Dotov, D. G., Bardy, B. G., & Dalla Bella, S. (2016). The role of environmental constraints in walking: Effects of steering and sharp turns on gait dynamics. *Scientific Reports*, *6*(1), 28374.

Ducharme, S. W., Kent, J. A., & Van Emmerik, R. E. (2019). Comparable stride time fractal dynamics and gait adaptability in active young and older adults under normal and asymmetric walking. *Frontiers in physiology*, *10*, 1318.

Ducharme, S. W., Liddy, J. J., Haddad, J. M., Busa, M. A., Claxton, L. J., & van Emmerik, R. E. (2018). Association between stride time fractality and gait adaptability during unperturbed and asymmetric walking. *Human movement science*, *58*, 248–259.

Earhart, G. M. (2009). Dance as therapy for individuals with parkinson disease. *European journal of physical and rehabilitation medicine*, *45*(2), 231.

Eke, A., Hermán, P., Bassingthwaighte, J., Raymond, G., Percival, D., Cannon, M., Balla, I., & Ikrényi, C. (2000). Physiological time series: Distinguishing fractal noises from motions. *Pflügers Archiv*, *439*(4), 403–415.

Eskinazi, I., & Fregly, B. J. (2018). A computational framework for simultaneous estimation of muscle and joint contact forces and body motion using optimization and surrogate modeling. *Medical Engineering & Physics*, *54*, 56–64.

Ezzina, S., Pla, S., & Delignières, D. (2025). Restoring the complexity of walking in the elderly and its impact on clinical measures around the risk of falls. *Frontiers in Network Physiology*, *5*, 1532700.

Fadel, P. J., Barman, S. M., Phillips, S. W., & Gebber, G. L. (2004). Fractal fluctuations in human respiration. *Journal of Applied Physiology*, *97*(6), 2056–2064.

Faivre, F., Joshi, A., Bezard, E., & Barrot, M. (2019). The hidden side of parkinson's disease: Studying pain, anxiety and depression in animal models. *Neuroscience & Biobehavioral Reviews*, *96*, 335–352.

Falisse, A., Serrancolí, G., Dembia, C. L., Gillis, J., Jonkers, I., & De Groote, F. (2019). Rapid predictive simulations with complex musculoskeletal models suggest that diverse healthy and pathological human gaits can emerge from similar control strategies. *Journal of The Royal Society Interface*, *16*(157).

Fasano, A., Mazzoni, A., & Falotico, E. (2022). Reaching and Grasping Movements in Parkinson's Disease: A Review. *Journal of Parkinson's Disease*, *12*(4), 1083.

Franz, J. R., Francis, C. A., Allen, M. S., & Thelen, D. G. (2017). Visuomotor entrainment and the frequency-dependent response of walking balance to perturbations. *IEEE Transactions on Neural Systems and Rehabilitation Engineering*, *25*(8), 1135–1142.

Frenkel-Toledo, S., Giladi, N., Peretz, C., Herman, T., Gruendlinger, L., & Hausdorff, J. M. (2005). Treadmill walking as an external pacemaker to improve gait rhythm and stability in parkinson's disease. *Movement disorders: official journal of the Movement Disorder Society*, *20*(9), 1109–1114.

Gao, J., Hu, J., Mao, X., & Perc, M. (2012). Culturomics meets random fractal theory: insights into long-range correlations of social and natural phenomena over the past two centuries. *J. R. Soc. Interface*, *9*, 1956–1964.

Gao, J., Hu, J., & Tung, W. w. (2011). Facilitating Joint Chaos and Fractal Analysis of Biosignals through Nonlinear Adaptive Filtering. *PLOS ONE*, *6*(9), e24331.

Garcia, M., Chatterjee, A., Ruina, A., & Coleman, M. (1998). The simplest walking model: Stability, complexity, and scaling. *Journal of Biomechanical Engineering*, *120*(2), 281–288.

Gates, D. H., & Dingwell, J. B. (2007). Peripheral neuropathy does not alter the fractal dynamics of stride intervals of gait. *Journal of Applied Physiology*, *102*(3), 965–971.

Gates, D. H., Su, J. L., & Dingwell, J. B. (2007). Possible biomechanical origins of the long-range correlations in stride intervals of walking. *Physica A: Statistical Mechanics and its Applications*, *380*(1-2), 259–270.

Ghai, S., & Ghai, I. (2018). Effects of rhythmic auditory cueing in gait rehabilitation for multiple sclerosis: A mini systematic review and meta-analysis. *Frontiers in neurology*, *9*, 386.

Ghai, S., & Ghai, I. (2019). Effects of (music-based) rhythmic auditory cueing training on gait and posture post-stroke: A systematic review & dose-response meta-analysis. *Scientific reports*, *9*(1), 2183.

Gilden, D. L., Thornton, T., & Mallon, M. W. (1995). 1/f Noise in Human Cognition. *Science*, *267*(5205), 1837–1839.

Ginis, P., Nackaerts, E., Nieuwboer, A., & Heremans, E. (2018). Cueing for people with parkinson's disease with freezing of gait: A narrative review of the state-of-the-art and novel perspectives. *Annals of physical and rehabilitation medicine*, *61*(6), 407–413.

Goetz, C. G., Poewe, W., Rascol, O., Sampaio, C., Stebbins, G. T., Counsell, C., Giladi, N., Holloway, R. G., Moore, C. G., Wenning, G. K., et al. (2004). Movement disorder society task force report on the hoehn and yahr staging scale: Status and recommendations the movement disorder society task force on rating scales for parkinson's disease. *Movement disorders*, *19*(9), 1020–1028.

Gonabadi, A. M., Antonellis, P., & Malcolm, P. (2021). Differentiating fallers from nonfallers using nonlinear variability analyses of data from a low-cost portable footswitch device: A feasibility study. *Acta of bioengineering and biomechanics*, *23*(2), 139–145.

Grahn, J. A., & Brett, M. (2007). Rhythm and Beat Perception in Motor Areas of the Brain. *Journal of cognitive Neuroscience*, *19*(5), 893–906.

Haar, S., & Donchin, O. (2020). A Revised Computational Neuroanatomy for Motor Control. *Journal of cognitive neuroscience*, *32*(10), 1823–1836.

Hammond, C., Bergman, H., & Brown, P. (2007). Pathological synchronization in parkinson's disease: Networks, models and treatments. *Trends in neurosciences*, *30*(7), 357–364.

Harcourt-Smith, W. E., & Aiello, L. C. (2004). Fossils, feet and the evolution of human bipedal locomotion. *Journal of anatomy*, *204*(5), 403–416.

Hausdorff, J. M., Peng, C. K., Ladin, Z., Wei, J. Y., & Goldberger, A. L. (1995). Is walking a random walk? Evidence for long-range correlations in stride interval of human gait. *Journal of Applied Physiology*, *78*(1), 349–358.

Hausdorff, J. M. (2005). Gait variability: methods, modeling and meaning. *J NeuroEngineering Rehabil*, *2*(19).

Hausdorff, J. M. (2007). Gait dynamics, fractals and falls: Finding meaning in the stride-to-stride fluctuations of human walking. *Human Movement Science*, *26*(4), 555–589.

Hausdorff, J. M. (2009). Gait dynamics in Parkinson's disease: Common and distinct behavior among stride length, gait variability, and fractal-like scaling. *Chaos: An Interdisciplinary Journal of Nonlinear Science*, *19*(2), 026113.

Hausdorff, J. M., Ashkenazy, Y., Peng, C. K., Ivanov, P. C., Stanley, H. E., & Goldberger, A. L. (2001). When human walking becomes random walking: fractal analysis and modeling of gait rhythm fluctuations. *Physica A: Statistical Mechanics and its Applications*, *302*(1-4), 138–147.

Hausdorff, J. M., Cudkowicz, M. E., Firtion, R., Wei, F. Y., & Goldberger, A. L. (1998). Gait Variability and Basal Ganglia Disorders: Stride-to-S tride Variations of Gait Cycle Timing in Parkinson's Disease and Huntington's Disease. *Movement Disorders*, *13*(3), 428–437.

Hausdorff, J. M., Lertratanakul, A., Cudkowicz, M. E., Peterson, A. L., Kaliton, D., & Goldberger, A. L. (2000). Dynamic markers of altered gait rhythm in amyotrophic lateral sclerosis. *Journal of applied physiology*.

Hausdorff, J. M., Mitchell, S. L., Firtion, R., Peng, C.-K., Cudkowicz, M. E., Wei, J. Y., & Goldberger, A. L. (1997). Altered fractal dynamics of gait: Reduced stride-interval correlations with aging and huntington's disease. *Journal of applied physiology*, *82*(1), 262–269.

Hausdorff, J. M., Nelson, M. E., Kaliton, D., Layne, J. E., Bernstein, M. J., Nuernberger, A., & Singh, M. A. F. (2001). Etiology and modification of gait instability in older adults: A randomized controlled trial of exercise. *Journal of Applied Physiology*.

Hausdorff, J. M., Purdon, P. L., Peng, C.-k., Ladin, Z., Wei, J. Y., GOLDBERGER Charles A, A. L., & Goldberger Fractal, A. L. (1996). *Fractal dynamics of human gait: stability of long-range correlations in stride interval fluctuations*.

Haussler, A. M., Baudendistel, S. T., Harrison, E. C., Tueth, L. E., Rawson, K. S., & Earhart, G. M. (2026). Exploring maintenance of spatiotemporal gait parameters during internal and external rhythmic auditory cueing in parkinson's disease. *Neurodegenerative disease management*, 1–13.

Hayashi, R., Hashimoto, T., Tada, T., & Ikeda, S. (2001). Relation between changes in long-latency stretch reflexes and muscle stiffness in Parkinson's disease – comparison before and after unilateral pallidotomy. *Clinical Neurophysiology*, *112*(10), 1814–1821.

Herman, T., Giladi, N., Gurevich, T., & Hausdorff, J. M. (2005). Gait instability and fractal dynamics of older adults with a "cautious" gait: Why do certain older adults walk fearfully? *Gait and Posture*, *21*(2), 178–185.

Herssens, N., Verbecque, E., Hallemans, A., Vereeck, L., Van Rompaey, V., & Saeys, W. (2018). Do spatiotemporal parameters and gait variability differ across the lifespan of healthy adults? a systematic review. *Gait & posture*, *64*, 181–190.

Hoehn, M. M., & Yahr, M. D. (1967). Parkinsonism: Onset, progression, and mortality. *Neurology*, *17*(5), 427–427.

Hollman, J. H., Lee, W. D., Ringquist, D. C., Taisey, C., & Ness, D. K. (2022). Comparing adaptive fractal and detrended fluctuation analyses of stride time variability: Tests of equivalence. *Gait & Posture*, *94*, 9–14.

Hollman, J. H., McDade, E. M., & Petersen, R. C. (2011). Normative spatiotemporal gait parameters in older adults. *Gait & posture*, *34*(1), 111–118.

Hollman, J. H., Von Arb, H. M., Budreck, A. M., Muehlemann, A., & Ness, D. K. (2020). Treadmill walking alters stride time dynamics in parkinson's disease. *Gait & Posture*, *77*, 195–200.

Hollman, J. H., Watkins, M. K., Imhoff, A. C., Braun, C. E., Akervik, K. A., & Ness, D. K. (2016). A comparison of variability in spatiotemporal gait parameters between treadmill and overground walking conditions. *Gait & posture*, *43*, 204–209.

Holt, K. G., Hamill, J., & Andres, R. O. (1991). Predicting the minimal energy costs of human walking. *Medicine and science in sports and exercise*, *23*(4), 491–498.

Hove, M. J., Suzuki, K., Uchitomi, H., Orimo, S., & Miyake, Y. (2012). Interactive Rhythmic Auditory Stimulation Reinstates Natural 1/f Timing in Gait of Parkinson's Patients. *PLoS ONE*, *7*(3), 32600.

Hunt, N., McGrath, D., & Stergiou, N. (2014). The influence of auditory-motor coupling on fractal dynamics in human gait. *Scientific reports*, *4*(1), 5879.

Hurst, H. E. (1951). Long-term storage capacity of reservoirs. *Transactions of the American society of civil engineers*, *116*(1), 770–799.

Iverson, J. M. (2010). Developing language in a developing body: The relationship between motor development and language development. *Journal of child language*, *37*(2), 229–261.

Jankovic, J. (2008). Parkinson's disease: Clinical features and diagnosis. *Journal of neurology, neurosurgery & psychiatry*, *79*(4), 368–376.

Jenkinson, N., & Brown, P. (2011). New insights into the relationship between dopamine, beta oscillations and motor function. *Trends in neurosciences*, *34*(12), 611–618.

Jordan, K., Challis, J. H., & Newell, K. M. (2007). Walking speed influences on gait cycle variability. *Gait and Posture*, *26*(1), 128–134.

Jordão, S., Cortes, N., Gomes, J., Brandão, R., Santos, P., Pezarat-Correia, P., Oliveira, R., & Vaz, J. R. (2022). Synchronization performance affects gait variability measures during cued walking. *Gait and Posture*, *96*, 351–356.

Jurado-Parras, M. T., Safaie, M., Sarno, S., Louis, J., Karoutchi, C., Berret, B., & Robbe, D. (2020). The Dorsal Striatum Energizes Motor Routines. *Current Biology*, *30*(22), 4362–4372.

Kaipust, J. P., Huisinga, J. M., Filipi, M., & Stergiou, N. (2012). Gait variability measures reveal differences between multiple sclerosis patients and healthy controls. *Motor control*, *16*(2), 229–244.

Kaipust, J. P., McGrath, D., Mukherjee, M., & Stergiou, N. (2013). Gait variability is altered in older adults when listening to auditory stimuli with differing temporal structures. *Annals of Biomedical Engineering*, *41*(8), 1595–1603.

Kalia, L. V., & Lang, A. E. (2015). Parkinson's disease. *The lancet*, *386*(9996), 896–912.

Kang, H. G., & Dingwell, J. B. (2008). Separating the effects of age and walking speed on gait variability. *Gait & posture*, *27*(4), 572–577.

Kirchner, M., Schubert, P., Liebherr, M., & Haas, C. T. (2014). Detrended fluctuation analysis and adaptive fractal analysis of stride time data in parkinson's disease: Stitching together short gait trials. *PloS one*, *9*(1), e85787.

Knill, D. C., Bondada, A., & Chhabra, M. (2011). Flexible, Task-Dependent Use of Sensory Feedback to Control Hand Movements. *Journal of Neuroscience*, *31*(4), 1219–1237.

Kobsar, D., Olson, C., Paranjape, R., & Barden, J. M. (2014). The validity of gait variability and fractal dynamics obtained from a single, body-fixed triaxial accelerometer. *Journal of applied biomechanics*, *30*(2), 343–347.

Konczak, J., Corcos, D. M., Horak, F., Poizner, H., Shapiro, M., Tuite, P., Volkmann, J., & Maschke, M. (2009). Proprioception and motor control in parkinson's disease. *Journal of motor behavior*, *41*(6), 543–552.

Kosse, N. M., Vuillerme, N., Hortobágyi, T., & Lamoth, C. J. (2016). Multiple gait parameters derived from ipod accelerometry predict age-related gait changes. *Gait & posture*, *46*, 112–117.

Kozlowska, K., Latka, M., & West, B. J. (2020). Significance of trends in gait dynamics. *PLoS Computational Biology*, *16*(10).

Krajewski, K. T., Dever, D. E., Johnson, C. C., Mi, Q., Simpson, R. J., Graham, S. M., Moir, G. L., Ahamed, N. U., Flanagan, S. D., Anderst, W. J., & Connaboy, C. (2020). Load Magnitude and Locomotion Pattern Alter Locomotor System Function in Healthy Young Adult Women. *Frontiers in Bioengineering and Biotechnology*, *8*.

Kuo, A. D. (2001). A Simple Model of Bipedal Walking Predicts the Preferred Speed–Step Length Relationship. *Journal of Biomechanical Engineering*, *123*(3), 264–269.

Kuo, A. D., Donelan, J. M., & Ruina, A. (2005). Energetic consequences of walking like an inverted pendulum: Step-to-step transitions. *Exercise and sport sciences reviews*, *33*(2), 88–97.

Kuznetsov, N. A., & Rhea, C. K. (2017). Power considerations for the application of detrended fluctuation analysis in gait variability studies. *PLoS One*, *12*(3), e0174144.

Lamoth, C. J., van Deudekom, F. J., van Campen, J. P., Appels, B. A., de Vries, O. J., & Pijnappels, M. (2011). Gait stability and variability measures show effects of impaired cognition and dual tasking in frail people. *Journal of neuroengineering and rehabilitation*, *8*(1), 2.

Lang, C., Hausdorff, J. M., Bruijn, S. M., Brodie, M. A., Okubo, Y., Maetzler, W., van Leeuwen, M., Singh, N. B., van Dieen, J. H., & Ravi, D. K. (2026). Foot placement coordination is impaired in people with parkinson's disease. *Journal of neuroengineering and rehabilitation*, *23*(1), 10.

Lheureux, A., Warlop, T., Cambier, C., Chemin, B., Stoquart, G., Detrembleur, C., & Lejeune, T. (2020). Influence of Autocorrelated Rhythmic Auditory Stimulations on Parkinson's Disease Gait Variability: Comparison With Other Auditory Rhythm Variabilities and Perspectives. *Frontiers in physiology*.

Lillebæk, B. S., Tran, J., Dalgas, U., & Langeskov-Christensen, M. (2025). Effects of oral levodopa on motor symptoms and gait impairments in Parkinson's disease: a systematic review and meta-analysis. *Expert Review of Neurotherapeutics*, *25*(12), 1435–1449.

Lim, I., van Wegen, E., De Goede, C., Deutekom, M., Nieuwboer, A., Willems, A., Jones, D., Rochester, L., & Kwakkel, G. (2005). Effects of external rhythmical cueing on gait in patients with parkinson's disease: A systematic review. *Clinical rehabilitation*, *19*(7), 695–713.

Lizrova Preiningerova, J., Novotna, K., Rusz, J., Sucha, L., Ruzicka, E., & Havrdova, E. (2015). Spatial and temporal characteristics of gait as outcome measures in multiple sclerosis (edss 0 to 6.5). *Journal of neuroengineering and rehabilitation*, *12*(1), 14.

Ma, Q. D., Bartsch, R. P., Bernaola-Galván, P., Yoneyama, M., & Ivanov, P. C. (2010). Effect of extreme data loss on long-range correlated and anticorrelated signals quantified by detrended fluctuation analysis. *Physical Review E - Statistical, Nonlinear, and Soft Matter Physics*, *81*(3).

Madison, G. (2001). Variability in isochronous tapping: Higher order dependencies as a function of intertap interval. *Journal of Experimental Psychology: Human Perception and Performance*, *27*(2), 411.

Maeda, R. S., O'Connor, S. M., Donelan, J. M., & Marigold, D. S. (2017). Foot placement relies on state estimation during visually guided walking. *Journal of Neurophysiology*, *117*(2), 480–491.

Malatesta, D., Simar, D., Dauvilliers, Y., Candau, R., Borrani, F., Préfaut, C., & Caillaud, C. (2003). Energy cost of walking and gait instability in healthy 65-and 80-yr-olds. *Journal of applied physiology*, *95*(6), 2248–2256.

Mancini, M., Smulders, K., Harker, G., Stuart, S., & Nutt, J. G. (2018). Assessment of the ability of open-and closed-loop cueing to improve turning and freezing in people with parkinson's disease. *Scientific reports*, *8*(1), 12773.

Mandelbrot, B. (1967). How long is the coast of britain? statistical self-similarity and fractional dimension. *science*, *156*(3775), 636–638.

Mandelbrot, B. B., & Van Ness, J. W. (1968). Fractional Brownian Motions, Fractional Noises and Applications. *Review*, *10*(4), 422–437.

Marchal-Crespo, L., & Riener, R. (2018). Robot-assisted gait training. *Rehabilitation Robotics*, 227–240.

Marchand-Pauvert, V., Gerdelat-Mas, A., Ory-Magne, F., Calvas, F., Mazevet, D., Meunier, S., Brefel-Courbon, C., Vidailhet, M., & Simonetta-Moreau, M. (2011). Both L-DOPA and HFS-STN restore the enhanced group II spinal reflex excitation to a normal level in patients with Parkinson's disease. *Clinical Neurophysiology*, *122*(5), 1019–1026.

Marmelat, V., & Meidinger, R. L. (2019). Fractal analysis of gait in people with parkinson's disease: Three minutes is not enough. *Gait & posture*, *70*, 229–234.

Marmelat, V., Reynolds, N. R., & Hellman, A. (2018). Gait dynamics in parkinson's disease: Short gait trials "stitched" together provide different fractal fluctuations compared to longer trials. *Frontiers in physiology*, *9*, 861.

Marmelat, V., Torre, K., Beek, P. J., & Daffertshofer, A. (2014). Persistent fluctuations in stride intervals under fractal auditory stimulation. *PLoS ONE*, *9*(3).

Mates, J. (1994). A model of synchronization of motor acts to a stimulus sequence I. Timing and error corrections. *Biol. Cybern*, *70*, 463–473.

Mazzoni, P., Hristova, A., & Krakauer, J. W. (2007). Why don't we move faster? Parkinson's disease, movement vigor, and implicit motivation. *Journal of Neuroscience*, *27*(27), 7105–7116.

McGregor, M. M., & Nelson, A. B. (2019). Circuit mechanisms of parkinson's disease. *Neuron*, *101*(6), 1042–1056.

McNeely, M. E., Duncan, R. P., & Earhart, G. M. (2012). Medication improves balance and complex gait performance in parkinson disease. *Gait & posture*, *36*(1), 144–148.

Mirelman, A., Bonato, P., Camicioli, R., Ellis, T. D., Giladi, N., Hamilton, J. L., Hass, C. J., Hausdorff, J. M., Pelosin, E., & Almeida, Q. J. (2019). Gait impairments in parkinson's disease. *The Lancet Neurology*, *18*(7), 697–708.

Mohammadi, F., Bruijn, S. M., Vervoort, G., Van Wegen, E. E., Kwakkel, G., Verschueren, S., & Nieuwboer, A. (2015). Motor switching and motor adaptation deficits contribute to freezing of gait in Parkinson's disease. *Neurorehabilitation and Neural Repair*, *29*(2), 132–142.

Moisello, C., Perfetti, B., Marinelli, L., Sanguineti, V., Bove, M., Feigin, A., Di Rocco, A., Eidelberg, D., & Ghilardi, M. F. (2011). Basal ganglia and kinematics modulation: Insights from Parkinson's and Huntington's diseases. *Parkinsonism & Related Disorders*, *17*(8), 642–644.

Moon, Y., Sung, J., An, R., Hernandez, M. E., & Sosnoff, J. J. (2016). Gait variability in people with neurological disorders: A systematic review and meta-analysis. *Human movement science*, *47*, 197–208.

Morris, M. E. (2000). Movement Disorders in People With Parkinson Disease: A Model for Physical Therapy. *Physical therapy*, *80*(6), 578–597. https://academic.oup.com/ptj/article/80/6/578/2842508

Moumdjian, L., Buhmann, J., Willems, I., Feys, P., & Leman, M. (2018). Entrainment and synchronization to auditory stimuli during walking in healthy and neurological populations: A methodological systematic review. *Frontiers in Human Neuroscience*, *12*.

Moumdjian, L., Maes, P.-J., Dalla Bella, S., Decker, L. M., Moens, B., Feys, P., & Leman, M. (2020). Detrended fluctuation analysis of gait dynamics when entraining to music and metronomes at different tempi in persons with multiple sclerosis. *Scientific reports*, *10*(1), 12934.

Nambu, A., Tokuno, H., & Takada, M. (2002). Functional significance of the cortico–subthalamo–pallidal 'hyperdirect'pathway. *Neuroscience research*, *43*(2), 111–117.

Nanhoe-Mahabier, W., Snijders, A., Delval, A., Weerdesteyn, V., Duysens, J., Overeem, S., & Bloem, B. (2011). Walking patterns in parkinson's disease with and without freezing of gait. *Neuroscience*, *182*, 217–224.

Nashed, J. Y., Crevecoeur, F., & Scott, S. H. (2012). Influence of the behavioral goal and environmental obstacles on rapid feedback responses. *Journal of neurophysiology*, *108*(4), 999–1009.

Negrotti, A., Secchi, C., & Gentilucci, M. (2005). Effects of disease progression and L-dopa therapy on the control of reaching-grasping in Parkinson's disease. *Neuropsychologia*, *43*(3), 450–459.

Nutt, J. G., Bloem, B. R., Giladi, N., Hallett, M., Horak, F. B., & Nieuwboer, A. (2011). Freezing of gait: Moving forward on a mysterious clinical phenomenon. *The Lancet Neurology*, *10*(8), 734–744.

O'Connor, S. M., Xu, H. Z., & Kuo, A. D. (2012). Energetic cost of walking with increased step variability. *Gait & Posture*, *36*(1), 102–107.

Osborne, J. A., Botkin, R., Colon-Semenza, C., DeAngelis, T. R., Gallardo, O. G., Kosakowski, H., Martello, J., Pradhan, S., Rafferty, M., Readinger, J. L., et al. (2022). Physical therapist management of parkinson disease: A clinical practice guideline from the american physical therapy association. *Physical therapy*, *102*(4), pzab302.

Ota, L., Uchitomi, H., Ogawa, K.-i., Orimo, S., & Miyake, Y. (2014). Relationship between neural rhythm generation disorders and physical disabilities in parkinson's disease patients' walking. *PLoS One*, *9*(11), e112952.

Otlet, V., & Ronsse, R. (2022). Predicting the effects of oscillator-based assistance on stride-to-stride variability of Parkinsonian walkers. *IEEE International Conference on Robotics and Automation*, 8090–8096.

Otlet, V., & Ronsse, R. (2023). Adaptive walking assistance does not impact long-range stride-to-stride autocorrelations in healthy people. *Journal of Neurophysiology*, *130*(2), 417–426.

Otlet, V., Vandamme, C., Warlop, T., Crevecoeur, F., & Ronsse, R. (2023). Effects of overground gait training assisted by a wearable exoskeleton in patients with parkinson's disease. *Journal of neuroengineering and rehabilitation*, *20*(1), 156.

Ou, Z., Pan, J., Tang, S., Duan, D., Yu, D., Nong, H., & Wang, Z. (2021). Global trends in the incidence, prevalence, and years lived with disability of parkinson's disease in 204 countries/territories from 1990 to 2019. *Frontiers in public health*, *9*, 776847.

Papoulis, A., & Pillai, S. U. (2002). *Probability*. McGraw-hill.

Peng, C. K., Buldyrev, S. V., Havlin, S., Simons, M., Stanley, H. E., & Goldberger, A. L. (1994). Mosaic organization of DNA nucleotides. *Physical Review E*, *49*(2), 1685.

Peng, C. K., Havlin, S., Stanley, H. E., & Goldberger, A. L. (1995). Quantification of scaling exponents and crossover phenomena in nonstationary heartbeat time series. *Chaos: An Interdisciplinary Journal of Nonlinear Science*, *5*(1), 82–87.

Pierrynowski, M. R., Gross, A., Miles, M., Galea, V., McLaughlin, L., & McPhee, C. (2005). Reliability of the long-range power-law correlations obtained from the bilateral stride intervals in asymptomatic volunteers whilst treadmill walking. *Gait & Posture*, *22*(1), 46–50.

Pressing, J., & Jolley-Rogers, G. (1997). Spectral properties of human cognition and skill. *Biol. Cybern*, *76*, 339–347.

Pruszynski, J. A., Kurtzer, I., & Scott, S. H. (2011). The long-latency reflex is composed of at least two functionally independent processes. *Journal of neurophysiology*, *106*(1), 449–459.

Rangarajan, G., & Ding, M. (2000). Integrated approach to the assessment of long range correlation in time series data. *Physical Review E*, *61*(5), 4991.

Ravi, D. K., Marmelat, V., Taylor, W. R., Newell, K. M., Stergiou, N., & Singh, N. B. (2020). Assessing the temporal organization of walking variability: A systematic review and consensus guidelines on detrended fluctuation analysis. *Frontiers in physiology*, *11*, 562.

Redgrave, P., Rodriguez, M., Smith, Y., Rodriguez-Oroz, M. C., Lehericy, S., Bergman, H., Agid, Y., DeLong, M. R., & Obeso, J. A. (2010). Goal-directed and habitual control in the basal ganglia: Implications for parkinson's disease. *Nature Reviews Neuroscience*, *11*(11), 760–772.

Repp, B. H., & Su, Y. H. (2013). Sensorimotor synchronization: A review of recent research (2006-2012). *Psychonomic Bulletin and Review*, *20*(3), 403–452.

Rhea, C. K., Kiefer, A. W., Wittstein, M. W., Leonard, K. B., MacPherson, R. P., Wright, W. G., & Haran, F. J. (2014). Fractal gait patterns are retained after entrainment to a fractal stimulus. *PLoS ONE*, *9*(9).

Riley, M. A., Bonnette, S., Kuznetsov, N., Wallot, S., & Gao, J. (2012). A tutorial introduction to adaptive fractal analysis. *Frontiers in Physiology*, *3*, 371.

Rochester, L., Baker, K., Nieuwboer, A., & Burn, D. (2011). Targeting dopa-sensitive and dopa-resistant gait dysfunction in parkinson's disease: Selective responses to internal and external cues. *Movement Disorders*, *26*(3), 430–435.

Roemmich, R. T., Hack, N., Akbar, U., & Hass, C. J. (2014). Effects of dopaminergic therapy on locomotor adaptation and adaptive learning in persons with Parkinson's disease. *Behavioural Brain Research*, *268*, 31–39.

Ronsse, R., Vitiello, N., Lenzi, T., Van Den Kieboom, J., Carrozza, M. C., & Ijspeert, A. J. (2011). Human-Robot synchrony: Flexible assistance using adaptive oscillators. *IEEE Transactions on Biomedical Engineering*, *58*(4), 1001–1012.

Rothwell, J. C., Obeso, J. A., & Marsden, C. D. (1983). The behaviour of the long-latency stretch reflex in patients with Parkinson's disease. *Neurosurgery, and Psychiatry*, *46*, 35–44.

Roume, C., Ezzina, S., Blain, H., & Delignières, D. (2019). Biases in the Simulation and Analysis of Fractal Processes. *Computational and Mathematical Methods in Medicine*, *2019*.

Salat, D., & Tolosa, E. (2013). Levodopa in the treatment of parkinson's disease: Current status and new developments. *Journal of Parkinson's disease*, *3*(3), 255–269.

Sarbaz, Y., Gharibzadeh, S., Towhidkhah, F., Banaie, M., & Jafari, A. (2011). A Gray-Box Neural Network Model of Parkinson's Disease Using Gait Signal. *Basic and Clinical Neuroscience*, *2*(3), 33–42.

Schapira, A. H., Chaudhuri, K. R., & Jenner, P. (2017). Non-motor features of parkinson disease. *Nature reviews neuroscience*, *18*(7), 435–450.

Scott, S. H. (2004). Optimal feedback control and the neural basis of volitional motor control. *Nature Reviews Neuroscience*, *5*(7), 532–545.

Seidel, K., Mahlke, J., Siswanto, S., Krüger, R., Heinsen, H., Auburger, G., Bouzrou, M., Grinberg, L. T., Wicht, H., Korf, H.-W., et al. (2015). The brainstem pathologies of parkinson's disease and dementia with lewy bodies. *Brain pathology*, *25*(2), 121–135.

Sejdić, E., Findlay, B., Merey, C., & Chau, T. (2013). The effects of listening to music or viewing television on human gait. *Computers in biology and medicine*, *43*(10), 1497–1501.

Sejdić, E., Fu, Y., Pak, A., Fairley, J. A., & Chau, T. (2012). The effects of rhythmic sensory cues on the temporal dynamics of human gait. *PLoS ONE*, *7*(8).

Shadmehr, R., & Krakauer, J. W. (2008). A computational neuroanatomy for motor control. *Experimental brain research*, *185*(3), 359–381.

Sheridan, M. R., & Flowers, K. A. (1990). Movement variability and bradykinesia in Parkinson's disease. *Brain*, *113*, 1149–1161.

Sloot, L. H., Van der Krogt, M., & Harlaar, J. (2014). Self-paced versus fixed speed treadmill walking. *Gait & posture*, *39*(1), 478–484.

Smulders, K., Dale, M. L., Carlson-Kuhta, P., Nutt, J. G., & Horak, F. B. (2016). Pharmacological treatment in parkinson's disease: Effects on gait. *Parkinsonism & related disorders*, *31*, 3–13.

Sowalsky, K. L., Okun, M. S., Terza, M., Martinez-Nunez, A. E., Lee, H., McFarland, N. R., Stergiou, N., Almeida, L., & Hass, C. J. (2026). Regular metronome, fractal metronome, and music for parkinson gait. *JAMA Network Open*, *9*(4), e262744.

Spaulding, S. J., Barber, B., Colby, M., Cormack, B., Mick, T., & Jenkins, M. E. (2013). Cueing and gait improvement among people with Parkinson's disease: A meta-analysis. *Archives of Physical Medicine and Rehabilitation*, *94*(3), 562–570.

Stergiou, N., & Decker, L. M. (2011). Human movement variability, nonlinear dynamics, and pathology: Is there a connection? *Human Movement Science*, *30*(5), 869–888.

Stergiou, N., Harbourne, R. T., & Cavanaugh, J. T. (2006). Optimal movement variability: A new theoretical perspective for neurologic physical therapy. *Journal of neurologic physical therapy*, *30*(3), 120–129.

Stout, R. D., Wittstein, M. W., LoJacono, C. T., & Rhea, C. K. (2016). Gait dynamics when wearing a treadmill safety harness. *Gait & Posture*, *44*, 100–102.

Surmeier, D. J. (2018). Determinants of dopaminergic neuron loss in parkinson's disease. *The FEBS journal*, *285*(19), 3657–3668.

Takakusaki, K. (2017). Functional Neuroanatomy for Posture and Gait Control. *Journal of Movement Disorders*, *10*(1), 1–17.

Terrier, P. (2016). Fractal fluctuations in human walking: Comparison between auditory and visually guided stepping. *Annals of biomedical engineering*, *44*(9), 2785–2793.

Terrier, P. (2020). Gait complexity assessed by detrended fluctuation analysis is sensitive to inconsistencies in stride time series: A modeling study. *arXiv preprint arXiv:2008.06367*.

Terrier, P., & Dériaz, O. (2012). Persistent and anti-persistent pattern in stride-to-stride variability of treadmill walking: Influence of rhythmic auditory cueing. *Human Movement Science*, *31*(6), 1585–1597.

Terrier, P., & Schutz, Y. (2003). Variability of gait patterns during unconstrained walking assessed by satellite positioning (GPS). *European Journal of Applied Physiology*, *90*(5-6), 554–561.

Terrier, P., Turner, V., & Schutz, Y. (2005). GPS analysis of human locomotion: Further evidence for long-range correlations in stride-to-stride fluctuations of gait parameters. *Human Movement Science*, *24*(1), 97–115.

Thaut, M. H., McIntosh, G. C., & Rice, R. R. (1997). Rhythmic facilitation of gait training in hemiparetic stroke rehabilitation. *Journal of the neurological sciences*, *151*(2), 207–212.

Thaut, M. H., Rice, R. R., Braun Janzen, T., Hurt-Thaut, C. P., & McIntosh, G. C. (2019). Rhythmic auditory stimulation for reduction of falls in parkinson's disease: A randomized controlled study. *Clinical rehabilitation*, *33*(1), 34–43.

Theiler, J., Eubank, S., Longtin, A., Galdrikian, B., & Farmer, J. D. (1992). Testing for nonlinearity in time series: The method of surrogate data. *Physica D: Nonlinear Phenomena*, *58*(1-4), 77–94.

Todorov, E. (2005). Stochastic Optimal Control and Estimation Methods Adapted to the Noise Characteristics of the Sensorimotor System. *Neural Computation*, *17*(5), 1084–1108.

Todorov, E., & Jordan, M. I. (2002a). A Minimal Intervention Principle for Coordinated Movement. *Advances in Neural Information Processing Systems*, *15*.

Todorov, E., & Jordan, M. I. (2002b). Optimal feedback control as a theory of motor coordination. *Nature neuroscience*, *5*(11), 1226–1235.

Torre, K., Vergotte, G., Viel, É., Perrey, S., & Dupeyron, A. (2019). Fractal properties in sensorimotor variability unveil internal adaptations of the organism before symptomatic functional decline. *Scientific Reports*, *9*(1), 15736.

Tosserams, A., Keijsers, N., Kapelle, W., Kessels, R. P., Weerdesteyn, V., Bloem, B. R., & Nonnekes, J. (2022). Evaluation of compensation strategies for gait impairment in patients with parkinson disease. *Neurology*, *99*(20), e2253–e2263.

Tosserams, A., Weerdesteyn, V., Bal, T., Bloem, B. R., Solis-Escalante, T., & Nonnekes, J. (2022). Cortical correlates of gait compensation strategies in parkinson disease. *Annals of neurology*, *91*(3), 329–341.

Trojaniello, D., Cereatti, A., Pelosin, E., Avanzino, L., Mirelman, A., Hausdorff, J. M., & Della Croce, U. (2014). Estimation of step-by-step spatio-temporal parameters of normal and impaired gait using shank-mounted magneto-inertial sensors: Application to elderly, hemiparetic, parkinsonian and choreic gait. *Journal of neuroengineering and rehabilitation*, *11*(1), 152.

Tunik, E., Poizner, H., Adamovich, S. V., Levin, M. F., & Feldman, A. G. (2004). Deficits in adaptive upper limb control in response to trunk perturbations in Parkinson's disease. *Experimental Brain Research 2004 159:1*, *159*(1), 23–32.

Uchitomi, H., Ota, L., Ogawa, K. i., Orimo, S., & Miyake, Y. (2013). Interactive Rhythmic Cue Facilitates Gait Relearning in Patients with Parkinson's Disease. *PLOS ONE*, *8*(9), e72176.

Van Wegen, E., De Goede, C., Lim, I., Rietberg, M., Nieuwboer, A., Willems, A., Jones, D., Rochester, L., Hetherington, V., Berendse, H., et al. (2006). The effect of rhythmic somatosensory cueing on gait in patients with parkinson's disease. *Journal of the neurological sciences*, *248*(1-2), 210–214.

Vandamme, C., Otlet, V., Ronsse, R., & Crevecoeur, F. (2023). Model of Gait Control in Parkinson's Disease and Prediction of Robotic Assistance. *IEEE Transactions on Neural Systems and Rehabilitation Engineering*, *31*, 1374–1383.

Vandamme, C., Otlet, V., Ronsse, R., & Crevecoeur, F. (2025). Measured and modeled transitions between self-paced walking and synchronization with rhythmic auditory cues. *Journal of Neurophysiology*, *134*(6), 1939–1952.

Vaz, J. R., Groff, B. R., Rowen, D. A., Knarr, B. A., & Stergiou, N. (2019). Synchronization dynamics modulates stride-to-stride fluctuations when walking to an invariant but not to a fractal-like stimulus. *Neuroscience Letters*, *704*, 28–35.

Vaz, J. R., Knarr, B. A., & Stergiou, N. (2020). Gait complexity is acutely restored in older adults when walking to a fractal-like visual stimulus. *Human Movement Science*, *74*, 102677.

Vaz, J. R., Rand, T., Fujan-Hansen, J., Mukherjee, M., & Stergiou, N. (2020). Auditory and Visual External Cues Have Different Effects on Spatial but Similar Effects on Temporal Measures of Gait Variability. *Frontiers in Physiology*, *11*.

Wagenmakers, E.-J., Farrell, S., & Ratcliff, R. (2004). Estimation and interpretation of $1/f\alpha$ noise in human cognition. *Psychonomic Bulletin & Review*, *11*(4), 579–615.

Warlop, T., Bollens, B., Detrembleur, C., Stoquart, G., Lejeune, T., & Crevecoeur, F. (2017). Impact of series length on statistical precision and sensitivity of autocorrelation assessment in human locomotion. *Human Movement Science*, *55*, 31–42.

Warlop, T., Detrembleur, C., Bollens, B., Stoquart, G., Crevecoeur, F., Jeanjean, A., & Lejeune, T. (2016). Temporal organization of stride duration variability as a marker of gait instability in Parkinson's disease. *Journal of Rehabilitation Medicine*, *48*(10), 865–871.

Warlop, T., Detrembleur, C., Stoquart, G., Lejeune, T., & Jeanjean, A. (2018). Gait complexity and regularity are differently modulated by treadmill walking in parkinson's disease and healthy population. *Frontiers in physiology*, *9*, 68.

Warlop, T. B., Bollens, B., Crevecoeur, F., Detrembleur, C., & Lejeune, T. M. (2013). Dynamics of Revolution Time Variability in Cycling Pattern: Voluntary Intent Can Alter the Long-Range Autocorrelations. *Annals of biomedical engineering*, *41*(8), 1604–1612.

Weiler, J., Gribble, P. L., & Pruszynski, J. A. (2015). Goal-dependent modulation of the long-latency stretch response at the shoulder, elbow and wrist. *J Neurophysiol*, *114*, 3242–3254.

Welford, W. T., Welford, A. T., Brebner, J. M. T., Brebner, J. M., & Kirby, N. (1980). *Reaction Times*. Academic Press. https://books.google.be/books?id=ZjT4d08b-YcC

West, B. J., & Scafetta, N. (2003). Nonlinear dynamical model of human gait. *Physical Review E - Statistical Physics, Plasmas, Fluids, and Related Interdisciplinary Topics*, *67*(5), 10.

Williams-Gray, C., Foltynie, T., Brayne, C., Robbins, T., & Barker, R. (2007). Evolution of cognitive dysfunction in an incident parkinson's disease cohort. *Brain*, *130*(7), 1787–1798.

Yano, S., Nakamura, A., Suzuki, Y., Smith, C. E., & Nomura, T. (2024). Smartphone usage during walking decreases the positive persistency in gait cycle variability. *Scientific reports*, *14*(1), 16410.

Yogev, G., Giladi, N., Peretz, C., Springer, S., Simon, E. S., & Hausdorff, J. M. (2005). Dual tasking, gait rhythmicity, and Parkinson's disease: Which aspects of gait are attention demanding? *European Journal of Neuroscience*, *22*(5), 1248–1256.